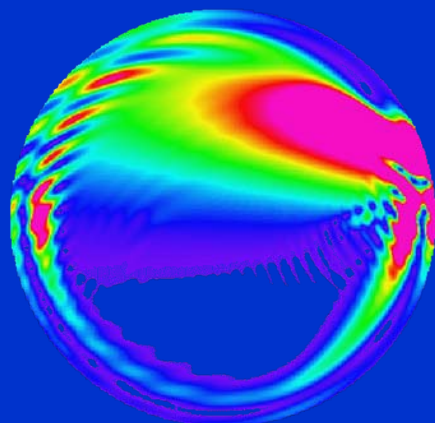




Universität Bremen



Martin-Luther-Universität
Halle-Wittenberg



Mie Theory 1908-2008

Present developments and
Interdisciplinary aspects
of light scattering

Wolfram Hergert, Thomas Wriedt
Editors



Universität Bremen



Martin-Luther-Universität
Halle-Wittenberg

Mie Theory 1908-2008

Present developments and
Interdisciplinary aspects
of light scattering

Martin Luther University Halle-Wittenberg
Halle, Germany
15th – 17th September 2008

Wolfram Hergert, Thomas Wriedt
Editors

Universität Bremen, Bremen 2008

ISBN 978-3-88722-701-2

© Universität Bremen, Bremen 2008

**Druck:
Digital Druckservice Halle GmbH
06108 Halle**

**Vertrieb:
Universitäts-Buchhandlung Bremen
Bibliotheksstr. 3, 28349 Bremen
Tel.: +49-421-211878
Fax: +49-421-217074
Email: info@unibuch-bremen.de**

Acknowledgement

We would like to thank the following institutions for their support:



Palas GmbH, Greschbachstr. 3B, 76229 Karlsruhe



Codixx AG, Steinfeldstraße 3, 39179 Barleben



Martin-Luther-Universität Halle-Wittenberg

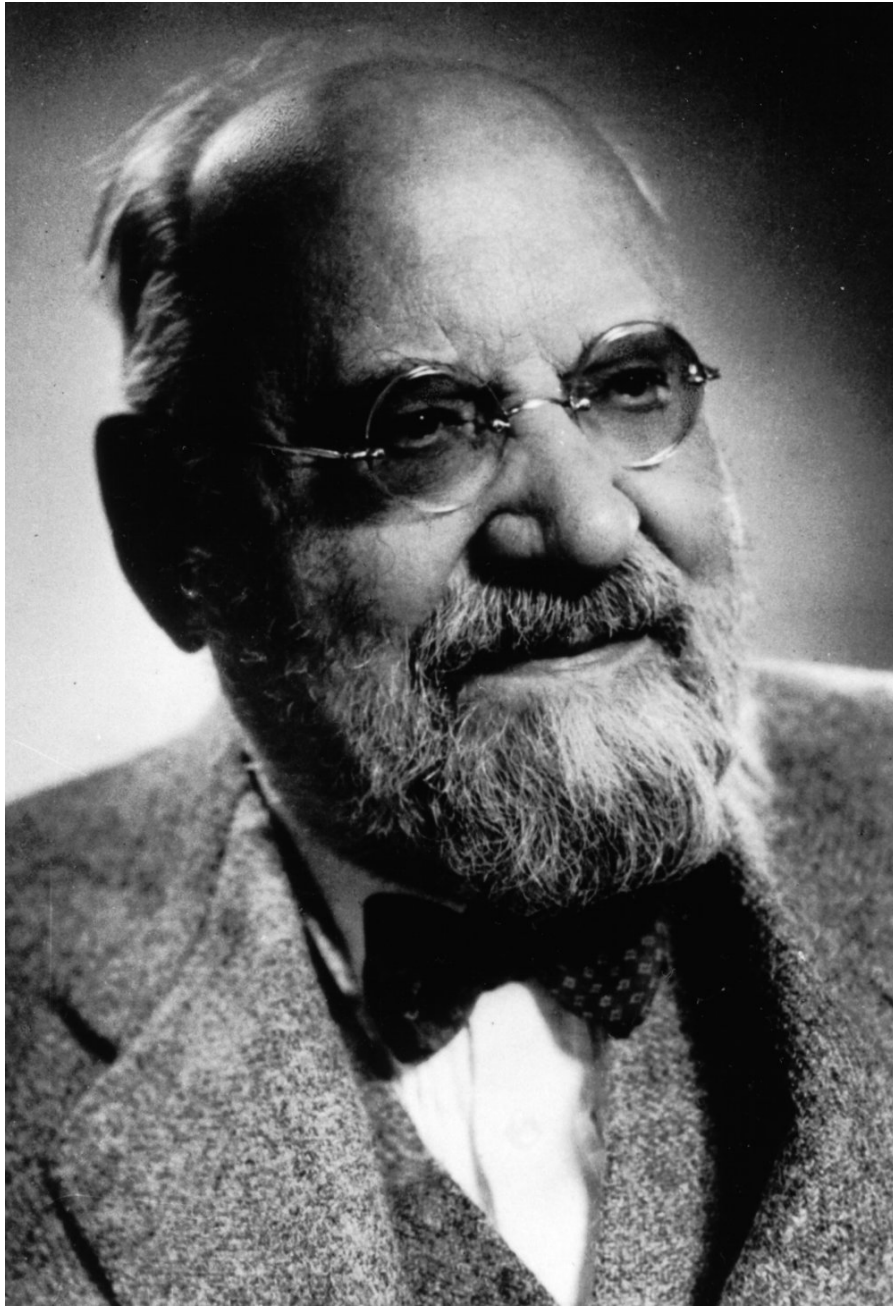


Universität Bremen

Deutsche
Forschungsgemeinschaft



Deutsche Forschungsgemeinschaft



GUSTAV MIE
(1868 – 1957)

With kind permission of Universitätsarchiv der Albert-Ludwigs-Universität Freiburg

Contents

1	Program of the conference	13
1.1	Monday, September 15th 2008 (VSP 1.04, 1.03)	13
1.2	Tuesday, September 16th 2008 (VSP 1.04)	15
1.3	Wednesday, September 17th 2008 (VSP 1.04)	16
2	Mie Theory 1908-2008	
	Introduction to the conference	17
3	Invited talks	22
3.1	The importance of Mie theory for understanding the formation of Supernovae and White Dwarfs (Andersen)	22
3.2	From Lidar Signals to Aerosol Properties via Mie’s Theory by advanced Regularization (Böckmann <i>et al.</i>)	22
3.3	Particle characterization by rainbow techniques (Damaschke)	24
3.4	Scattering by system of particles on or near a plane surface (Doicu)	26
3.5	Application of Lorenz-Mie Theory in Graphics (Frisvad)	26
3.6	Light scattering from features on surfaces (Germer)	28
3.7	Lorenz-Mie and Duhem-Quine (Gouesbet)	29
3.8	Measurement and modelling of light scattering by small particles (Hesse)	31
3.9	Rainbows, coronas and glories (Laven)	34
3.10	Harry Bateman, Gustav Mie and Maxwell’s equations (Martin)	36
3.11	What can Lorenz–Mie theory do for optical tweezers? (Nieminen <i>et al.</i>)	37
3.12	Optical trapping of microsized spheres in aberrated Hermite-Gauss fields (Saija <i>et al.</i>)	38
3.13	Optical Resonances, Mie-Theory and beyond (Schweiger)	40
4	Contributed Talks	41
4.1	Speeding up mesh-based nanooptics calculations (Alegret, Martín-Moreno)	41
4.2	Particle characterization by pulse induced Mie scattering and time resolved analysis of scattered light (Bech, Leder)	42
4.3	Field distribution of plasmons on Ag nanospheres in a dielectric matrix (Benghorieb <i>et al.</i>)	45
4.4	Nanoplasmonics and an extension of the Lorentz-Mie theory by the method of additional boundary conditions (Datsuyk)	48
4.5	Light Transport in Random Media with Internal Resonances (Frank <i>et al.</i>)	49
4.6	Mie scattering and topological charge (Garbin <i>et al.</i>)	49

4.7	Particle sizing from the measurement of the effective refractive index of colloids (García-Valenzuela <i>et al.</i>)	51
4.8	Efficiency of frequency-pulsed excitation of a micron-sized spherical microcavity by chirped ultrashort laser radiation (Geints <i>et al.</i>)	53
4.9	Interstellar Extinction curve from Mie, TMatrix and DDA models (Gupta, Vaidya)	53
4.10	Gustav Mie - From Electromagnetic Scattering to a General Theory of Matter (Hergert)	55
4.11	UV radiation inside interstellar grain aggregates (Iatì <i>et al.</i>)	56
4.12	Novel interferometric laser imaging for spray and micobubble sizing – one of the successful Mie scattering application (Kawaguchi <i>et al.</i>)	58
4.13	Optical properties of densely packed small particles (Okada, Kokhanovsky)	60
4.14	Gas Density Measurements via Rayleigh Scattering (Rausch <i>et al.</i>)	62
4.15	Use of the Mie-theory in optical aerosol spectrometers (Schmidt, Mölter)	63
4.16	Mie Scattering for Particle Size Analysis (Stübinger <i>et al.</i>)	64
4.17	Applying Mie Theory to determine single scattering of arbitrarily shaped precipitation particles at microwave frequencies (Teschl, Randeu)	66
4.18	Rigorous modeling of light scattering in dielectric structures by the generalized source method (Shcherbakov, Tishchenko)	67
4.19	Interactions of layered spheres with dipoles in direct and inverse scattering theory (Tsitsas)	71
4.20	The use of nano particles for patterned polarizers within the whole transparent window of soda lime glass (Volke)	73
4.21	Using Light Scattering for Fast Particle Sizing in Atmospheric Science (Wollny)	73
4.22	Considerations to Rayleigh’s hypothesis (Wauer, Rother)	76
4.23	Optical force distribution on the surface of a spheroid (Xu <i>et al.</i>)	76
5	Poster contributions	78
5.1	Investigation of volume scattering from size distributed MgO and TiO ₂ particles using Mie theory (Ahmed <i>et al.</i>)	78
5.2	Optical properties of dielectric media in the presence of metallic nanoparticles (Benghorieb <i>et al.</i>)	79
5.3	FEM simulation of light scattering by nonspherical objects (Burger <i>et al.</i>)	82
5.4	Experimental determination of light scattering properties of spheroidal titania particles and its comparison with Mie theory (Gogoi <i>et al.</i>)	84
5.5	Mie Resonances in Femtosecond Pulse Absorption by metallic Nanoparticles (Grigorchuk, Tomchuk)	85
5.6	Resonance spectra of typical particles (Han <i>et al.</i>)	87
5.7	Categorization of light scattering programs (Hellmers, Wriedt)	88
5.8	Aggregate of spherical primary particle and approximations for light scattering cross section (Jacquier, Gruy)	91
5.9	Probing the composition of a drying microdroplet of water suspension of nanoparticles with optical methods (Jakubczyk <i>et al.</i>)	93

5.10	Photonic/Plasmonic Structures in Nanocomposite Glass(Kiriyenko <i>et al.</i>)	95
5.11	Theory of strong localization effects of classical waves in disordered loss or gain media (Lubatsch <i>et al.</i>)	96
5.12	Optical Trapping of Carbon Nanotubes and Gold Nanorods (Maragò <i>et al.</i>)	97
5.13	Field enhancement through particle plasmons (Miclea <i>et al.</i>)	99
5.14	Experimental determination of size and refractive index of colloidal particles by coherent refraction and transmittance of light (Sánchez-Pérez <i>et al.</i>)	99
5.15	Equivalent refractive index for biaxially anisotropic scatterers using T-matrix approach (Schmidt, Wriedt)	101
5.16	Interstellar Extinction by Spheroidal Grains (Vaidya)	104
5.17	New life of Mie's approach with other bases, potentials, methods, etc. (Farafonov <i>et al.</i>)	105
5.18	Scattering data base <code>scatdb</code> (Wauer, Rother)	106

1 Program of the conference

Invited talks (I) 30 min. talk, 10 min. discussion

Contributed talks 15 min. talk, 5 min. discussion

Posters should be fixed Monday morning during the coffee break and remain on the stands till Tuesday.

1.1 Monday, September 15th 2008 (VSP 1.04, 1.03)

08:50 - 09:00 Opening of the workshop
(Prof. Dr. H. Graener; Dean of the Faculty, Th. Wriedt, W. Hergert)

I. Session (Chair: Wriedt)

09:00 - 09:40	W. Hergert (Halle, Germany)	55
	Gustav Mie -From Electromagnetic Scattering to a General Theory of Matter	
09:40 - 10:20 (I)	F. Mie (Berlin, Germany)	
	Wer war dieser Geheimrat und Professor Mie?	
10:20 - 10:40	<i>Coffee break (Fix posters)</i>	

II. Session (Chair: Kokhanovsky)

10:40 - 11:20 (I)	G. Gouesbet (Rouen, France)	29
	Lorenz-Mie and Duhem-Quine	
11:20 - 12:00 (I)	P.A. Martin (Golden, USA)	36
	Harry Bateman, Gustav Mie and Maxwell's equations	
12:00 - 12:20	T. Kawaguchi (Tokyo, Japan)	58
	Novel interferometric laser imaging for spray and microbubble sizing - one of the successful Mie scattering applications	
12:20 - 12:40	A. Garcia-Valenzuela (Mexico)	51
	Particle sizing from the measurement of the effective refractive index of colloids	
12:40 - 14:00	<i>Lunch break</i>	

III. Session (Chair: Gousbet)

14:00 - 14:40 (I)	Th. Germer (Gaithersburg, USA)	28
	Light scattering features at surfaces	
14:40 - 15:00	S. Benghorieb (Saint-Etienne, France)	45
	Field distribution of plasmons on Ag nanospheres in a dielectric matrix	
15:00 - 15:20	V.V. Datsyuk (Kyiv, Ukraine)	48
	Nanoplasmonics and an extension of the Lorentz-Mie theory by the method of additional boundary conditions	
15:20 - 15:40	<i>Coffe break</i>	

IV. Session (Chair: Schweiger)

15:40 - 16:20 (I)	A. Doicu (Oberpfaffenhofen, Germany)	26
	System of particles near surfaces	
16:20 - 16:40	J. Wauer (Leipzig, Germany)	76
	Considerations to Rayleigh's hypothesis	
16:40 - 17:00	V. Garbin (Twente, Netherlands)	49
	Mie scattering and topological charge	
17:00 - 17:20	M. Schmidt (Pallas GmbH, Germany)	63
	Use of the Mie theory in optical aerosol spectrometers with digital single signal evaluation of scattered light impulses	
17:20 - 17:40	<i>Break</i>	

V. Session (Chair: Martin)

17:40 - 18:00	A. Volke (Codixx AG, Germany)	73
	The use of nano particles for patterned polarizers within the whole transparent window of soda lime glass	
18:00 - 18:20	Y. Okada (Osaka, Japan)	60
	Optical properties of densely packed small particles	

VI. Postersession (VSP 1.03)

18:30 - 20:00	Postersession (lecture hall VSP 1.03)	
---------------	---------------------------------------	--

1.2 Tuesday, September 16th 2008 (VSP 1.04)

I. Session (Chair: Saija)

09:00 - 09:40 (I)	P. Laven (Horley, Surrey, UK) Rainbows, coronas, glories	34
09:40 - 10:20 (I)	N. Damaschke (Rostock, Germany) Particle characterization by rainbow techniques	24
10:20 - 10:50	<i>Coffee break</i>	

II. Session (Chair: Germer)

10:50 - 11:30 (I)	C. Böckmann (Potsdam, Germany) From LIDAR Signals to Aerosol Properties via Mie's Theory by advanced regularization	22
11:30 - 11:50	F. Teschl (Graz, Austria) Applying Mie theory to determine single scattering of arbitrarily shaped precipitation particles at microwave frequencies	66
11:50 - 12:10	H. Bech (Rostock, Germany) Particle characterization by pulse induced Mie scattering and time resolved analysis of light scattering	42
12:10 - 12:30	A. Shcherbakov (Moscow, Russia) Rigorous modelling of light scattering in dielectric structures by the generalized source method	67
12:30 - 14:00	<i>Lunch break</i>	

III. Session (Chair: Hesse)

14:00 - 14:40 (I)	G. Schweiger (Bochum, Germany) Optical resonances: Mie theory and beyond	40
14:40 - 15:00	Th. Stübinger (Sympatec GmbH, Germany) Mie Scattering for Particle Size Analysis: Expanded Size Ranges by Extreme Precision Calculations	64
15:00 - 15:20	N.L. Tsitsas (Athens, Greek) Interactions of layered spheres with dipoles in direct and inverse scattering theory	71
15:20 - 15:50	<i>Coffee break</i>	

IV. Session (Chair: Frisvad)

15:50 - 16:30 (I)	A.C. Andersen (Copenhagen, Denmark) The importance of Mie theory for understanding the formation of Supernovae and White Dwarfs	22
-------------------	--	----

16:30 - 16:50	M.A. Iatí (Messina, Italy)	56
	UV radiation inside interstellar grain aggregates: Implications for interstellar photochemistry and formation of prebiotic molecules	
16:50 - 17:10	R. Gupta (Pune, India)	53
	Interstellar Extinction curve from Mie, TMatrix and DDA models	
17:10 - 17:30	<i>Break</i>	
17:30 - 18:10 (I)	Nieminen, T. A. (Queensland, Australia)	37
	What can Lorenz–Mie theory do for optical tweezers?	
18:10 - 18:30	J. Alegret (Zaragoza, Spain)	41
	Speeding up mesh-based nanooptics calculations	
18:30 - 18:50	R. Franck (Bonn, Germany)	49
	Light transport in Random Media with Internal Resonances	
19:30	<i>Dinner</i>	

1.3 Wednesday, September 17th 2008 (VSP 1.04)

I. Session (Chair: Doicu)

09:00 - 09:40 (I)	J.R. Frisvad (Lyngby, Denmark)	26
	Application of Lorenz-Mie Theory in Graphics	
09:40 - 10:20 (I)	E. Hesse (Hatfield, UK)	31
	Measurement and modelling of light scattering by small particles	
10:20 - 10:50	<i>Coffee break</i>	

II. Session (Chair: Hergert)

10:50 - 11:30 (I)	R. Saija (Messina, Italy)	38
	Optical trapping of microsized spheres in aberrated Hermite-Gauss fields	
11:30 - 11:50	A. Rausch (Berlin, Germany)	62
	Gas Density Measurements via Rayleigh Scattering	
11:50 - 12:10	A. Wollny (Mainz, Germany)	73
	Using Light Scattering for Fast Particle Sizing in Atmospheric Science: an Up-to-date White Light Optical-Particle-Counter	
12:10 - 12:30	F. Xu (Darmstadt, Germany)	76
	Optical force distribution on the surface of a spheroid	
12:30 - 12:40	<i>Final remarks</i>	

2 Mie Theory 1908-2008

Introduction to the conference

Thomas Wriedt

Verfahrenstechnik, FB4, Universität Bremen, Bremen, Germany

Electromagnetic scattering by a homogeneous, isotropic sphere is commonly referred to as Mie theory, although *Gustav Mie* (1868–1957) was not the first to formulate this electromagnetic scattering problem. Before him *Alfred Clebsch* (1833–72), solving the elastic point source scattering problem of a perfectly rigid sphere using potential functions [1], and *Ludvig Lorenz* (1829–91) [3, 2] contributed to this problem [4]. In 1909 *Peter Debye* (1884 – 1966) considered the related problem of radiation pressure on a spherical particle [5] utilizing two scalar potential functions. Therefore plane wave scattering by a homogeneous isotropic sphere is also referred to as Lorenz-Mie theory [6], or even Lorenz-Mie-Debye theory [7]. The incorrect name Lorentz-Mie theory seems also to be quite common (e.g. in Burlak [8]). Kerker provides an extensive postscript on the history of scattering by a sphere [9].

German physicist *Gustav Mie* published his classical paper on the simulation of the colour effects connected with colloidal gold particles using the classical Maxwell equations in 1908 [10] when he was professor of physics in Greifswald. This paper gave an outline of how to compute light scattering by small spherical particles and it became the classic contribution to this subject. To cite *Eugene Garfield* from his 1985 investigation on articles most cited in the SCI from 1961 to 1982 [11]: "The oldest paper was published in *Annalen der Physik* in 1908 by Gustav Mie. It is one of three articles in Table 1 written in German. This paper discusses the electric and magnetic vibrations and optical properties of particles in colloidal solutions. Interestingly, it continues to be heavily cited even today - 45 times in 1983 alone, 75 years later. It is interesting to speculate why it has not become the common wisdom of physics, which often leads to obliteration of citations to classic work."

Cardona and Marx [12] comment, that this paper was almost ignored until about 1945 but its importance rose with increasing interest in colloids starting from the 1950s such that hundred years after publication the paper is still much cited [14] with currently 160 citations a year (Fig. 2.0.1). The paper is called *Dornröschen* (Sleeping Beauty) by the researchers at Information Retrieval Services of Max Planck Society [13] because of its low recognition considering the number of citations during the first years after its publication. But in the 1930s contemporary scientists acknowledged the importance of his contribution. In a special issue devoted to Mie's 70s birthday *Ilse Fränz-Gotthold* and *Max von Laue* [15] dedicate their paper to "Gustav Mie whom physics owes the

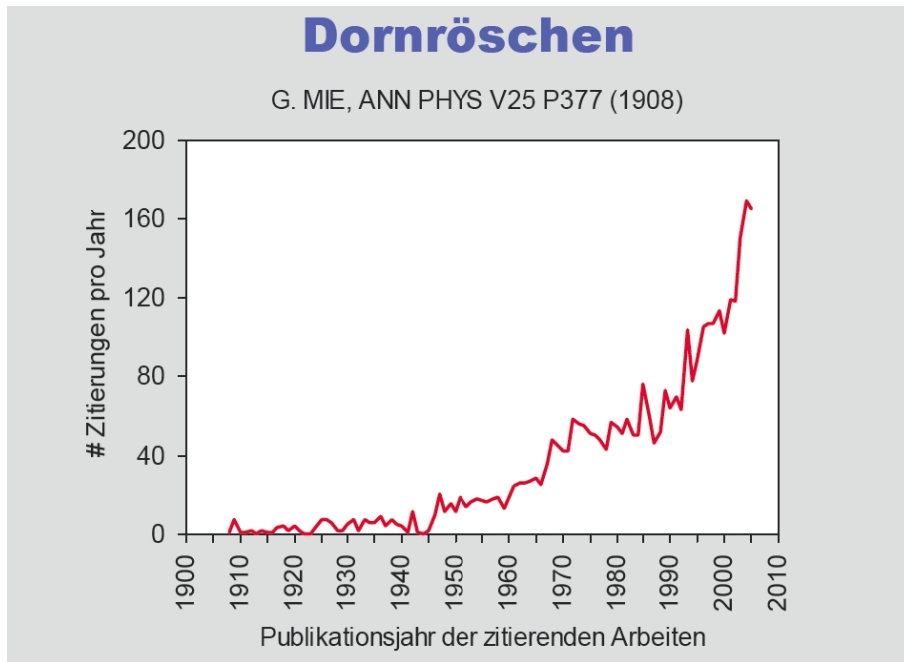


Figure 2.0.1: Number of citations of Mie’s paper according to *Bowman and Marx* [13].

mathematical treatment of diffraction by a sphere”.

The current citations of Mie’s paper show that the applications of Mie theory cover a wide range of subjects like climate research, optical particle characterization or interstellar dust in astrophysics.

Understandably prior to the development of electronic computers in the middle of last century not many papers were published on computing scattering problems using Mie’s theory since the computational labour involved in evaluating functions such as Ricatti-Bessel functions was quite extreme.

Even with the rapid evolution of the computer it took some time before stable algorithms were developed. Gradually reliable and stable scattering programs were published. Early well known algorithms were published by *Giese* [16] and *Dave* [17]. The IBM report by *Dave* from 1968 was still send out on request in the 1990s. Nowadays a number of efficient algorithms and programs are available. A major step was the program MIEV0 written by *Wiscombe* [18, 19], which is based on *Lentz’s* continued-fraction method for the calculation of spherical Bessel functions [20]. It has been demonstrated that Mie’s theory can be successfully applied up to size parameters of 500 [21, 4, 23] and this year Mie’s theory has even been programmed on a Java enabled Mobile Phone using a Matlab clone [24]. As the scattering of a plane electromagnetic wave by a dielectric sphere is considered a canonical problem, Mie’s theory is still used as a standard reference to validate methods intended for more complex scattering problems [25, 26, 27].

Apparently one of the first English language versions of Mie’s theory was published by *Bateman* [28]. Mie’s original paper was translated into the English language as late as

1976 by the Royal Aircraft Establishment in the UK [29] and two years later by Sandia Laboratories in US [30]. Recently a Spanish translation of the original paper became available [31] and Chinese and Hebrew translations are on the way [32].

In the published literature, when citing derivation of Mie's theory first major references of a full description of the theory were to *Stratton* [33], *Born and Wolf* [34] and *van de Hulst* [35]. Later *Bohren and Huffman* [36] were cited commonly.

As in 2008 hundred years after its publication scientists from various disciplines all over the world still deal with Mie's theory applying or extending it, it seems that this year might be suitable date to celebrate this 100 years history by having a close look at *Present developments and interdisciplinary aspects of light scattering*.

Acknowledgment

We would like to acknowledge support of this conference by Deutsche Forschungsgemeinschaft (DFG).

Bibliography

- [1] Alfred Clebsch: Über die Reflexion an einer Kugelfläche. Journal für Mathematik, Band 61, 1863, Heft 3, p 195-262.
- [2] Ludvig Lorenz: Lysbevaegelsen i og uden for en af plane Lysbolger belyst Kugle. Det Kongelige Danske Videnskabernes Selskabs Skrifter, 6. Raekke, 6. Bind, 1890,1, p 1-62.
- [3] Ludvig Lorenz: Sur la lumière réfléchié et réfractée par une sphère (surface) transparente. in Oeuvres scientifiques de L. Lorenz. revues et annotées par H. Valentiner. Tome Premier, Libraire Lehmann & Stage, Copenhague, 1898, p 403-529.
- [4] N. A. Logan: Survey of some early studies of the scattering of plane waves by a sphere. Proc. IEEE (1965) 773–785.
- [5] Peter Debye: Der Lichtdruck auf Kugeln von beliebigem Material. Annalen der Physik, Vierte Folge, Band 30, 1909, No. 1, p 57-136.
- [6] Walter T. Grandy: Scattering of waves from large spheres. Cambridge University Press 2005.
- [7] E.J. Davis, G. Schweiger: The Airborne Microparticle. Springer, Berlin, Heidelberg 2002.
- [8] Gennadiy Burlak: The Classical and Quantum Dynamics of the Multispherical Nanostructures. Imperial College Press, London 2004.
- [9] Milton Kerker: The Scattering of Light, and Other Electromagnetic Radiation. Academic Press, New York, London 1969.

- [10] Gustav Mie: Beiträge zur Optik trüber Medien, speziell kolloidaler Metallösungen. *Annalen der Physik*, Vierte Folge, Band 25, 1908, No. 3, p 377-445.
- [11] Eugene Garfield: The Articles Most Cited in the SCI from 1961 to 1982. 6. More Citation Classics to Think About. *Current Contents* 14 (1985) April 8, 3-10.
- [12] Manuel Cardona, Werner Marx: Verwechselt, vergessen, wieder gefunden. *Physik Journal* 3 (2004) 11, 27-29.
- [13] Benjamin F. Bowman, Werner Marx: Bibliometrie in der Forschungsevaluierung. www.biochem.mpg.de/iv/AgFN_Bibliometrie.pdf, accessed 15. Aug. 2008.
- [14] Werner Marx: Dornröschen und Mauerblümchen. Nachzügler und vergessene Arbeiten in der Physik. *Phys. Unserer Zeit* (2007) 1, 34-39.
- [15] Ilse Fränz-Gotthold, Max von Laue: Beugung konvergierender Lichtwellen. *Annalen der Physik* 425 (1938) 3, 249-258.
- [16] R.-H. Giese: Die Berechnung der Lichtstreuung an kugelförmigen Teilchen mit einem Digitalrechner. *Elektron. Rechenanl.* 3 (1961) 6, 240-245.
- [17] J. V. Dave: Subroutines for Computing the Parameters of the Electromagnetic Radiation Scattered by a Sphere, Rep. No. 320-3237, IBM Scientific Center, Palo Alto, Calif. (1968).
- [18] W. J. Wiscombe: Mie Scattering Calculations: Advances in Technique and Fast, Vector-Speed Computer Codes, National Center for Atmospheric Research Technical Note NCAR/TN-140+STR (1979).
- [19] W. J. Wiscombe: Improved Mie scattering algorithms, *Appl. Opt.* 19 (1980), 1505–1509.
- [20] W. J. Lentz: Generating Bessel functions in Mie scattering calculations using continued fractions, *Appl. Opt.* 15 (1976), 668–67.
- [21] Guei-Gu Siu, Lu Cheng: Mie solution of light scattering from spheres of radii up to 80λ with digit-array method. *JOSA B*, 19 (2002) 8, 1922-1929.
- [22] H. Du: Mie-scattering calculation. *Applied Optics* 43 (2004) 9, 1951-1956.
- [23] Jianqi Shen: Algorithm of Numerical Calculation on Lorentz Mie Theory. *PIERS Online* 1 (2005) 6, 691-694.
- [24] Thomas Wriedt: Mie theory 1908, on the mobile phone 2008. *Journal of Quantitative Spectroscopy & Radiative Transfer* 109 (2008), 1543–1548.
- [25] Thomas Grosjes, Alexandre Vial, Dominique Barchiesi: Models of near-field spectroscopic studies: comparison between Finite-Element and Finite-Difference methods. *Optics Express* 13 (2005) 21, 8484.

- [26] Ruo-Jian Zhu , Jia Wang, Guo-Fan Jin: Mie scattering calculation by FDTD employing a modified Debye model for Gold material. *Optik* 116 (2005), 419–422.
- [27] Peng-Wang Zhai, Changhui Lia, George W. Kattawar and Ping Yang: FDTD far-field scattering amplitudes: Comparison of surface and volume integration methods. *Journal of Quantitative Spectroscopy and Radiative Transfer* 106 (2007) 1-3, 590-594.
- [28] Harry Bateman: The mathematical analysis of electrical and optical wave-motion on the basis of Maxwell’s equations. Cambridge University Press, 1915. <http://www.archive.org/download/mathematicalanal00baterich/mathematicalanal00baterich.pdf>, accessed 15. Aug. 2008.
- [29] Gustav Mie: Contributions to the optics of turbid media, particularly of colloidal metal solutions. Royal Aircraft Establishment, Library Translation 1873, 1976, RAE-Lit-Trans-1873. <http://diogenes.iwt.uni-bremen.de/vt/laser/papers/RAE-LT1873-1976-Mie-1908-translation.pdf>, accessed 15. Aug. 2008.
- [30] Gustav Mie: Contributions on the optics of turbid media, particularly colloidal metal solutions — Translation. Sandia Laboratories, Albuquerque, New Mexico, 1978, SAND78-6018. National Translation Center, Chicago, ILL, Translation 79-21946.
- [31] Gustav Mie: Consideraciones sobre la óptica de los medios turbios, especialmente soluciones coloidales. http://www.ugr.es/~aquiran/ciencia/mie/mie1908_spanish.pdf, accessed 15. Aug. 2008.
- [32] Arturo Quirantes: Mie Translation Project, <http://www.ugr.es/~aquiran/mie.htm>, accessed 15. Aug. 2008.
- [33] J. A. Stratton: *Electromagnetic Theory*. McGraw-Hill, New York 1941.
- [34] M. Born, E. Wolf: *Principles of Optics*. Pergamon Press, London 1959.
- [35] H. C. van de Hulst: *Light Scattering by Small Particles*. Wiley, New York 1957.
- [36] C. F. Bohren, D. R. Huffman: *Absorption and Scattering of Light by Small Particles*. Wiley, New York 1983.

3 Invited talks

3.1 The importance of Mie theory for understanding the formation of Supernovae and White Dwarfs

A. C. Andersen¹

¹Dark Cosmology Centre, Niels Bohr Institute, University of Copenhagen, Denmark, anja@dark-cosmology.dk

Massive stars end their life by becoming supernovae, while less massive stars end their life as a white dwarf. It was shown by Chandrasekhar that white dwarfs have a mass limit of less than 1.4 solar masses. From observations it seems that stars with a main-sequence mass of less than 8 solar masses reach the end stellar stage of a white dwarf. These stars therefore undergo significant mass loss in their late stellar stages. This mass loss influences both their evolution and their observable properties. The mass loss is driven by pulsation-enhanced dust driven wind. The dust particles form in the cool outer layers and are accelerated away from the star by radiation pressure. The composition of the particles is determined by the elemental abundance in the stellar atmosphere, with carbon-rich stars forming mostly amorphous carbon particles and oxygen-rich stars producing silicate particles. The detailed understanding of how the dust drives the stellar wind which explain this immense mass loss have been a mystery. The solution to this mystery now seems to have been found by a proper treatment of Mie theory.

3.2 From Lidar Signals to Aerosol Properties via Mie's Theory by advanced Regularization

C. Böckmann¹, L. Osterloh¹, P. Pornsawad¹

¹Institute of Mathematics, University of Potsdam, Am Neuen Palais 10, 14469 Potsdam, Germany

Knowledge on the amount of aerosol in the Earth's atmosphere is not sufficient to calculate or even to estimate the impact of aerosols on global and regional climate. One of the techniques to gain more knowledge is advanced lidar remote sensing. Indeed, there are several problems connected with the retrieval of microphysical parameters from the data gained by Raman lidar measurements. The calculation can be reduced to two basic steps; in the first step, the aerosol extinction and backscatter profiles have to be

extracted from the Raman signals, then those profiles are used for the retrieval of the microphysical properties. Unfortunately, both problems are of an ill-posed nature. To gain extinction profiles, one can solve the equation

$$\alpha_{\text{aer}}(\lambda_L, z) = \left\{ \frac{d}{dz} \ln \left[\frac{N(z)}{z^2 P(\lambda_R, z)} \right] - \alpha_{\text{mol}}(\lambda_L, z) - \alpha_{\text{mol}}(\lambda_R, z) \right\} / \left\{ 1 + \left(\frac{\lambda_L}{\lambda_R} \right)^k \right\},$$

with α_{aer} being the sought aerosol extinction profile, λ_L the emitted wavelength, λ_R the receiving Raman wavelength, $N(z)$ the density of the atmospheric Raman scatterer, z the height, P the power received and α_{mol} the molecular extinction. As shown in [2], this is an ill-posed problem that needs regularization for the derivative calculation. After the

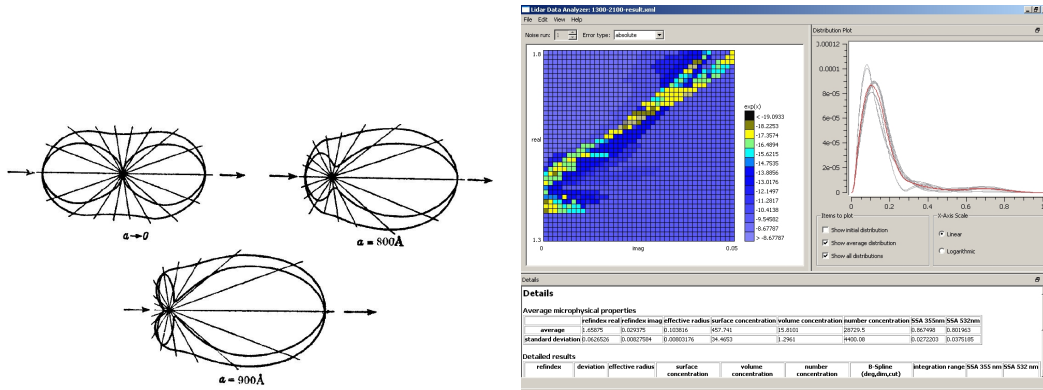


Figure 3.2.1: Left: Polar diagrams for the scattering of light by a spherical gold particle by Mie [1]. Right: Screen shot of the developed software.

backscatter and extinction profiles have been calculated, suitable height layers in these profiles are chosen for microphysical retrieval; this is, again, an ill-posed problem. The equation we need to solve with kernel functions for Mie particles [1] is

$$\Gamma(\lambda) = \int_{r_0}^{r_1} \pi r^2 Q_{\pi/\text{ext}}^n(r, \lambda, m) n(r) dr, \quad Q_{\pi} = k^{-2} r^{-2} \left| \sum_{n=1}^{\infty} (2n+1) (-1)^n (a_n - b_n)^2 \right|.$$

Here, ext denotes extinction and π backscatter. k is the wave number defined by $k = 2\pi/\lambda$, and a_n and b_n are coefficients derived by the boundary conditions. r_0 and r_1 are sensible lower and upper bounds for the size of the particles. m is the complex refractive index. Thus, an algorithm to solve this ill-posed problem has been proposed in [3] which splits the nonlinear problem into several linear problems at every refractive index in a certain predefined grid. The solution at each point is obtained by a hybrid regularization technique employing both B-spline collocation and truncated singular value decomposition. For solving this problem, a software (see Fig. 3.2.1, right) is being developed. Ongoing research on this topic includes new regularization schemes like Runge-Kutta type iterations, see [4], and the influence of the choice of nodes for the B-spline collocation on the quality of the solution.[5]

Acknowledgement

The support by the European Commission under grant RICA- 025991 via project Earlinet-ASOS is gratefully acknowledged.

References

- [1] G. Mie, "Beiträge zur Optik trüber Medien," *Ann. d. Physik* 25, 377-445 (1908).
- [2] P. Pornsawad, C. Böckmann, C. Ritter and M. Rafler, "The ill-posed retrieval of aerosol extinction coefficient profiles by regularization," *Appl. Opt.* 47, 1649-1661 (2008).
- [3] C. Böckmann, I. Mironova, D. Müller, R. Nessler and L. Schneidenbach, "Microphysical aerosol parameters from multiwavelength lidar," *J. Opt. Soc. Am. A* 22, 518-528 (2005).
- [4] C. Böckmann, A. Kirsche, "Iterative regularization method for lidar remote sensing," *Comput. Phys. Commun.* 174, 607-615 (2006).
- [5] L. Osterloh, C. Böckmann, "Retrieval of aerosol distribution from lidar data with adaptive base points," *Proceedings of 24th ILRC Boulder*, 165-168 (2008).

3.3 Particle characterization by rainbow techniques

N. Damaschke¹

¹ **University of Rostock, Institute of General Electrical Engineering, Optoelectronics and Photonic Systems, Rostock, Albert-Einstein-Str.**

Since the theoretical contribution of Gustav Mie there are a tremendous number of applications of Mie scattering phenomena. Beside the extensions of the Lorenz-Mie theory for description of complex scattering also the scattering from one single homogeneous spherical particle in a plane wave initiated a number of developments. Optical sizing and characterization of individual particles is one application example. Especially small droplets or bubbles tend to become spherical and can fulfill the requirements of the Lorenz-Mie theory. The field of application varies from fuel injection, lacquer processes, spray forming and temperature measurements to sizing of cavitation bubbles. The rainbow technique is one example of such measurement systems. Rainbows are generated by two wave interference from the same scattering order in the region of the deflection point of the outgoing rays. The generated interference fringes are sensitive to particle size and refractive index. Therefore rainbow techniques are used to measure diameter and droplet temperature via the refractive index (e.g. [1]). Nevertheless, additional wave phenomena's disturb the ideal rainbow, predicted from the geometrical optics or the Airy theory. Interference with reflection or surface waves generates the ripple structure,

which partially hide the rainbow interference. A number of theoretical and practical investigations were performed to solve these problems but always limits the accuracy of particle size and temperature estimation to about one micrometer and one Kelvin (e.g. [2-4]). A second approach uses the fineness in the scattering functions, ripple structure and optical resonances, for diameter and refractive index estimations with very high accuracy. Some of these inversion strategies can detect diameter changes down to 10nm and small changes in the refractive index and refractive index profile. Otherwise this accuracy requires perfect spherical droplets and is limited to laboratory investigations of single droplets (e.g. [5], [6]). Currently the rainbow is used as a contact-free and optical measurement technique for particle diameter and refractive index with very high resolution. Most of the applications were performed under laboratory conditions for single droplets and results in very precise measurements for calibration of evaporation models. Beside these specialized setups, one commercial instrument was provided for some years ([7]). Against the background of these investigations the present contribution will give an overview of available rainbow techniques, the current research activities and future potential for characterization of individual particles.

References

- [1] J. P. A. J. van Beeck, Rainbow phenomena: development of a laser based, non-intrusive technique for measuring droplet size temperature and velocity, (Techn. Uni Eindhoven, Eindhoven Netherlands, 1997).
- [2] N. Damaschke, Light Scattering Theories and Their Use for Single Particle Characterization, in *Fachgebiet Strömungslehre und Aerodynamik*, (Technische Universität Darmstadt, Darmstadt Germany, 2003).
- [3] J. P. A. J. van Beeck, L. Zimmer, and M. L. Riethmuller, Global Rainbow Thermometry for Mean Temperature and Size Measurement of Spray Droplets, Part. Part. Syst. Charact. **18**, 196-204 (2001).
- [4] M. Peil, I. Fischer, W. Elsäßer, S. Bakić, N. Damaschke, C. Tropea, S. Stry, and J. Sacher, Rainbow refractometry with a tailored incoherent semiconductor laser source, Appl. Phys. Lett. **89**, 091106 (2006).
- [5] J. Wilms, Evaporation of Multicomponent Droplets, in *Institut für Thermodynamik der Luft- und Raumfahrt*, (Universität Stuttgart, Stuttgart Germany, 2005), p. 157.
- [6] S. Saengkaew, T. Charinpanitkul, H. Vanisri, W. Tanthapanichakoon, Y. Biscos, N. Garcia, G. Lavergne, L. Mees, G. Gouesbet, and G. Grehan, Rainbow refractrometry on particles with radial refractive index gradients, Exp. Fluids **43**, 595-601 (2007).
- [7] S. V. Sankar, K. M. Ibrahim, D. H. Buermann, M. J. Fidrich, and W. D. Bachalo, An integrated phase Doppler/Rainbow refractometer system for simultaneous measure-

ment of droplet size, velocity and refractive index, in *3rd International Conference on Optical Particle Sizing*, (Yokohama Japan 1993), pp. 275-283.

3.4 Scattering by system of particles on or near a plane surface

Doicu, A.¹

¹Remote Sensing Technology Institute, German Aerospace Centre, Oberpfaffenhofen, Wessling, Germany

Computation of light scattering from particles deposited upon a surface is of great interest in the simulation, development and calibration of surface scanners for wafer inspection. More recent applications include laser cleaning, scanning near-field optical microscopy and plasmon resonances effects in surface-enhanced Raman spectroscopy. In this paper we address the electromagnetic scattering by a system of particles on or near a plane surface. The formalism is based on the null-field method and the integral representation of vector spherical wave functions over plane waves. Essentially, the theoretical model accounts on the multiple scattering effects between the individual particles and on the interaction between the system of particles and the plane surface.

3.5 Application of Lorenz-Mie Theory in Graphics

Frisvad, J. R.¹

¹DTU Informatics, Technical University of Denmark, Richard Petersens Plads, Building 321, DK-2800 Kgs. Lyngby, Denmark

This talk has two purposes: firstly to show what the Lorenz-Mie theory has been used for in computer graphics, secondly to discuss the generalisations of the theory that are available and why they are important in a graphics context. Some details are provided in the following.

In order to produce photo-realistic images that capture a digitally modelled scene, we need scattering properties for all the materials that are present in the scene. To acquire such scattering properties, one option is to measure them. Another option is to compute them from the particle contents of the materials. The second option is made possible by the Lorenz-Mie theory, and it provides us with a very flexible way of modelling how the appearance of a material changes when we change its contents. Nevertheless, the Lorenz-Mie theory has only reluctantly been adopted in graphics. In the two papers [1,2] where the theory was first considered for graphics applications, it was found to be either too complicated [1] or too restricted [2] to be useful. The problematic restrictions are that the material should consist of nearly spherical particles embedded in a non-absorbing host medium. This significantly limits the number of materials that

can be modelled by the original version of the theory. Even so, the original theory has proven useful for modelling the appearance of some special materials: Callet [3] used the theory to model pigmented materials (such as paints, plastics, inks, and cosmetics which consist of pigmented particles in a transparent solvent). Jackèl and Walter [4] used it to model the atmosphere and rainbows. Nishita and Dobashi [5] used the theory to model various other materials consisting of particles in air (clouds, smoke/gas, fog/haze, snow, and sand). Most recently, we have seen a development towards generalisation of the Lorenz-Mie theory such that it becomes useful for a wider range of materials. These new developments were adapted for graphics by Frisvad et al. [6]. I will discuss this and other generalisations of the theory. Figure 3.5.1 exemplifies how we can use the Lorenz-Mie theory to compute the visual significance of each individual component in a material. Of course, we can also use it to compute the appearance of materials with different mixed particle concentrations.



Figure 3.5.1: From the paper by Frisvad et al. [6]: Rendered images of the components in milk as well as mixed concentrations. The scattering properties of the components and the milk have been computed using a new scheme for robust evaluation of the Lorenz-Mie coefficients when the host medium is absorbing. From left to right the glasses contain: Pure water, the host medium (water and dissolved vitamin B2), water and protein, water and fat, skimmed milk, regular milk, and whole milk.

References

- [1] T. Nishita, Y. Miyawaki, and E. Nakamae, "A shading model for atmospheric scattering considering luminous intensity distribution of light sources," *Computer Graphics (Proceedings of ACM SIGGRAPH 87)* 21(4), 303–310 (July 1987).
- [2] H. Rushmeier. "Input for participating media," in *Realistic Input for Realistic Images*, ACM SIGGRAPH 95 Course Notes (1995).
- [3] P. Callet, "Pertinent data for modelling pigmented materials in realistic rendering," *Computer Graphics Forum* 15(2), 119-127 (1996).

- [4] D. Jackèl and B. Walter, "Modeling and rendering of the atmosphere using Mie-scattering," *Computer Graphics Forum* 16(4), 201-210 (1997).
- [5] T. Nishita and Y. Dobashi, "Modeling and rendering of various natural phenomena consisting of particles," In *Proceedings of Computer Graphics International 2001*, IEEE Computer Society, 149-156 (2001).
- [6] J. R. Frisvad, N. J. Christensen, and H. W. Jensen, "Computing the scattering properties of participating media using Lorenz-Mie theory," *ACM Transactions on Graphics* 26(3), Article 60 (July 2007).

3.6 Light scattering from features on surfaces

Germer, T.A.¹

¹National Institute of Standards and Technology, Gaithersburg, MD 20899, USA

In this talk, I will describe recent work that highlights the power of computational electromagnetics as it applies to process control and inspection in the semiconductor industry. A variety of methodologies are available for investigating surface features, whether they be unintentional particles or intentionally fabricated structures, but few of them have the non-contact, high-throughput, and inline-friendly advantages afforded to optical methods. Analysis of the signals in optical measurements, however, is non-trivial because most of the structures of interest are on the order of or smaller than the wavelength of the light used. Thus, the relationship between the optical signature and the details of the feature is not necessarily straightforward.

One example that will be given is the distinction between surface roughness, subsurface defects and particles. In this case, polarization can play a key role in distinguishing between these cases. Light scattering from small amounts of surface roughness yields a specific polarization behavior that is dependent only upon the measurement geometry, the wavelength of the light, and the optical constants of the material. The specific details of the surface roughness, quantified by the power spectrum of the surface height function, imparts itself only upon the scattered light intensity. Similar behavior can be found for some classes of subsurface defects, such as material inhomogeneity or very small spherical defects, although the polarization behavior will be different. These findings can potentially improve the sensitivity of inspection tools to particulate contamination.

Recent interest has been directed towards the problem of scattering by a sphere above a surface. The solution of this problem involves a merging of two classic electromagnetic problems: the Mie scattering by a sphere and the Fresnel reflection from a planar interface. While spherical particles are rarely found during inspection of smooth surfaces, they are often used to calibrate those instruments. Having a robust theory for scattering by a sphere has improved such calibration by enabling a model-based calibration scheme. While polystyrene spheres are usually used for calibration standards, their lifetime under

ultraviolet irradiation is short. With the model-based calibration scheme, other materials, such as silica, which are more stable, can be used instead, without changing the overall scale of the instrument.

Computational electromagnetic methods are being used extensively now for the metrology of microfabricated structures. Optical scatterometry, whereupon the reflectance of a grating is measured as a function of angle or wavelength, is becoming a useful tool for determining line width, sidewall angle, height, and other shape parameters. When one has a pretty good idea of what structure one is looking at, the inverse scattering problem becomes tractable by comparing the reflectance signature to a large library of possible structures or by performing a regression analysis. The sensitivity of this method to the various dimensions of a structure is often in the sub-nanometer regime.

In all of the above cases, there are many details that continue to need exploring. Roughness of thin films complicates the scatter by interfaces. Shape issues become important for optimally spherical particles, when they are attached to surfaces. Robust methods for solutions to the grating problem continue to need development.

3.7 Lorenz-Mie and Duhem-Quine

G.Gouesbet¹

¹ **LESP, CORIA, UMR CNRS 6614, Rouen University, Rouen INSA, BP12, avenue de l'université, 76801, Saint-Etienne du Rouvray, France.**

One of the most famous theories in electromagnetism, more particularly in light scattering, is the one published by Mie in 1908, that we are currently now commemorating in this conference. This theory is based on Maxwell's equations. However, another theory solving the same problem has actually been published about twenty years before by Lorenz. Both Mie and Lorenz theories are empirically equivalent as discussed by Logan or Kragh. But the extraordinary fact is that Lorenz theory does not rely on Maxwell's equations, but on the old theory of aether, this aether which has been rejected after Einstein and his relativity. When I became aware of this fact, about thirty years ago, I found this very puzzling and guessed that something very important, from an epistemological point of view, was hidden behind such a thing which, surely, should not be a mere coincidence, but deserved some kind of explanation. It is only recently that I understood what was going on. There exists a theorem called Duhem-Quine theorem which is of a philosophical nature (although a philosophical theorem may look like an oxymoron) and which, furthermore, has never been demonstrated. After many precursors (like Oslander, Urbain VIII, Galileo Galilei, Descartes or Pascal), a modern formulation of the theorem is that theories are under-determined by experiments. In other words, you may have conflicting theories which produce the same experimental predictions. The possibility of an under-determination of theories by experiments is usually much disliked by physicists, and the actual vagueness which remains attached to this concept (a theo-

rem not demonstrated, or even ill-stated) does not help. It is however very important because, if it is true, it questions the possibility of a realistic description of the world, the kind of description which was praised so much by Einstein and shaken so much by quantum mechanics. But, is the theorem true? A way to answer this question, before may be possessing a genuine statement and a genuine demonstration (we likely need a new Gödel for this) is to provide examples. Here is a first example. It is impossible to discriminate between Lorenz and Mie on the basis of their respective abilities of making correct experimental predictions, since they both make the same predictions. Therefore, the choice between Lorenz and Mie is under-determined by experiments. This is a case to which the Duhem-Quine theorem applies. For a second example, let us start with classical mechanics, and consider two of its formulation, the one of Newton and the one of Hamilton-Jacobi. In Newton's formulation, the representation of the world is based on the concept of trajectory (I restrict my discussion to the case of matter points). Provide initial conditions, integrate the equations of motion, and you obtain a Newtonian trajectory of a matter point. That's all. There is nothing more to understand with Newton. With the Hamilton-Jacobi's formulation, we obtain another picture of the world. In this formulation, we possess an unobservable action field S and the trajectories are orthogonal to the surfaces of equi-values of S . The two formulations (say theories) of Newton and Hamilton-Jacobi make the same experimental predictions, but they do not provide the same picture of the world. From this point of view, they are incompatible theories. This is our second example of applications of the Duhem-Quine theorem. You may try to use an ampliative argument which, by definition, is a supplementary argument used to remove the under-determination. Such an argument may run as follows. We are used to trajectories (we observe trajectories every day) and we are not used to an unobservable action field S . Therefore, surely, this action field is may be a convenient intermediary for computations, but it does not have any physical reality. Therefore, Newton is right, at least better connected with reality than Hamilton-Jacobi. However, I am going to claim that the reverse opinion is actually true. Consider a sub-topic of classical mechanics, namely classical scattering. More specifically, let us consider the non relativistic motion of a matter point in a central potential $V(r)$. It is known that, under certain circumstances, this may generate rainbow singularities, where the differential scattering cross-section becomes infinite. Such an actual (in the sense of Aristotle) infinity in physics is, I claim, inadmissible (this is a non-singularity principle, NSP). It means that classical mechanics is inadmissible (it contained the germs of its own destruction) and, also, that Newtonian trajectories of matter points do not exist. Therefore, Hamilton-Jacobi is better than Newton. Now, having removed the trajectories from the Hamilton-Jacobi picture, what should we do with the action field S ? Since classical mechanics is inadmissible due to the singularities it generates, it has to be lifted to a wave mechanics (waves remove singularities). Assuming that the classical mechanics is an approximation to the wave mechanics to be built, we may then reach a set of generalized Schrödinger's equations, the Schrödinger's equation itself being the simplest equation in this set. The worrying unobservability of S is then conveyed to the non worrying unobservability of the wave function. NPS has been used as an ampliative argument to discriminate between Newton and Hamilton-Jacobi, and to

escape from the Duhem-Quine under-determination. It can also be used to show that wave mechanics is the result of an a priori rational necessity. As a third example, let us compare the orthodox quantum mechanics, with its intrinsic indeterminacy generated by the von Neumann's postulate of projection, and a deterministic version, named pilot wave, initiated by Louis de Broglie, and developed to its logical conclusion by Bohm. The orthodox quantum mechanics and the pilot wave are experimentally equivalent, although one is indeterministic, and the other deterministic. They are therefore Duhem-Quine equivalent. But the pilot wave theory relies on the existence of hidden objective particle trajectories. Since the existence of such trajectories has been rejected in classical mechanics, we may use an ampliative argument, and refuse to accept them in quantum mechanics. Therefore, the orthodoxy of Copenhagen is here winning against the heterodoxy of Bohm. Finally, we may now again use an ampliative argument to reject Lorenz, and preserve Mie, an ampliative argument which tells us that the old aether has indeed to be rejected and that, hence, Lorenz is to be rejected. Thirty years after I asked myself the question, here is, I believe an answer. For lack of room, I did not provide references in this abstract. But more is to come in a paper on Duhem-Quine to be written and in a book (hidden worlds in quantum kingdom) under preparation. I apologize if the reader feel a bit frustrated and I intend to work hard to tell more soon.

3.8 Measurement and modelling of light scattering by small particles

Hesse, E.¹, Ulanowski, Z.¹, Mc Call, D.S.¹, Stopford, C.¹, Kaye, P.H.¹

¹Science and Technology Research Institute, University of Hertfordshire, Hatfield AL10 9AB, U.K.

Abstract

At the University of Hertfordshire we measure and model light scattering by small particles, in particular by such relevant for climate research. The measurements comprise phase functions, linear polarization of single levitated particles (ice analogues, Saharan dust) and 2D scattering patterns for interpretation of airborne instrument data (Small Ice Detector). In order to extend the applicability of geometric optics towards lower size parameters, we have developed the Ray Tracing with Diffraction on Facets (RTDF) model. It combines geometric optics with diffraction on flat facets, and is suitable for rapid computation of scattering on faceted dielectric objects such as ice crystals or faceted approximations of more complex shapes. Due to its low computational cost it allows the calculation of 2D scattering patterns, which are useful for deriving particle shape from scattering data.

Introduction

The importance of ice and mixed-phase clouds to the earth-atmosphere radiation balance and climate is well established. Though studied for many years, there is still a large uncertainty over the radiative properties of cirrus clouds [1]. This is partly due to inadequate theoretical models of light scattering by the constituent ice crystals of realistic shapes and sizes. Therefore, laboratory measurements of single particle scattering properties as well as the development of suitable light scattering models - capable of predicting scattering properties of complex particles of intermediate size - are important.

Measurements on single particles levitated in an electrodynamic balance

An electrodynamic balance (EDB) of the double ring double disc type has been designed for studying single microparticles [2]. The EDB has small dimensions in order to facilitate the use of high resolution microscope objectives (14mm focal length). It allows electrostatic particle injection and recovery. By applying suitable ac-parameters to the EDB, elongated particles can be aligned randomly or at certain fixed orientations. For injection into the trap, the selected particle is picked up by a sharp tungsten needle and contact charged. Light scattering measurements are carried out using a laser diffractometer [3]. Results for ice analogue crystals (which are stable at room temperature and have the same refractive index and hexagonal crystal structure as water ice [4]), and Saharan dust particles will be presented.

The RTDF model

The ray tracing with diffraction on facets (RTDF) model combines geometric optics (GO) with diffraction on flat facets. The model calculates diffraction using an approximation for the far field direction of the Poynting vector. Phase functions for near random orientation of hexagonal columns have been compared with SVM [8], which is an analytical method, and with GO with projected area diffraction [9]. The RTDF results approximate those by SVM much better than GO over the whole angular range, and in particular in near forward and backscattering regions, in the halo region and between 142° and 160° . Comparisons with T-matrix calculations [10] have been carried out for randomly oriented circular cylinders. The RTDF method can be applied to arbitrary faceted objects or faceted approximations of objects with curved surfaces and can be used to calculate 2D scattering patterns for fixed and random orientation.

Measurements and modelling of 2D scattering patterns

Most in situ probes for shape characterization of cloud particles rely on direct imaging of particles onto 1D or 2D sensors. Therefore, resolution is limited due to diffraction, optical aberrations, and constrained depth-of-field. However, light scattering patterns of single particles are not bound by depth-of-field and optical resolution constraints. The spatial distribution of the light depends on particle size, shape, orientation and internal structure. This approach has been used for a series of detectors developed at the

University of Hertfordshire (Small Ice Detectors SID-1 and SID-2). A new instrument employs a gated intensified charge coupled device camera (ICCD) to record particle light scattering patterns with single photon sensitivity [11]. Discriminating between droplets and nonspherical ice crystals is straightforward, since the former produce highly symmetric scattering patterns and the latter generally do not [12]. Frequency analysis can be used to group recorded images into various classes of ice crystal habits [13]. To develop this method further, reference scattering patterns from known particles, such as ice analogs [4] and 2D scattering patterns modeled using RTDF can be used.

Acknowledgement

This work was supported by the Natural Environment Research Council of the UK.

References

- [1] Intergovernmental Panel on Climate Change, 2007. Fourth Assessment Report.
- [2] E. Hesse, Z. Ulanowski, P.H. Kaye, Stability characteristics of cylindrical fibers in an electrodynamic balance designed for single particle investigation, *J. Aerosol Sci.* **33**, 149-163 (2002).
- [3] Z. Ulanowski, R.S. Greenaway, P.H. Kaye, and I.K. Ludlow. Laser diffractometer for single- particle scattering measurements , *Meas. Sci. Technol.* **13**, 292-296 (2002).
- [4] Z. Ulanowski, E. Hesse, P.H. Kaye and A.J. Baran, Light scattering by complex ice-analogue crystals , *J. Quantit. Spectr. Rad. Transf.* **100** (1-3), 382-392 (2006).
- [5] E. Hesse, Z. Ulanowski. Scattering from long prisms using ray tracing combined with diffraction on facets , *J Quantit Spectrosc Radiat Transf* **79-80C**, 721-732 (2003).
- [6] A.J.M.Clarke, E. Hesse, Z. Ulanowski and P.H. Kaye, A 3D implementation of ray-tracing with diffraction on facets: Verification and a potential application , *J Quantit Spectrosc Radiat Transf* **100**, 103-114 (2006).
- [7] E. Hesse, Modelling diffraction during ray-tracing using the concept of energy flow lines , *J. Quantit. Spectr. Rad. Transf.* **109**, 1374-1383 (2008).
- [8] S. Havemann, T. Rother, K. Schmidt. Light scattering by hexagonal ice crystals . In: M.I. Mishchenko, L.D. Travis, J.W. Hovenier, editors. *Conference on Light Scattering by Nonspherical Particles: Theory, Measurements and Applications*, 29th September-1st October 1998. New York: American Meteorological Society, p.253-6.
- [9] A. Macke, J. Mueller, E. Raschke, Single scattering properties of atmospheric ice crystals , *J Atmos Sci* **53**, 2813-2825 (1996).
- [10] M.I. Mishchenko, A. Macke, How big should hexagonal ice crystals be to produce halos?, *Appl. Opt.* **38**, 1626-1629 (1999).

- [11] P.H. Kaye et al. Classifying atmospheric ice crystals by spatial light scattering . Submitted to Optics Letters.
- [12] E. Hirst, P. H. Kaye, R. S. Greenaway, P. R. Field, and D. W. Johnson, Discrimination of micrometre-sized ice and super-cooled droplets in mixed-phase cloud , Atmos. Environ. 35, 33- 47 (2001).
- [13] Z. Ulanowski, C. Stopford, E. Hesse, P.H. Kaye, E. Hirst, and M. Schnaiter, Characterization of small ice crystals using frequency analysis of azimuthal scattering patterns , 10th Int. Conf. on Electromagnetic & Light Scattering 2007, June, 17-22, Bodrum, Turkey, pp.225-228.

3.9 Rainbows, coronas and glories

Laven, P.¹

¹ 9 Russells Crescent, Horley, Surrey, RH6 7DJ, United Kingdom
(philip@philiplaven.com)

The rainbow, corona and glory are examples of atmospheric optical phenomena caused by the scattering of sunlight from spherical drops of water. Eminent scientists (such as Descartes, Newton, Young, Airy and others) offered various explanations for the formation of rainbows - and thus made major contributions to our understanding of the nature of light. Given the availability since 1908 of Mie's rigorous solution for scattering of light by homogeneous spherical particles, it might be assumed that everything is now known about the rainbow, corona and glory. However, it is only in recent years that rapid advances in computing power have allowed Mie's solution to be used to investigate these phenomena - and to produce full-colour simulations, such as those shown in Fig. 1 [1-4].

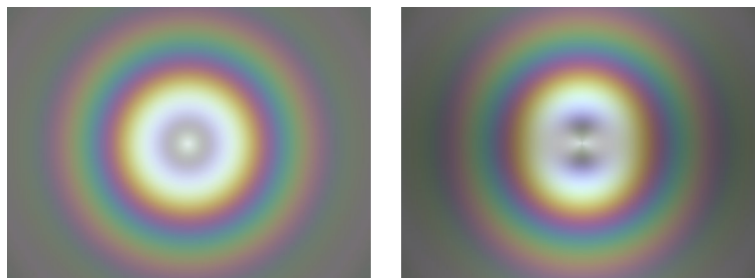


Figure 3.9.1: Left: Simulation of a glory caused by scattering of sunlight from water droplets with radius $10 \mu\text{m}$. Right: Simulation of the same glory as seen through a vertical polarising filter.

Although Mie's solution permits excellent simulations of glories, it provides no information about the scattering processes that cause glories. In 1947, van de Hulst [5]

suggested that the glory was caused by surface waves generated by light rays suffering one internal reflection. The final paper will report on tests [6] of this hypothesis, including scattering calculations for Gaussian beams.

What would glories look like if they were caused by scattering from substances more exotic than water, such as the clouds of ethane as found on Titan? The left side of Fig. 2 is a false-colour map [7] showing the intensity of scattering of 650 nm light by a sphere of radius $10\ \mu\text{m}$ for scattering angles between 170° and 180° as a function of refractive index n of the sphere. Note that the zones of moderate intensity around 178° , 176° , 174.1° and 172.2° correspond to the rings of the glory: the horizontal alignment of these zones indicate that the angular size of the glory's rings is almost independent of n . This is confirmed in the right side of Fig.2, which compares simulations of the glory caused by scattering of sunlight by a sphere of radius $10\ \mu\text{m}$ with various values of n .

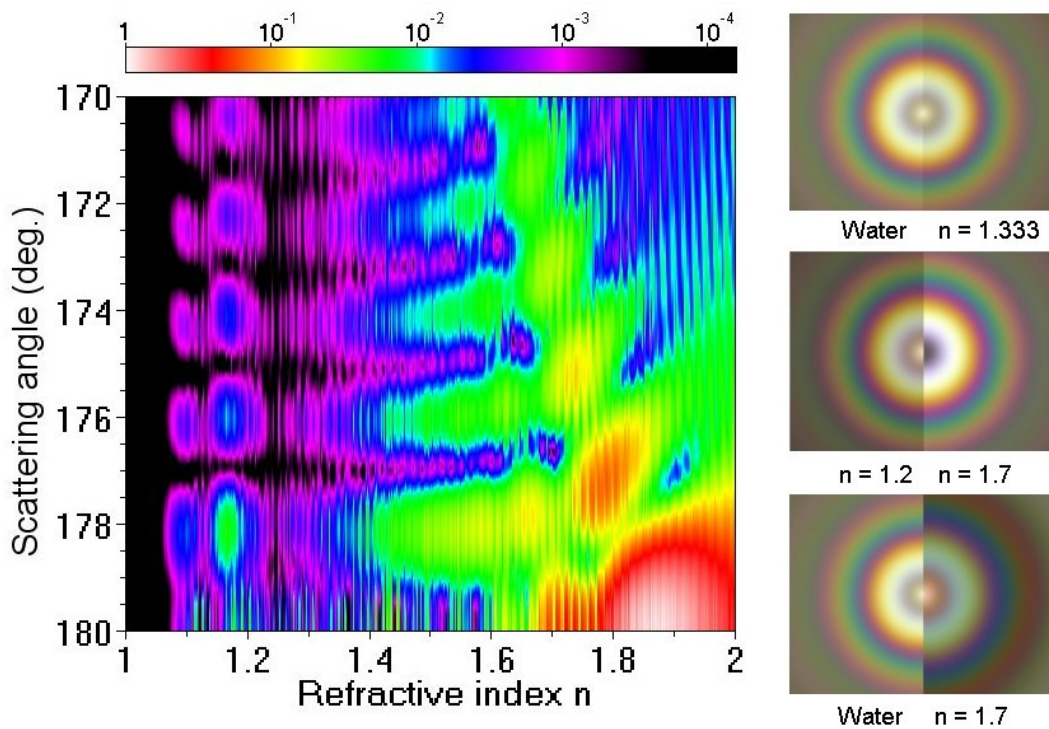


Figure 3.9.2: Left: False-colour map showing the intensity of scattering of red light (650 nm) from a sphere of radius $10\ \mu\text{m}$ as a function of refractive index n of the sphere. Right: Comparisons of the glory caused by scattering of sunlight from a sphere of radius $10\ \mu\text{m}$ for various values of n (for water, n varies between 1.3445 at 400 nm and 1.3314 at 700 nm).

References

- [1] R. L. Lee, Jr, *Mie theory, Airy theory, and the natural rainbow*, Appl. Opt., 37, 1506-1519 (1998).

- [2] S. D. Gedzelman, *Simulating glories and cloudbows in color*, Appl. Opt., 42, 429-435 (2003)
- [3] P. Laven, *Simulation of Rainbows, Coronas, and Glories by use of Mie Theory* Appl. Opt., 42, 436-445 (2003)
- [4] P. Laven, *Atmospheric glories: simulations and observations*, Appl. Opt., 44, 5667-5674 (2005).
- [5] H. C. van de Hulst, *A theory of the anti-coronae*, J. Opt. Soc. Am. 37, 16-22 (1947).
- [6] P. Laven, *How are glories formed?*, Appl. Opt. 44, 5675-5683 (2005).
- [7] P. Laven, *Effects of refractive index on glories*, submitted to Appl. Opt. (2008).

3.10 Harry Bateman, Gustav Mie and Maxwell's equations

Martin, P. A.¹

¹Department of Mathematical and Computer Sciences, Colorado School of Mines, Golden, CO 80401-1887, USA

Bateman (1882–1946) was an English mathematician who emigrated to the USA in 1910. His first book (1915) contains a detailed discussion on scattering of a plane electromagnetic wave by a penetrable sphere, with several citations of Mie's famous paper. Bateman was interested in this particular problem because it can be solved exactly. More generally, he was interested in finding exact solutions of Maxwell's equations mainly because of his development of elaborate electron theories. Nowadays, Bateman is perhaps best known for the Bateman Manuscript Project (which produced five red books on special functions and integral transforms after his death). In fact, Bateman was a mathematician with a very broad range of interests, including partial differential equations, integral equations and fluid dynamics.

The talk will describe some of Bateman's life and work, with emphasis on his contributions to the mathematics of waves.

3.11 What can Lorenz–Mie theory do for optical tweezers?

Nieminen, T. A.¹, Stilgoe, A. B.¹, Hu, Y.^{1,2}, Knöner, G.¹, Heckenberg, N. R.¹, Rubinsztein-Dunlop, H.¹

¹Centre for Biophotonics and Laser Science, School of Physical Sciences, The University of Queensland, Brisbane QLD 4072, Australia, ²Department of Bioengineering, Rice University, PO Box 1892, MS-142, Houston TX 77251-1892, USA

Optical tweezers [1], in which a laser beam focussed by a high numerical aperture microscope objective is used to trap or manipulate microscopic particles, provide an interesting physical system to which Lorenz–Mie theory can be applied. Notably, the most commonly trapped particles are spherical, on the order of the wavelength or a few wavelengths in size, and they are typically trapped away from surfaces, and apart from the complication of the , classic Lorenz–Mie theory is directly applicable.

The forces that are responsible for the trapping of particles in optical tweezers arise from the exchange of momentum between the trapping beam and the particle within the trap as it scatters the beam. Therefore, Lorenz–Mie theory provides a method for the calculation of the optical forces within the trap [2].

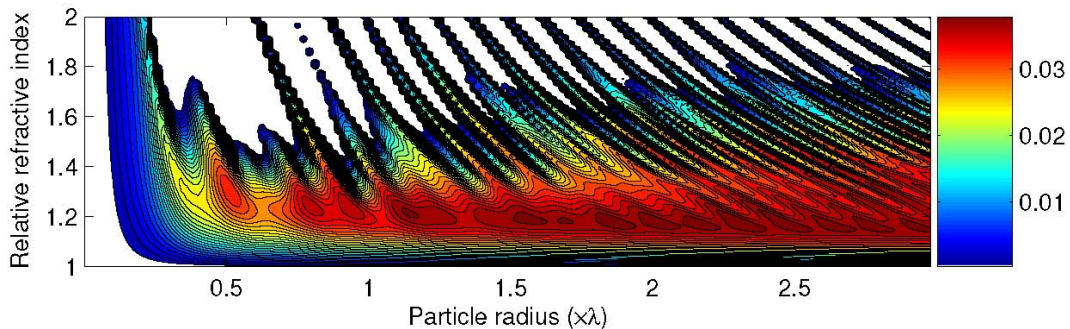


Figure 3.11.1: Trapping landscape

Major applications of optical tweezers include the non-contact trapping and manipulation of micro-organisms, including bacteria, eukaryote cells, and the measurement of piconewton-scale forces in microscopic systems, which are typical of many of the forces seen in biological systems. Both types of applications can benefit from computational modelling of the performance of optical tweezers. Firstly, knowledge of the performance of one’s optical trap can allow the design to be optimised, such as minimising the laser power used, reducing the likelihood of damage to or optication of live biological specimens. Secondly, we can consider what types of particles are best for trapping for particular applications [2], or even design special particle for better trapping [3]. Figure 1 is a “trapping landscape”, showing the variation of trap strength with particle size

and refractive index, and illustrates the type of information that can be found. One striking feature is the prediction of trapping for high refractive index particles of specific sizes (the “fingers” in the upper region of the figure), which is related to the resonances seen in Mie scattering.

However, it is quantitative application where computational modelling is likely to be of most benefit. For example, it can allow better understanding of errors affecting force measurements made by optical tweezers through the investigation of the effects of the variation of probe particle size. Furthermore, the ability to calculate forces opens new possibilities for quantitative applications, such as the measurement of the refractive index of microparticles, even if only a single particle is available, or they are highly polydisperse [4].

References

- [1] A. Ashkin, J. M. Dziedzic, J. E. Bjorkholm, S. Chu, ”Observation of a single-beam gradient force optical trap for dielectric particles,” *Opt. Lett.* 11, 288-290 (1986).
- [2] T. A. Nieminen, V. L. Y. Loke, A. B. Stilgoe, G. Knöner, A. M. Brańczyk, N. R. Heckenberg, H. Rubinsztein-Dunlop, ”Optical tweezers computational toolbox,” *J. Opt. A* 9, S196-S203 (2007).
- [3] Y. Hu, T. A. Nieminen, N. R. Heckenberg, H. Rubinsztein-Dunlop, ”Antireflection coating for improved optical trapping,” *J. Appl. Phys.* 103, 093119 (2008).
- [4] G. Knöner, S. Parkin, T. A. Nieminen, N. R. Heckenberg, H. Rubinsztein-Dunlop, ”Measurement of the index of refraction of single microparticles,” *Phys. Rev. Lett.* 97, 157402 (2006).

3.12 Optical trapping of microsized spheres in aberrated Hermite-Gauss fields

Saija R.¹, Denti P.¹, Borghese F.¹, Maragò O.², Iatì M. A.²

¹Dip. Fisica della Materia e Ingegneria Elettronica,

Università di Messina, Salita Sperone 31, 98166 Messina, Italy

²Istituto per i Processi Chimico-Fisici del CNR, Salita Sperone, 98158 Faro Superiore, Messina, Italy

The transition matrix approach proved to be effective in describing the forces and torques exerted by a focalized laser beam on nonspherical particles [1,2]. This approach has been used to calculate the trapping of microsized latex spheres in aberrated Hermite-Gauss fields with a twofold aim. On one hand we validate our result by comparison with some theoretical calculations on the trapping of spheres in radially-polarized beams [3,4], on

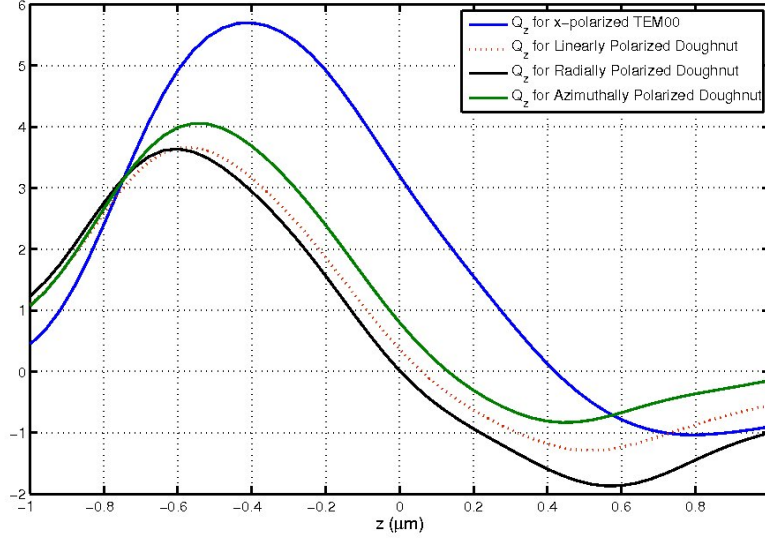


Figure 3.12.1: $Q_z(0, 0, z)$ for a homogeneous sphere of latex with radius $1.0 \mu\text{m}$

the other hand we give theoretical support to the experimental work that is in progress in Messina on the trapping and manipulation of nanostructures. In fact, our results, when the calculations refer to non-aberrated fields, coincide with those reported by Nieminen et al. [3].

The optical system we deal with has $\text{NA}=1.3$ and the exit pupil is immersed in oil ($n = 1.6$). The trapping particle is embedded in water ($n = 1.33$) and oil and water are separated by a cover slip orthogonal to the optical axis and located at $z = -20 \mu\text{m}$ with respect to the nominal focus of the lens, which was chosen as origin of the coordinates. The profile of the laser beam was chosen to be a pure gaussian profile TEM_{00} linearly polarized along the x axis, or a combination of Hermite-Gauss profiles HG_{01} and HG_{10} that give a radially polarized or an azimuthally polarized doughnut shaped field. Of course, due to the aberration, the maximum field intensity does not occur at the focus but at $z \approx -4.0 \mu\text{m}$. In Fig. 3.12.1 we report the trapping efficiency along the z axis for a homogeneous sphere of latex ($n = 1.59$) of radius $1.0 \mu\text{m}$. Note that the z axis zero is shifted just by $z = -4.0 \mu\text{m}$. As a preliminary comment, we notice that trapping sphere is larger than the trapping spot, so that any approximation turns out to be non applicable. This is the probable cause of the discrepancy between the results of Nieminen et al [3] and those of Kawauchi et al. [4].

References

- [1] F. Borghese, P. Denti, R. Saia, M. A. Iatì, O. M. Maragò, “Radiation torque and force on optically trapped linear nanostructures,” *Phys. Rev. Lett.* 100, 163903 (2008).

- [2] F. Borghese, P. Denti, R. Saija, M. A. Iatì, “Optical trapping of nonspherical particles in the T -matrix formalism,” *Opt. Express* 15, 11984–1998 (2007).
- [3] H. Kawauchi, K. Yonezawa, Y. Kozawa, S. Sato, “Calculatios of optical trapping forces on a dielectric sphere in the ray optics regime produced by a radially polarizad laser beam,” *Optics Lett.* 32, 1839–1841 (2007)
- [4] T. A. Nieminen, N. R. Heckenberg, H. Rubinztein-Dunlop, “Forces in optical tweezers with radially and azimuthally polarized trapping beams,” *Optics Lett.* 33, 122–124 (2008).

3.13 Optical Resonances, Mie-Theory and beyond

Schweiger, G.¹

¹Ruhr-Universität Bochum, Bochum, Germany

Mie theory, also called Lorenz-Mie theory or Lorenz-Mie-Debye theory, is a complete analytical solution of Maxwell’s equation for the scattering of electromagnetic radiation by spherical particles. Mathematically, the electromagnetic field inside and outside of the particle is represented by a series of functions that are special solutions of the Maxwell equations. The technique of representing the electromagnetic field by a series of special functions, each representing a special wave solution of the Maxwell equations was highly refined especially in the last two decades. With these methods very powerful techniques are available today to solve nearly any scattering problem of electromagnetic radiation. However, the physics behind this powerful mathematical tool is not obvious. In contrast to this exact theory approximate theories have been developed that are much closer to human intuition and reveal the physics behind the various phenomena. Geometrical optics is one of these theories and we will demonstrate how this theory can be used to describe the phenomenon of optical resonances also known as morphology dependent resonances (MDR) or whispering gallery modes nearly as precisely as the exact theory but with much better insight to the underlying physics. In the framework of geometrical optics the existence of narrow and broad resonances as well as the appearance of resonances of various mode numbers and orders becomes obvious. The resonance condition can be formulated in a simple way. The physical reason why the index of refraction or the size and shape of the resonator affects the resonances becomes clear. Recently, an increasing number of investigations was and is made to understand in detail the optical properties of micro resonators and their interaction with the surroundings, especially with light guiding structures. We will give some examples of the use of micro resonators as sensor.

4 Contributed Talks

4.1 Speeding up mesh-based nanooptics calculations

Alegret, J.¹, Martín-Moreno, L.¹

¹Departamento de Física de la Materia Condensada, Universidad de Zaragoza, Pedro Cerbuna 12, 50009 Zaragoza, Spain

Numerical methods play an important role in studying the scattering of light by nanoparticles, as they allow the probing, albeit virtually, of certain physical quantities that would be very difficult or downright impossible to obtain by experiments. For instance, one can obtain the electric field inside a metallic nanoparticle, and relate this quantity to the far-field scattering, which can be measured experimentally. Mesh-based methods, like the discrete-dipole approximation (DDA) [1] or the Green's tensor (GT) formalism [2,3], are suitable numerical algorithms to obtain the response of nanoparticles to an incoming electric field, such as a plane wave or a laser beam. These methods work by discretising the particles into small pieces, called mesh elements, and self-consistently calculating the electric field inside these elements, under the assumption that the field is constant inside each individual mesh element.

DDA and GT both yield, in general, good accuracy when compared to experiments. Additionally, they can be extended to consider layered backgrounds [4,5], which are suitable, for instance, to perform calculations of particles on a substrate or on a film. However, this type of calculations can be time-consuming if the number of mesh elements is large, and/or there are several layers in the calculation.

In this work, we present an overview of several methods that can be utilised to speed up mesh-based calculations. In particular, we review the top-down extended meshing algorithm (TEMA) [6], which is a simple but powerful method to create non-homogeneous meshes optimised for nanooptics calculations. Typical gains in speed with this algorithm are of a factor of 4, compared to a regular mesh with all elements of the same size. We also look at the Fourier transform method, which however is only valid for homogeneous backgrounds, and enumerate the symmetries of the equations that can be used to speed up the calculations in a layered background. Finally, we present a comparison of the times and precisions achieved with the different methods.

References

- [1] B. T. Draine. The discrete-dipole approximation and its applications to interstellar graphite grains. *Astrophys. J.*, 333:848, 1988.
- [2] O. J. F. Martin, A. Dereux, and C. Girard. Iterative scheme for computing exactly the total field propagating in dielectric structures of arbitrary shape. *J. Opt. Soc. Am. A*, 11:1073, 1994.
- [3] O. J. F. Martin and N. B. Piller. Electromagnetic scattering in polarizable backgrounds. *Phys. Rev. E*, 58:3909, 1998.
- [4] M. Paulus, P. Gay-Balmaz, and O. J. F. Martin. Accurate and efficient computation of the Green's tensor for stratified media. *Phys. Rev. E*, 62:5797, 2000.
- [5] M. Paulus and O. J. F. Martin. Light propagation and scattering in stratified media: a Green's tensor approach. *J. Opt. Soc. Am. A*, 18:854, 2001.
- [6] J. Alegret, P. Johansson, and M. Käll. Top-down extended meshing algorithm and its applications to green's tensor nano-optics calculations. *Phys. Rev. E*, 75:046702, 2007.

4.2 Particle characterization by pulse induced Mie scattering and time resolved analysis of scattered light

H. Bech¹, A. Leder¹

¹Universität Rostock, Lehrstuhl Strömungsmechanik, Albert-Einstein-Str. 2, 18059 Rostock, Germany

The use of laser pulses as source of light for Mie-scattering offers new possibilities for particle characterization since the pulse width is small enough compared with characteristic distances of spatial propagation (10 fs corresponds to 3 μm in vacuum). If the path of light through the particle is known, then the particle diameter results from the temporal intervals between the detected orders of scattered light. Fig. 4.2.1 shows the path of scattered light for reflection and refraction of second order as it's known from geometrical optics. The spatial propagation of the pulse induced scattered light of reflection and second order refraction is shown in Fig. 4.2.2.

Far from the particle, that means earlier in time, appears the order of reflection and near the particle is to find the second order of refraction because of the longer optical path through the particle. From Fig. 4.2.2 it is evident, that the temporal distance between the detection of these two scattering orders can be used for particle sizing. For

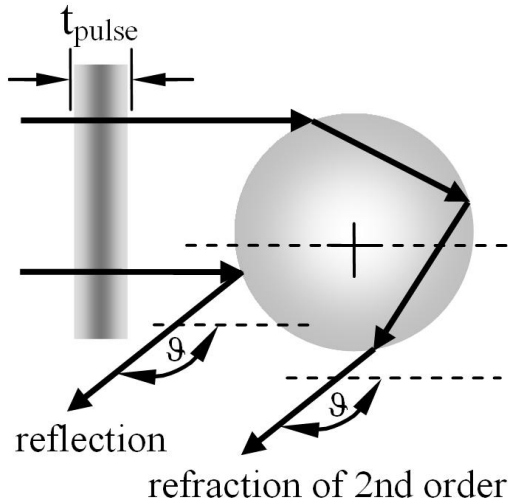


Figure 4.2.1: Simplified ray path for detection in the back scattering region

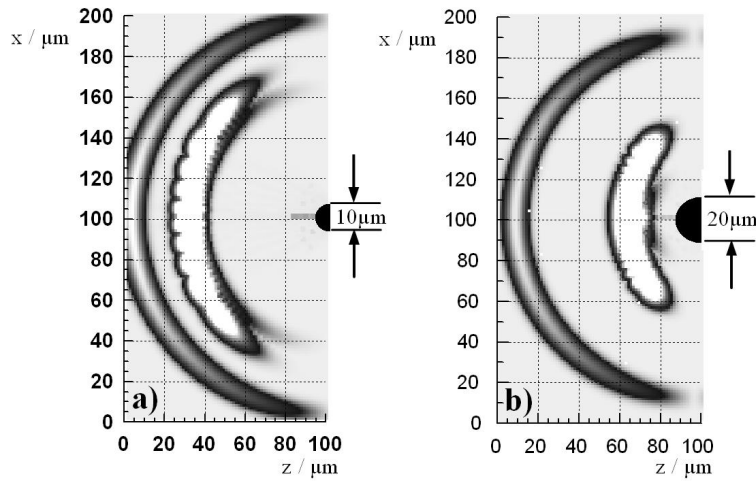


Figure 4.2.2: Pulse induced scattered light of reflection and second order of refraction, a) $d_p = 10\mu\text{m}$, spreading time $t_s = 300\text{fs}$ b) $d_p = 20\mu\text{m}$, $t_s = 250\text{fs}$

study of the temporal behaviour of a single scattering order it is useful to decompose the total Mie scattered light by application of Debye-series. The result is presented in Fig. 4.2.3. The second order of refraction splits into two different pulses. This is the consequence of the fact that different optical paths produce specific contributions simultaneously for this order of refraction (rainbow, surface waves) [1]. For particle sizing it is necessary to determine the temporal distance between the scattered light signals of reflection and second order of refraction. Dependent on the particle size the time difference between both signals can arise to a delay in order of picoseconds, (see Fig. 4.2.3 a, b).

Fig. 4.2.4 shows the temporal behaviour of the total Mie-scattered light for a small particle compared with Fig. 4.2.3. This case was calculated by using an algorithm for

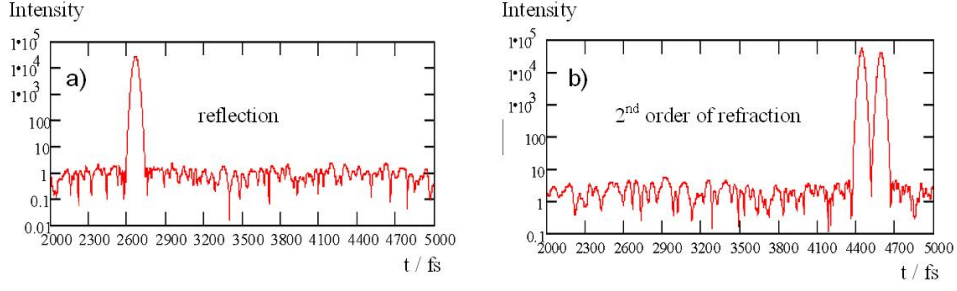


Figure 4.2.3: Temporal behaviour of pulse induced scattered light, $\vartheta = 180^\circ$, $m = 1.33$, $d_p = 200\mu\text{m}$, a) reflection, b) second order of refraction

multiple scattering by spheres (Generalized Multiparticle Mie solution, GMM) [2].

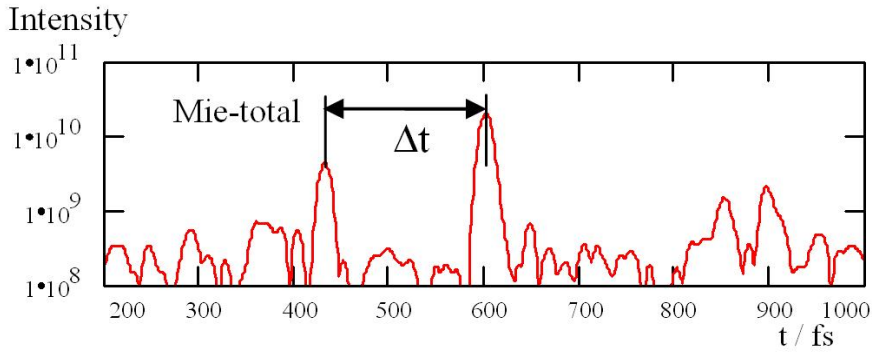


Figure 4.2.4: Temporal behaviour of the total Mie-scattered light detected in the back scattering region, $\vartheta = 150^\circ$, $d_p = 20\mu\text{m}$, $m = 1.330$

As a result the temporal difference between reflection and refraction amounts to $\Delta t = 173$ fs. Equation (4.2.1) for calculation of particle diameter d_p from the temporal delay Δt follows from geometrical optics. ϑ_{R1} means the scattering angle of first order of refraction corresponding to the scattering angle ϑ_{R2} of the second refraction order.

$$d_p = \frac{0.3\Delta t}{\sqrt{1 + m^2 - 2 \cdot m \cdot \cos(\vartheta_{R1}/2) + \sin(\vartheta_{R2}/2) + m \cdot \sin((\vartheta_{R2} - \vartheta_{R1})/2)}} \quad (4.2.1)$$

References

- [1] H. Bech, A. Leder, Particle sizing by time resolved Mie calculations - a numerical study. *Optik-International Journal for Light and Electron Optics* 117 (2006) 40-47
- [2] Yu-Lin Xu, Electromagnetic scattering by an aggregate of spheres, *Applied Optics*, Vol. 34, No. 21 (1995), 4573-4588

4.3 Field distribution of plasmons on Ag nanospheres in a dielectric matrix

S. Benghorieb¹, R. Saoudi¹, A. V. Tishchenko¹, F. Hobar²

¹Universitaire Jean Monnet, Laboratoire Hubert Curien, 18 rue Benoît Lauras, 42000 Saint-Etienne, France, ²Laboratoire Microsystèmes et Instrumentation, Université de Constantine, route d'Ail El Bey, Constantine 25000 Algérie

Abstract

We present a new method which extracts the field of the plasmon on a spherical metallic nanoparticle in a dielectric matrix. The Mie theory is applied to deliver this field in the case of a single nanosphere in visible range. We study also, the influence of perturbation by a spherical layer (shell) on the spectral position of the plasmon resonance.

1 Introduction

The interaction of light with spherical metallic particle reveals a particular behavior, consisting in a significant localized near-field at the surface of the particle. This is due to a collective electron oscillation at the surface of metal excited by the light in particularly resonant conditions. Many numerical methods are developed to modeling this effect [1]. The classical approaches look for a whole near-field, while our approach, based on Mie formulation, can extract the resonant part of the field and attribute it to the plasmon field.

2 Extraction of the plasmon field

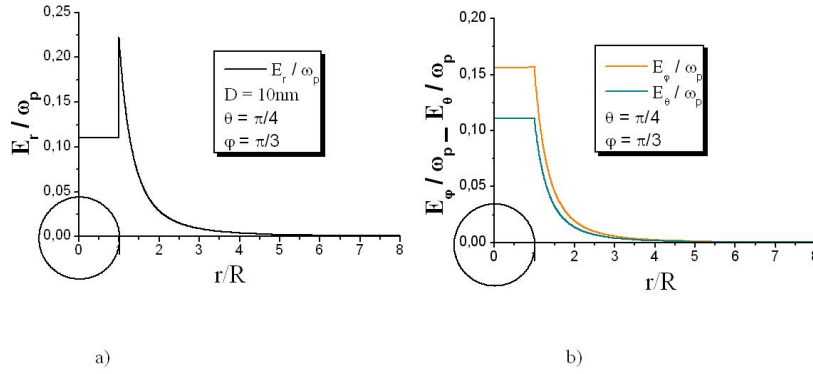


Figure 4.3.1: a) Radial, b) polar component of the plasmon field of an Ag nanosphere of diameter $D = 10\text{nm}$.

Mie theory is applied to filter the plasmon field. The field near the sphere is expressed as a sum of a regular and a singular term [2]:

$$\mathbf{E}(\mathbf{r}, \omega) = \frac{\mathbf{E}_p(\mathbf{r})}{\omega - \omega_p} + \sum_{n=0}^{\infty} \mathbf{E}_n(\mathbf{r}) (\omega - \omega_p)^n \quad (4.3.1)$$

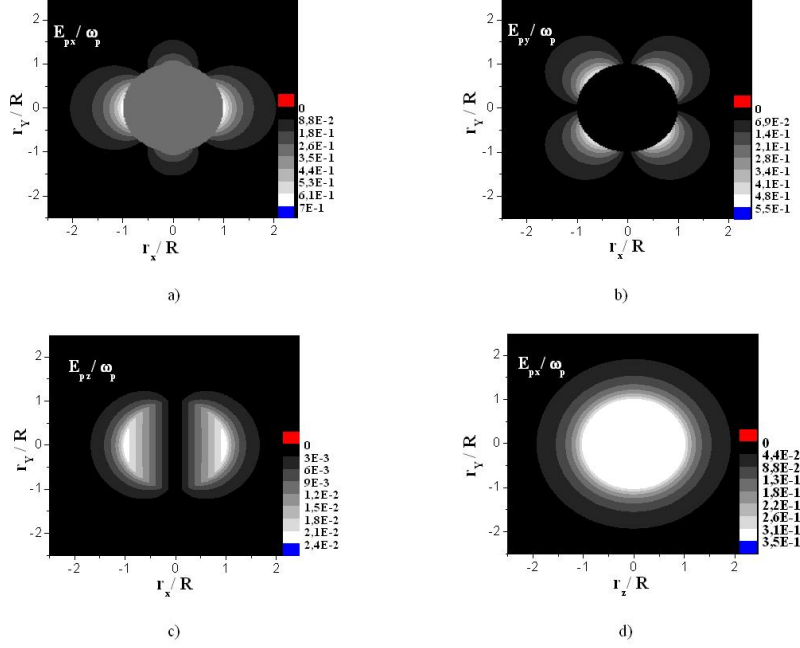


Figure 4.3.2: Distribution of the plasmon field of a silver nanosphere ($D = 20nm$) in glass. a) E_{xp} , b) E_{yy} , c) E_{zp} in the xy plane, d) E_{xp} in the yz plane

The regular term represents all spherical harmonics around the sphere, the singular term is the plasmon field related with the pole in the complex field expression. To extract the plasmon frequency ω_p , we use the special numerical technique developed earlier in [2]. The plasmon field $\mathbf{E}_p(\mathbf{r})$ is then found by the Laurent series extension to the resonance frequency ω_p .

2.1 Plasmon field in the spherical coordinate system

In this section, we show our preliminary numerical results for Ag nanospheres of diameter $D = 10nm$ in the glass matrix. The axis orientation is $\theta = \pi/4$ and $\varphi = \pi/3$. We represent three components of field in spherical coordinates E_r, E_θ, E_φ . All the field values of the singular part are normalized on resonance frequency ω_p . The distribution of the plasmon field is illustrated in Fig. 4.3.1. The radial component exhibits a homogenous enhancement interior the sphere this is predicted for small particles by the Maxwell-Garnett theory. At the interface silver/glass this field component is a discontinuous. The radial field decreases exponentially with distance r normalized by particle radius R , Fig. 4.3.1a. The exterior radial field decreases fast, this confirms that the plasmon field exists and is localized in the vicinity of the surface of the sphere. We observed similar field enhancement for the polar components Fig. 4.3.1b, with a constant value of the interior field. At the interface this field component has a maximum then decreases fast, it ceases at distance r greater then $2R$.

2.2 Plasmon field in the Cartesian coordinate system

The plasmon field is invariant to the incident and transmitted waves. This can be confirmed by simulation in the Cartesian coordinates. Fig. 4.3.1 illustrates the plasmon

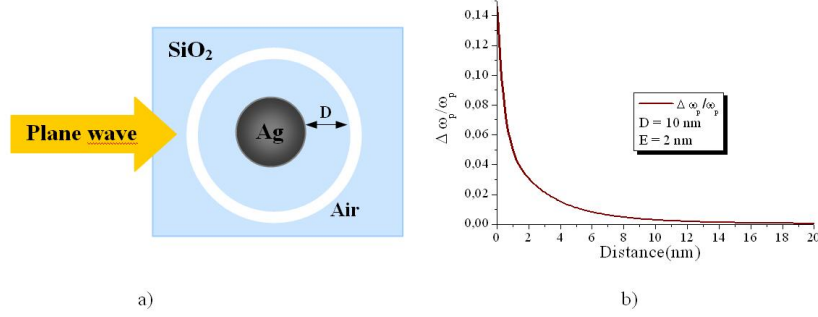


Figure 4.3.3: a) Nanoshell system, b) Depending of plasmon's position on a distance between Ag nanosphere with diameter fixed at $D = 10nm$ and air layer with a thickness $E = 2nm$.

field distribution in the xy plane for a silver nanosphere ($D = 20nm$). For E_{px} and E_{py} we observe a homogeneous behavior of the field in the interior of the sphere. In the exterior, the strong field exists at the surface of particle, then it is attenuated along the spherical interface. The energy is confined at the surface and the plasmon field decreases exponentially with distance from the interface. Such behavior is already observed in the previous section. In addition, the electric field distribution predicts zero values at four points. That can be explained by interference of two counter-propagated plasmons. They turn around the particle surface in two opposite directions and interfere to generate this field picture. On the contrary, field E_{pz} is practically zero, but numerical resolution shows (Fig. 4.3.1c) that there is a field with a low amplitude, this is caused by the effect of particle size. When the observation plane yz coincides with the polarization E_{px} (Fig. 4.3.1d), a strong field exhibits a homogeneous behavior in the interior of the particle. The plasmon field decreases exponentially in the exterior.

3 Nanoshell application

We consider an Ag nanosphere suspended in a homogenous isotropic glass matrix. Assume the existence of a spherical air shell at distance D from the Ag sphere. Fig. 4.3.3a illustrates this structure. We study the dependence of plasmon's resonance frequency versus this distance. The thickness of the shell which perturbs the plasmon field is $2nm$. We observed that the change of the resonance frequency is decreasing exponentially with D . This means that the plasmon field "sees" the refractive index variation only near the particle interface which confirms the small plasmon size.

4 Conclusion

The possibility of extracting the plasmon field by Mie theory opens perspectives for the investigation of this important property of a metallic nanosphere. The numerical results show that this field is localized around the metal/dielectric interface, it is independent from all other fields near this interface.

References

- [1] J.-W. Liaw, Simulation of surface plasmon resonance of metallic nanoparticles by the boundary-element method, *J. Opt. Soc. Am.*, v. 23, 108-116 (2006)
- [2] A.V. Tishchenko, M. Hamdoun, O. Parriaux, Two-dimensional coupled mode equation for grating waveguide excitation by a focused beam, *Opt. Quantum Electron.*, v. 35, 475-491 (2003)

4.4 Nanoplasmonics and an extension of the Lorentz-Mie theory by the method of additional boundary conditions

Datsuyk, V.V.¹

¹Kyiv National Taras Shevchenko University, Ukraine

In the past decades, metallo-optics and its branch nanoplasmonics have discovered new effects and originated new nanotechnologies. The most prominent among them are the effects of surface-enhanced Raman scattering, metal-enhanced fluorescence, non-diffraction-limited transport of light through metal nanostructures and pinholes, the technologies of scanning near-field optical microscopy, single-molecule spectroscopy, and nano-patterning. To model the engaged optical processes, the local density of states (LDOS) of electromagnetic field has to be calculated. It appears that the common Lorentz-Mie theory fails to determine the LDOS outside a metallic sphere. Space dispersion of the permittivity, or, in other words, nonlocality of the dielectric function, must be taken into account. This effect can be allowed for with the method of additional boundary conditions. The presented nonlocal theory predicts efficient excitation of the supplementary surface plasmon-polariton modes in a metal nanosphere. As a consequence, particular TM modes of low orders give rise to additional resonances in the spectral dependence of LDOS. The calculations show that the LDOS on the surface of a silver sphere of a radius of 10 nm placed in air can be enlarged in the UV region of spectrum up to five orders of magnitude. The peak amplitude is found to decrease by a power law if the distance from the center of the sphere increases.

4.5 Light Transport in Random Media with Internal Resonances

Frank, R.¹, Lubatsch, A.¹, Kroha, J.¹

¹Physikalisches Institut, Universität Bonn, Nußallee 12, 53115 Bonn, Germany

We present a systematical theory for the interplay of strong localization effects and absorption or gain of classical waves in 3-dimensional, disordered dielectrics, which is based on a selfconsistent resummation of self-interference (Cooperon) contributions. In the presence of absorption or gain, Anderson localized modes do not exist in a strict sense. However, in the case of linear gain (i.e. exponential intensity growth), causality in connection with the Cooperon pole structure predicts the appearance of a new finite length scale, which we interpret as the coherence length of a random laser mode. A characteristic dependence of this coherence length on the gain intensity is found, consistent with experiments.

4.6 Mie scattering and topological charge

Valeria Garbin¹, Giovanni Volpe², Enrico Ferrari³, Michel Versluis¹, Dan Cojoc³ and Dmitri Petrov^{2,4}

¹Physics of Fluids - University of Twente (The Netherlands), ²ICFO - Institut de Ciències Fòniques (Spain), ³CNR-INFN, Laboratorio Nazionale TASC (Italy), ⁴ICREA - Institutio Catalana de Recerca i Estudis Avancats (Spain)

Optical beams with a helical phase front, such as Laguerre-Gaussian (LG) beams, attract significant interest in many areas of optics and physics [1]. However, it was not until recently that the Mie scattering of LG beams by spherical particles has been first investigated theoretically [2]. Here we study this problem both numerically and experimentally.

We study the scattering from dielectric spheres (shown in the figure) and from metallic spheres (not shown) by varying both the modulus and the sign of the topological charge. In particular, we address the question whether the Mie scattering would enable to distinguish the sign and the modulus of the phase dislocation.

In the experiment a LG beam with various topological charges is generated by converting a 1064 nm linearly polarized Gaussian beam using diffractive optical elements (DOEs) implemented on a spatial light modulator (SLM). A microparticle attached to the coverslip of the sample is scanned through the focus of the beam with nanometer precision using a piezo stage. The forward-scattered light is collected by a second objective and transferred by a relay lens onto a quadrant photodiode (QPD) for recording

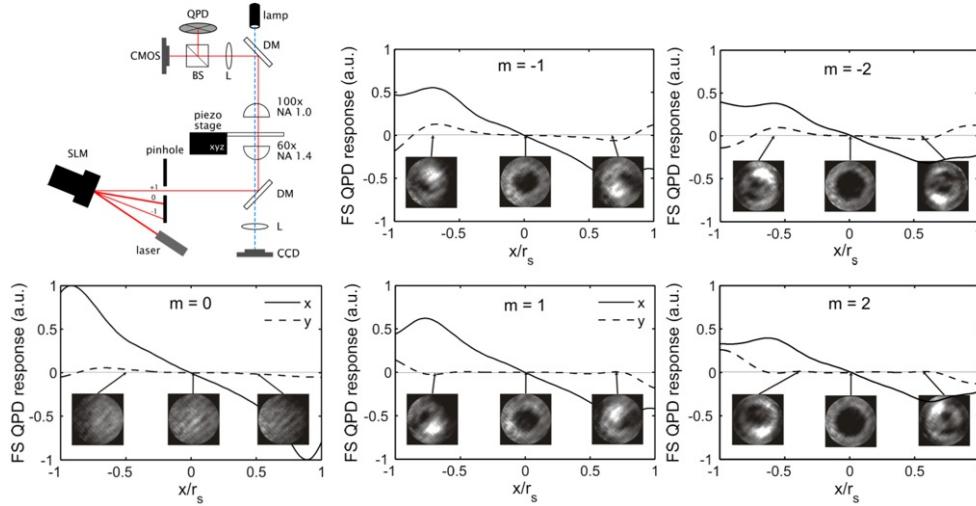


Figure 4.6.1: Experimental setup and experimental results for a dielectric sphere (radius $r_s = 2.4 \mu\text{m}$). Response of the QPD in the direction of the particle movement (x -signal, solid line) and in the direction perpendicular to the particle movement (y -signal, dashed line). Both the effect of the modulus and the sign of the charge are shown.

the x - and y -position signals.

Our approach to the calculation of the scattering from an arbitrary focussed beam on a spherical particle of arbitrary radius and refractive index is described in Ref. [3]. The numerical results (not shown) are in agreement with the experimental results.

Our numerical and experimental results verify that the sign of the topological charge can be discriminated by the Mie scattering both for dielectric and metallic particles. We anticipate that our observations have potential applications to the many fields for which Mie scattering and beams with orbital angular momentum are of relevance, and in particular for optical trapping and photonic force microscopy.

Acknowledgement

We would like to acknowledge useful discussions with Gregory Kozyreff.

References

- [1] L. Allen, S. M. Barnett, and M. Padgett. Optical angular momentum. (IoP Publishing, 2003).
- [2] A. S. van de Nes and P. Török, "Rigorous analysis of spheres in Gauss-Laguerre beam," Opt. Express 15, 13360-13374 (2007).
- [3] G. Volpe, G. Kozyreff, and D. Petrov, "Backscattering position detection for photonic force microscopy," J. Appl. Phys. 102, 084701 (2007).

4.7 Particle sizing from the measurement of the effective refractive index of colloids

García-Valenzuela, A.¹, Barrera, R.G.², Sánchez-Pérez, C.¹, Gutiérrez-Reyes, E.²

¹Centro de Ciencias Aplicadas y Desarrollo Tecnológico, Universidad Nacional Autónoma de México, Apartado Postal 70-186, Distrito Federal 04510, México., ²Instituto de Física, Universidad Nacional Autónoma de México, Apartado Postal 20-364, Distrito Federal 01000, México.

The optical properties of colloids have been a challenging area of research for many years providing also important applications. A colloid is a random system of particles embedded in a homogeneous matrix material. The appearance of a colloid can be turbid when the size of the particles composing the system is not very small compared to the wavelength. Since long ago some researchers have assigned an effective refractive index to turbid colloids [1]. This effective refractive index has been recognized to depend on the scattering properties of the particles, and not only on their refractive index. Recently, we showed experimentally that from this effective refractive index one may infer the size of the colloidal particles and their refractive index [2]. However, the existence of a diffuse field in a colloid, which manifests itself as turbidity, has been a source of confusion when referring to its effective optical parameters such as its effective refractive index. The concept of an effective refractive index of turbid colloids has actually remained rather vague. To develop a theory for the effective optical parameters of colloids one must first distinguish the presence of two types of fields: the coherent beam and the diffuse field. Then one must recognize that the effective optical parameters should be associated only the coherent beam, which is actually defined as an average field, where the average is usually a configurational one taken over all possible random locations of the colloidal particles. Thus, when one refers to the refractive index of a turbid colloid one actually refers to the effective refractive index that describes the optical behavior of the coherent beam. Very recently we have established formally the nature of the electromagnetic response of the effective medium associated to the coherent beam in a colloid, and it turned out that its effective electric permittivity and its effective magnetic permeability are actually non-local [3]. The length of non-locality is the diameter of the particles. This means that there is spatial dispersion thus the effective electric and magnetic response functions depend not only on the frequency but also on the wave vector of the propagating electromagnetic wave. The non-local effective-medium approach for the electromagnetic response of a dilute colloid was developed in detail in Ref. [3]. In this reference it was also shown that from the nonlocal dispersion relation for the transverse mode one is able to obtain an effective refractive that depends only on the frequency and the particle's parameters. When an effective index of refraction derived from the dispersion relation of a system with a non-local response is naively used as an effective refractive index in continuum electrodynamics, mistakes and misinterpretations might

definitely occur. For instance, if one tries to measure the effective index of refraction of a colloidal system by measuring the reflectance in the usual internal-reflection set up, and then uses Fresnel's relations to determine it, inconsistencies might be found [4,5]. However, in this work we show that with proper precautions one can use the effective refractive index of colloids in Snell's law in its generalized form for complex refractive indices in the same way as one would deal with a usual local medium with a complex refractive index. In this way one avoids the disputed use of Fresnel's reflection and transmission coefficients with an effective refractive index. We consider refraction in and out of the colloidal medium, as well as actual propagation of a refracted beam through the system.

In this work we provide firm theoretical grounds for the measurement and interpretation of the effective refractive index of dilute colloids. Then we show that from the measurement of the effective refractive index and the volume fraction occupied by the particles it is possible to derive the size and refractive index of small dielectric particles forming the colloid. We provide guidelines to the limits on the size and refractive index of the particles for which the method works well and has a unique solution. We also provide estimates of the sensitivity of the method and sources of error and discuss actual experiments performed recently in our laboratory with latex and glass colloidal particles.

References

- [1] M. Mohammadi, Colloidal refractometry: meaning and measurement of refractive index for dispersions; the science that time forgot, *Adv. Colloid & Interf. Sci.* **62**, 17 (1995).
- [2] A. Reyes Coronado, A. García-Valenzuela, C. Sánchez-Pérez, R. G. Barrera , Measurement of the effective refractive index of a turbid colloidal suspension using light refraction, *New Journal of Physics* **7**, 89 (2005).
- [3] R. G. Barrera, A. Reyes-Coronado, A. García-Valenzuela, "Nonlocal nature of the electrodynamic response of colloidal systems, *Physical Review B* **75**, 184202, 1-19 (2007).
- [4] G. H. Meeten and A. N. North, Refractive index measurement of absorbing and turbid fluids by reflection near the critical angle, *Meas. Sci. Technol.* **6**, 214 (1995).
- [5] A. García-Valenzuela, R. G. Barrera, C. Sánchez-Pérez, A. Reyes Coronado, E. R. Méndez , Coherent reflection of light from a turbid suspension of particles in an internal-reflection configuration: Theory versus experiment, *Optics Express* **13** (18), 6723-6737 (2005).

4.8 Efficiency of frequency-pulsed excitation of a micron-sized spherical microcavity by chirped ultrashort laser radiation

Geints, Yu.E.¹, Apeksimov, D.V.¹, Zemlyanov, A.A.¹

¹Institute of Atmospheric Optics, Siberian Branch of the Russian Academy of Sciences, Akademicheskii Avenue, 1, Tomsk, Russia

Excitation of internal optical field resonance in transparent spherical microparticle (microcavity) illuminated by a train of ultrashort laser pulses is simulated numerically. Our results show that the optimal tuning of incident radiation to a specific high-Q electromagnetic resonant mode (MDR) of the particle can be achieved by varying the time interval between pulses in a train together with linear frequency modulation of every pulse (chirping). Efficiency of MDR excitation by chirped laser pulse train can be highly increased as compared to plane-wave excitation.

4.9 Interstellar Extinction curve from Mie, TMatrix and DDA models

Gupta, R.¹, Vaidya, D.B.²

¹IUCAA, Post Bag 4, Ganeshkhind, Pune-411007, India &

²Ex-Gujrat College, Ahmedabad-380006, India

Conventionally, Mie theory has been used extensively for studying the light scattering of dust and in particular case of explaining the interstellar extinction [1,2]. We have used alternative methods based on Effective Medium Approximation (EMA), T-Matrix and Discrete Dipole Approximation (DDA) for modeling the observed interstellar extinction curve [3].

The need for the alternative models arises due to the fact that the dust grains are not homogeneous solid spheres as is assumed in the Mie theory. The real dust in interstellar context is highly porous, non-spherical and a mixture of various composite materials like silicates, graphites, PAHs etc. This is further supported by the fact that collected samples of dust particles from stratosphere and comet flyby missions are found to be highly porous, fluffy and non-spherical aggregates of a mixture of different materials.

In this paper we have used composite dust grain model [4] which is able to explain the interstellar extinction curve quite well. In this model we have used the DDA method and the dust grains consist of silicate dipoles with embedded graphite dipoles and also vacuum sites for porosity. This model also explains the interstellar polarization curve (Serkowski's Law, [5]) which essentially requires the dust grains to be of spheroidal shape. Finally, our composite porous model requires less amount of carbon and thus satisfies

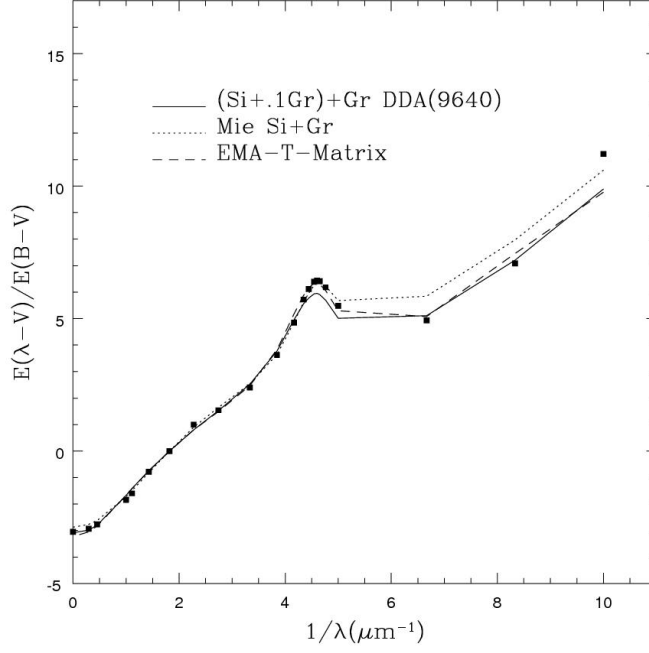


Figure 4.9.1: Fitting of observed interstellar extinction curve (solid square dots) with three models.

the carbon abundance constraint of the Interstellar medium (ISM) to closer values as compared to the other models which assume solid grains.

Figure 1.1 shows the fitting of the observed interstellar extinction curve with composite DDA; Mie and EMA-T-Matrix models.

Acknowledgement

The authors thank the grant from the ISRO-RESPOND project No. ISRO/RES/2/345/2007-08 under which this work has been carried out.

References

- [1] Mie, S., Ann. Phys., 1908, 25, 377
- [2] Mathis J.S., Rumpl W., Nordsieck K.H., 1977, ApJ, 217, 425
- [3] Whittet D.C.B., 2003, in Dust in the Galactic Environments, 2nd edn. IoP Publishing, Bristol, UK.
- [4] Vaidya D.B., Gupta R., Snow T.P., 2007, MNRAS, 379, 791
- [5] Serkowski K., Mathewson D.S. and Ford V.L., 1975, ApJ, 196, 261

4.10 Gustav Mie - From Electromagnetic Scattering to a General Theory of Matter

W. Hergert¹

¹Institute of Physics, Martin Luther University Halle-Wittenberg, Von-Seckendorff-Platz 1, 06120 Halle, Germany

Gustav Mie (1868-1957) studied in his hometown Rostock and in Heidelberg. Stations of his academic career were Karlsruhe, Greifswald, Halle and Freiburg. Hundert years ago his famous article *Contributions to the optics of turbid media, especially of colloid metal solutions* [1] was published. Although this work is cited in the specialized literature very often [2], Mie himself did not consider this as his most important achievement. Far more important he estimates his textbook *Lehrbuch der Elektrizität und des Magnetismus. Eine Experimentalphysik des Weltäthers für Physiker, Chemiker und Elektrotechniker*. [3] He said about himself:

So much I can judge about myself, it has become my occupation, to establish the connection between theoretical and experimental physics, which just at that time stood in danger to separate more and more. I believe, that my most important achievement has been the writing of a textbook on electricity in which above all I point out, that Maxwell's differential equations appearing so abstract to a further standing person, nevertheless, are nothing else than the shortest and the most exact formulation of the experimentally found laws, by which electric and magnetic fields with each other are tied together. [4]

The different history of reception of Gustav Mie's main contributions to theoretical physics is interesting. While his work to scattering theory in the first years is hardly perceived, he was a participant in the debate with Hilbert and Einstein about the basics of the theory of general relativity. The work *Bases of a theory of Matter* [5] played a significant role in this discussion. It was written to found an electromagnetic view of the world, but it became soon outdated due to the stormily developing quantum theory. In literature on the development of the theory of general relativity Mie's contribution is discussed in detail (see, e.g. [6]) but it plays no role anymore in actual research. In contrast, the article about light scattering [1] won due to the extension of its field of application during the last decades increasingly in interest.[2]

The life of Gustav Mie will be discussed in this contribution more in detail on the bases of archive material of the university archives in Greifswald, Halle and Freiburg. The estate of Gustav Mie being in the Freiburg university archive is especially significant for this study.[7] The backgrounds of the offers of a chair at Greifswald, Halle and Freiburg are discussed. From the correspondence of Gustav Mie with colleagues conclusions can be drawn on his position among the theoretical physicists at the time. It also lights up the work and interconnections of the scientific community between 1900 and 1930.

Acknowledgement

The assistance of the archives of Ernst Moritz Arndt University Greifswald, Martin Luther University Halle-Wittenberg and Albert Ludwigs University Freiburg and of the German Academy of Sciences Leopoldina is gratefully acknowledged.

References

- [1] G. Mie, *Beiträge zur Optik trüber Medien, speziell kolloidaler Metallösungen*, Annalen der Physik, **25**,377-445 (1908).
- [2] W.Marx, *Dornröschen und Mauerblümchen, Nachzügler und vergessene Arbeiten in der Physik*, Physik in Unserer Zeit, No. 1, 34-39 (2007)
- [3] G. Mie, *Lehrbuch der Elektrizität und des Magnetismus. Eine Experimentalphysik des Weltäthers für Physiker, Chemiker und Elektrotechniker*, Verlag von Ferdinand Enke, Stuttgart, 1, Auflage, 1910.
- [4] G. Mie, *Aus meinem Leben*, Zeitenwende, **19**, 733-743 (1948).
- [5] G. Mie, *Grundlagen einer Theorie der Materie*, Annalen der Physik, **37**, 511 (1912); **39**, 1 (1912); **40**, 1 (1913).
- [6] L. Corry, *David Hilbert and the Axiomatization of Physics (1898-1918)*, Kluwer Academic Publishers, Dordrecht/Boston/London, 2004.
- [7] Universitätsarchiv der Albert-Ludwigs-Universität Freiburg, Bestände E012, E14, C136

4.11 UV radiation inside interstellar grain aggregates. Implications for interstellar photochemistry and formation of prebiotic molecules.

Iatì, M. A.¹, Cacciola, A.², Cecchi-Pestellini, C.³, Saija, R.², Denti, P.², Borghese, F.²

¹CNR-Istituto per i Processi Chimico-Fisici, Salita Sperone, 98158 Faro Superiore, Messina, Italy

²Dip. di Fisica della Materia e Ingegneria Elettronica, Università di Messina, Salita Sperone 31, 98166 Messina, Italy

³INAF-Osservatorio Astronomico di Cagliari, Strada n.54, Loc. Poggio dei Pini, 09012 Capoterra (CA), Italy

A number of methods have been developed to calculate the optical properties of irregularly shaped particles such as the Discrete Dipole Approximation [1] and the Transition Matrix method [2]. Internal field effects have been, in general, ignored. However, there

are instances, such as e.g. the computation of the internal heating, in which it is necessary to know the electromagnetic field within the particle. The knowledge of internal fields and their polarization patterns may also have relevant implications in space chemistry.

Dust grains are generally porous and fluffy with much of their internal volume being vacuum. The internal volume may be partly filled with ices as a result of ice percolation and aggregation of smaller-sized grains. Duley (2000) noted that these environments offer the possibility of a peculiar, terrestrial type, chemistry induced by cosmic rays and/or high energy radiation [3]. As a consequence, a range of molecular species much wider than the ordinary gas-phase and surface chemistry in molecular clouds, e.g. complex organic molecules, is expected. Here we propose a scenario in which amino acids and sugars formed in the cavities of interstellar aggregates are exposed to asymmetric photolysis induced by an effective ultraviolet circularly polarized light (UVCPL) generated *in situ*.

We consider two kinds of cavities: interstitial cavities that form because of the aggregation process and cavities that may exist within the aggregating particles. We show that the incoming linearly polarized radiation depolarizes (becomes elliptically polarized) in an aggregate cavity giving rise to CPL. We use the transition matrix method to calculate exactly the field and its polarization inside the cavities of the aggregate [4,5]. An asymmetry in the sphere-cavities configuration is necessary for the depolarization effect to occur: only asymmetry can beget asymmetry[6]. In the interstitial material and in the cavities of the aggregate the direction of propagation of the field changes from point to point. Consequently, the state of polarization of the field cannot be described by the usual Stokes parameters but it needs a more general description [7].

Grain aggregates provide the perfect environment where interstellar molecules can evolve into complex organic species. The photolysis induced by the UVCPL inside the cavities drives an enantiomeric selection of the molecules during the formation process. At the same time, grain coagulation in the disk increases the size of the aggregates, thus producing an efficient shield against further destructive interaction with UV radiation. The final step of these molecules into biopolymers is dependent on their delivery to planets offering favourable conditions for life to become possible.

References

- [1] E. M. Purcell, C. R. Pennipacker, "Scattering and absorption of light by nonspherical dielectric grains," *Astrophys. J.* 186, 705-714 (1973).
- [2] P. C. Waterman, "Symmetry, unitarity, and geometry in electromagnetic scattering," *Phys. Rev. D* 3, 825-839(1971).
- [3] W. W. Duley, "Chemistry in grain aggregates: a source of complex molecules?," *Mon. Not. R. Astron. Soc.* 319, 791-796 (2000).
- [4] C. Cecchi-Pestellini, R. Saija, M. A. Iatì, A. Giusto, F. Borghese, P. Denti, S. Aiello,

- “Ultraviolet radiation inside interstellar grain aggregates. I. The density of radiation,” *Astrophys. J.* 624, 223-231 (2005)
- [5] R. Saija, C. Cecchi-Pestellini, Iatì, A. Giusto, F. Borghese, P. Denti, S. Aiello, “Ultraviolet radiation inside interstellar grain aggregates. II. Field depolarization,” *Astrophys. J.* 633, 953-966 (2005)
- [6] F. R. Japp, “Stereochemistry and vitalism,” *Nature* 58, 452-460 (1898)
- [7] T. Carozzi, R. Karlsson, J. Bergman, “Parameters characterizing electromagnetic wave polarization,” *Phys. Rev.E* 61, 2024-2028 (2000)

4.12 Novel interferometric laser imaging for spray and micobubble sizing – one of the successful Mie scattering application

Kawaguchi¹, Isao Satoh¹ and Takushi Saito¹

¹Tokyo Institute of Technology
Ookayama 2-12-1 Meguro-ku, Tokyo, Japan

Experimental investigations leading to an understanding of gas-liquid or liquid-liquid two phase flow, especially as dispersed gas bubbles or liquid droplets are important to many energy-related systems such as; optimization of fuel injection and combustion in engine cylinder, effective gas dissolution by microbubbles, realtime analysis of cavitation. In order to investigate the flow fields with particles and the heat and mass exchange rate, multidimensional and time-resolved measurement techniques that provide the information on the individual dispersed particles are required.

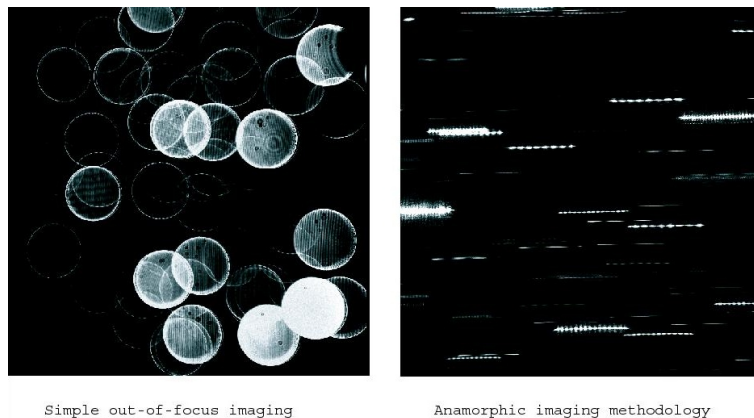


Figure 4.12.1: Comparison between conventional out-of-focus Mie scattering imaging and novel imaging technique

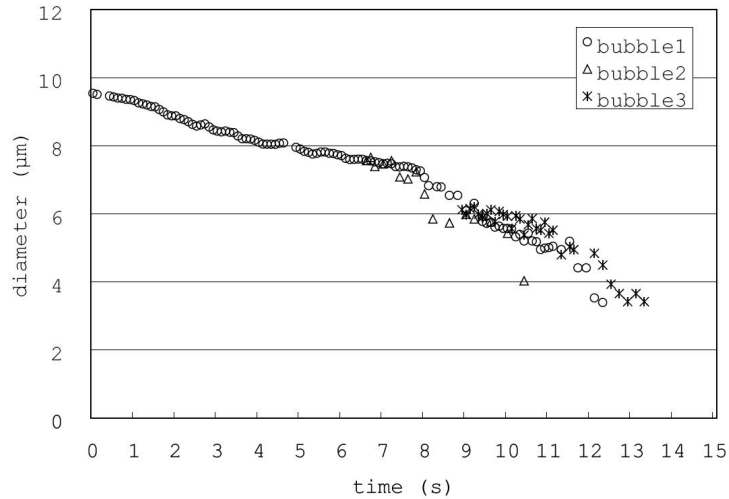


Figure 4.12.2: Size transition of dissolving O₂ bubble

For the last few decade, the imaging technique which observes the scattered light by sphere has been developed to measure the planar size distribution of transparent spheres in fluid flow[1]. The similar measurement techniques based on the out-of-focus imaging have been developed by many researchers such as ILIDS (Interferometric Laser Imaging for Droplet Sizing), IPI (Interferometric Particle Imaging), IMI (Interferometric Mie Imaging), PMSI (planar Mie scattering interferometry) and so on.

The author has developed the sophisticated optical imaging technique to increase the measurable particle concentration limits by an anamorphic optical design. An example of the captured images was shown in Figure 4.12.1. From the instantaneous image, the size of individual sphere such as droplet or bubble was obtained by the angular fringe separation or fringe count. Moreover, the velocity vectors of every sphere could be determined by the consecutive two images captured by CCD camera and pulsed laser system. Figure 4.12.2 shows the dissolution of Oxygen microbubbles measured by the technique. The experimental result demonstrated that the sizing technique which observes the Mie scattering by sphere enables to investigate the fluid dynamics, and such kind of optical technique contributes to the solution of the global issues in conjunction with the recent progress of the high-speed imaging devices as well as the high repetition rate pulsed laser systems.

Acknowledgement

This work was supported by Grant-in-Aid for Young Scientists (A) of Japan Society for the Promotion of Science.

References

- [1] König G, Anders K, Frohn A, A new light-scattering technique to measure the diameter of periodically generated moving droplets, *J Aerosol Sci.*, 17, 157–167 (1986).
- [2] Kawaguchi T., Akasaka Y. and Maeda M., Size measurements of droplets and bubbles by advanced interferometric laser imaging technique, *Meas. Sci. Technol.*, 13, 308–316 (2002).
- [3] Maeda M., Kawaguchi T. and Hishida K., Novel Interferometric Measurement of Size and Velocity Distributions of Spherical Particles in Fluid Flows, *Meas. Sci. Technol.*, 11, L13–L18 (2000).
- [4] Maeda M., Akasaka Y. and Kawaguchi T., Improvements of the interferometric technique for simultaneous measurement of droplet size and velocity vector field and its application to a transient spray, *Exp. in Fluids*, 33, 125–134 (2002).

4.13 Optical properties of densely packed small particles

Yasuhiko Okada¹, Alexander A. Kokhanovsky²

¹Kinki University, 3-4-1 Kowakae Higashi-Osaka, Osaka, 577-8502 Japan,

²University of Bremen, Otto Hahn Allee 1, D-28234 Bremen, Germany

The study of light scattering and absorption properties of a group of particles/aggregates is an interesting and important research topic. These properties are needed in many branches of modern science and technology (e.g., light scattering by soot chains, cometary aggregates, etc).

Okada et al. (JQSRT, submitted) proposed the numerical simulation method for light scattering by a group of particles [1]. The proposed method is a modification of the T-matrix method for clusters of spheres described in [2] with the analytical orientation averaging described in [3]. The new method does not use the analytical averaging procedure, instead it is based on the numerical averaging procedure. This enables to perform calculations for larger sizes of particles and also for larger numbers of particles compared to analytical orientation averaging.

Also, usually the analytical averaging leads to the shorter computational time. However, in our case, the numerical averaging procedure is carried out with following improvements:

- faster numerical averaging using Quasi-Monte-Carlo method [4]
- simulations for different orientations of particles are carried out in parallel on different computers

Table 4.13.1: Parameters used in our simulations

<i>Symbol</i>	<i>Note (unit)</i>
λ	wavelength of incident light (nm)
ρ	packing density of a group of particles (%)
r_p	radius of each particle (nm)
$m(= n + ik)$	complex refractive index
$C_{abs}(N)$	absorption cross sections of a group of N particles (nm ²)

With this method, we have investigated the influence of densities on optical properties of a group of particles for an increased number of particles ($N=600$). In our simulations, 1000 orientations are considered in the numerical orientation averaging. This is sufficiently large number for the calculation of scattering and absorption cross sections [4].

Table shows parameters of our numerical simulations. In our simulations, wavelength of incident light λ is fixed and equal to 550 nm.

The results of calculations of the absorption enhancement factor $k = C_{abs}(N)/N/C_{abs}(1)$ for groups of particles with various densities and various particle radii are shown in Figure. For smaller densities, the value of k is close to 1.0, which just a confirmation of the fact that the influence of multiple scattering and close-packed media effects is negligible in this case. The value increases for increased densities, which demonstrates how the close-packed media and multiple scattering influence becomes important.

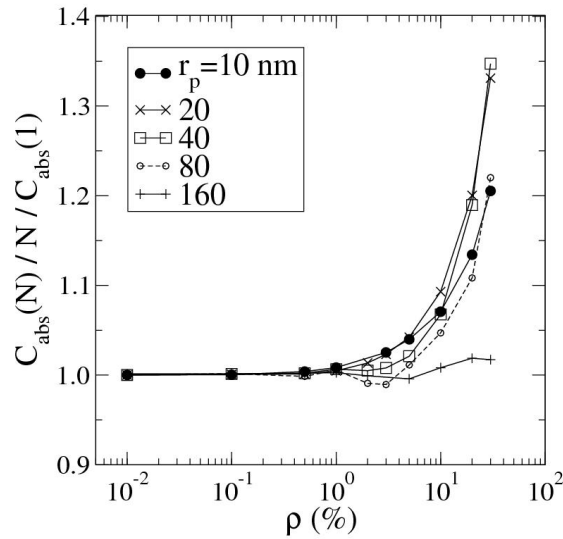


Figure 4.13.1: $C_{abs}(N)/N/C_{abs}(1)$ for groups of particles with different densities and different particle radii. $m=1.60+10^{-5}i$, $\lambda=500$ nm and $N=600$

References

- [1] Y. Okada, I. Mann, T. Mukai, M. Koehler, J.Q.S.R.T. (submitted).
- [2] D.W. Mackowski and M.I. Mishchenko, J. Opt. Soc. Am. A, 2266 (1996).
- [3] M.I. Mishchenko, J.Opt.Soc.Am.A, 8(6), 871 (1991).
- [4] Y. Okada, J.Q.S.R.T., doi:10.1016/j.jqsrt.2008.01.002.

4.14 Gas Density Measurements via Rayleigh Scattering

Rausch, A.¹, Doll, U.¹, Roehle, I.¹

¹Engine Acoustics Department, Institute of Propulsion Technology, DLR German Aerospace Center, Mueller-Breslau-Strasse 8, 10623 Berlin ,Germany

Gas density is an important parameter in turbomachinery diagnostics and simulation, especially in the development of combustion chambers and nozzels of aircraft engines. For example it provides information about the origin of noise and the formation of destructive feed-back-loops in combustion chambers.

Generally density measurements of gases are based on the ideal gas law, meaning that temperature and pressure in the investigated volume have to be measured. Thus sensors have to be installed in the measurement volume. Often the application of mechanical sensors is hinderd because the parameters of flow are disturbed by the sensor heads and in combustion chambers and in nozzels the environment is too harsh for most sensor types. Thus noninvasiv ruggedly designed measurement setups are needed for combustion diagnostics.

Measuring the intensity of light scattered by gas molecules enables the direct and non-invasiv investigation of gas density. Using a laser to generate an intense light beam or sheet to illuminate the investigation volume the gas density in a defined region can be determined via measuring the scattered light intensity [1,2]. Since Rayleigh Scattering is elastic, reflections from walls and windows and Mie Scattering from parasitic big particles like dust or soot trouble the measurement. Spectral narrow notch filters can be used to reduce these parasitic intensities. Thus Rayleigh Scattering Measurements can also be used in difficult measurement situations [3].

Measurements of density fluctuations of a pulsating flame and their comparison to thermocouple measurements and OH-chemiluminescence data will be presented. Furthermore the influence of several filters, especially the separation efficiency between Rayleigh and Mie scattering of spectral notch filters, will be shown.

Acknowledgement

The authors would like to thank the German Helmholtz Association for the financial support of the project.

References

- [1] Robert W. Dibble, M. B. L. "Investigation of differential diffusion in turbulent jet flows using planar laser Rayleigh scattering" *Combustion and Flame*, 2005, 143, 644-649 .
- [2] P. R. Medwell, P. Kalt B. B. Dally "Simultaneous imaging of OH, formaldehyde, and temperature of turbulent nonpremixed jet flames in a heated and diluted coflow" *Combustion and Flame*, 2007, 148, 48-61.
- [3] R. B. Miles, W. R. Lempert, J. N. Forkey, "Laser Rayleigh scattering" *Measurement Science and Technology*, 2001, 12, R33-R51.

4.15 Use of the Mie-theory in optical aerosol spectrometers with digital single signal evaluation of scattered light impulses

M. Schmidt¹, L. Mölter¹

¹Palas® GmbH, Greschbachstraße 3b, 76229 Karlsruhe, mail@palas.de, www.palas.de

Optical Aerosol Spectrometers (OAS) are used with large success for the particle size and particle quantity determination, e.g. for the characterisation of test aerosols, outside air aerosols, as well as for the fractional efficiency determination of separators.

OAS are detecting the size and concentration of particles with help of the scattered light analysis. Basically these instruments consist of a light source and a scattered light detector. Whenever a particle passes the light beam a scattered light impulse is measured.

To evaluate the particle concentration, the number of these signals in a certain time and under defined conditions is measured. The particle size can be determined from the intensity of the scattered light signal. The relation between the scattered light intensity and the particle size is given by the Mie-theory for a spherical single particle.

To prove the good function of the instrument and the relation between the particle size and the intensity signal OAS need to be calibrated with regard to the concentration as well as with regard to the detected particle size.

For sure the technical design of OAS is different for different types. The so called device parameters describe the quality of the measurement device in several technical standards. Looking at the Mie-theory OAS using white light in combination with a 90° scattered light angle offer the special advantage of a defined calibration curve, the basis for a high resolution in the detection of particle size.

The Mie-theory as well as the counting method with OAS is based on the detection of a single particle. If more than one particle is in the measuring zone at the same time the

so called coincidence error occurs. More than one signal is measured at the same time and as a result the particle size is measured too large and the concentration is measured too small.

Due the digital single signal analysis according to Dr. Umhauer and Dr. Sachweh one can now measure with an OAS in substantially higher concentrations up to larger 10^6 P/cm³ practically without coincidence error.

The function of the digital signal analysis, the coincidence correction and the effect on the particle size and particle quantity determination will be likewise described in this paper.

4.16 Mie Scattering for Particle Size Analysis: Expanded Size Ranges by Extreme Precision Calculations

Stübinger, Th.¹, Köhler, U.¹, Witt, W.¹

¹Sympatec GmbH, System-Partikel-Technik,
Am Pulverhaus 1, D-38678 Clausthal-Zellerfeld, Germany

Exactly 100 years after the invention of the fundamental theory of light scattering by homogeneous and isotropic spherical particles by the German physicist Gustav Mie (1868 - 1957) in 1908 [1] Mie scattering theory has still growing interest in the field of particle characterisation, especially in particle size analysis. In contrast to Fraunhofer Diffraction, which is a powerful and parameter free standard method used for evaluation in particle size analysis for a wide range of opaque materials and non-spherical particles, Mie Scattering theory is necessary for the evaluation of particle sizes especially in the submicron particle size range including different polarisation effects. Also for larger particle sizes, however, more optical parameters are needed for evaluation including optical effects resulting from reflecting or transparent spherical particles. Hence, Mie Scattering is complementary to Fraunhofer Diffraction, expanding particle size range to smaller particle sizes and enhancing the overall material portfolio in all size ranges. Significant changes in physical values can be explained dependent on the particle size including the relative refractive index of particles and the surrounding medium. Especially calculations of the Extinction Efficiency or of the Volume Concentration of particles are affected and lead to interesting results, e.g. related to material consumption.

There exist some important works describing theory and formulas of Mie scattering theory [2,3], but only a few of them deal with problems of precision and stability needs for calculation and the challenges to circumvent these problems when implementing calculation algorithms [3,4]. Mie Scattering calculations, however, were limited by the calculation accuracy in the past. In the range of coarse particles instability problems are significant, resulting from large numbers of series terms in the calculation. Furthermore,

calculation time and accuracy were limited by former computer systems. Today, more powerful computers allow for extreme precision calculation tools, and enable to expand the particle size range covered by Mie scattering calculations from submicron materials up to particles in the millimetre range.

We describe in this paper an extended precision calculation of Mie scattering theory for use in particle size analysis in order to extend the particle size range. By using precision digits of several hundreds and applied convergence criterions for the Mie expansion coefficients it was possible to create a Mie validation data set for different Mie parameter sets (see example in Table 4.16.1), which could be used for internal optimisation of calculation algorithms and therefore for accuracy checks of Mie light scattering calculations. Our Mie scattering calculations are based and verified on this precision analysis expanding the existing particle size ranges from submicron to millimetre particles including transparent spherical or reflecting materials.

Table 4.16.1: Mie scattering results using extended precision calculation for a given Mie parameter set (Q_{ext}, Q_{sca} : Extinction and Scattering Efficiency, i_s, i_p : relative intensity of scattered light with polarisation perpendicular (i_s) and parallel (i_p)).

<i>Mie parameter:</i>	1.0, <i>refractive index:</i> 1.50 - $i \cdot 0.10$, <i>scattering angle:</i> 85°
$Q_{ext} =$	0.4823704563469868561270187621636 ...
$Q_{sca} =$	0.208740018314837188477238385572 ...
$i_s =$	0.07815653982023038113148036344532 ...
$i_p =$	0.00172975830062537505959779732895 ...

References

- [1] G. Mie, "Beiträge zur Optik trüber Medien, speziell kolloidaler Metallösungen", *Annalen der Physik*, Vierte Folge, Band 25 (3), 377-445 (1908).
- [2] C.F. Bohren, D.R. Huffman, "Absorption and Scattering of Light by Small Particles", John Wiley & Sons, New York (1983).
- [3] W.J. Wiscombe, "Mie Scattering Calculations: Advances in Technique and Fast, Vector-Speed Computer Codes", NCAR/TN-140+STR, National Center for Atmospheric Research, Boulder, Colorado (1996).
- [4] H. Du, "Mie-scattering calculation", *Appl. Optics*, Vol. 43, Issue 9, 1951-1956 (2004).

4.17 Applying Mie Theory to determine single scattering of arbitrarily shaped precipitation particles at microwave frequencies

Teschl, F.¹, Randeu, W.L.¹

¹Department of Broadband Communications, Graz University of Technology, Austria.

Precipitation particles like raindrops, snowflakes, ice pellets, hail, graupel etc. scatter and absorb electromagnetic waves and so attenuate them. Electromagnetic scattering by precipitation particles concerns a variety of scientific and engineering disciplines. Particularly it concerns radar meteorology, remote sensing, and wireless communication. Liquid precipitation attenuates radar waves stronger than frozen precipitation because of the higher refractive index of water than that of ice. With increasing capacity requirements by radio-communication and -navigation services, associated with the need for higher frequencies (millimeter waves), knowledge about scattering and absorption by frozen precipitation particles becomes more important. In this study single scattering parameters like radar cross section, scattering cross section, absorption cross section and asymmetry factor were calculated for frozen precipitation particles applying the Discrete Dipole Approximation (DDA). The particles were modeled as hexagonal plates, columns, needles and dendrites as well as rather spherical graupel particles. The calculations were carried out over a wide range of centimeter- and millimeter-wavelengths, from 1 GHz to 200 GHz. The study results show that for arbitrarily shaped frozen precipitation particles with size parameters x smaller than 2 ($x = \text{circumference} / \text{wavelength}$), exclusively their ice volume is crucial for scattering and absorption and therefore the Mie Theory can be applied. If the size parameter however is greater than 2, the actual shape and the inner structure of the particle determines its scattering behavior and volume approximation methods should be used.

4.18 Rigorous modeling of light scattering in dielectric structures by the generalized source method

Shcherbakov, A.¹, Tishchenko, A.V.²

¹Moscow Institute of Physics and Technology, Institutsky Str. 9, 141701 Dolgoprudny, Russia ²Universitaire Jean Monnet, Laboratoire Hubert Curien, 18 rue Benoît Lauras, 42000 Saint Etienne, France

Abstract

On the base of the generalized source method we develop the new numerical technique for fast and rigorous modeling the light scattering on dielectric structures of arbitrary shape and composition. Due to the fast Fourier transform involved the proposed algorithm provides high resolution in short calculation time. This allows for modeling various complex-shaped particles/ensembles of particles. The Mie theory is used as a reference to compare numerical results.

Introduction

Whereas in the electromagnetic scattering theory of the only exact known solution is given by the Mie theory, a strong motivation exists to develop different numerical algorithms. Among other methods the most universal and often used are the discrete dipole approximation (DDA) and volume integral methods (VIE) [1]. The linear systems obtained in these approaches are usually solved by the conjugate gradient method [1]. There exist several publications [2-4] where authors apply the fast Fourier transform using special properties of the matrices under consideration. We believe that such idea is very promising and develop it in the frame of the generalized source method (GSM) [5].

Generalized source method

To describe GSM consider an electromagnetic problem with some permittivity distribution $\varepsilon(\mathbf{r})$. First we rely on a rigorous analytical solution of the related problem but concerning another distribution of dielectric permittivity $\varepsilon_b(\mathbf{r})$, that is called further a basic problem. This problem is supposed to have a complete solution, i.e., an exact solution is known for any given source distribution \mathbf{J} :

$$\mathbf{E} = \aleph_s(\mathbf{J}) \quad (4.18.1)$$

Looking for a solution to the initial problem we substitute into (4.18.1) generalized source $\mathbf{J} = -i\omega(\varepsilon - \varepsilon_b)\mathbf{E}$, which results in an implicit equation

$$\mathbf{E} = \aleph_s [(\mathbf{J}) - i\omega(\varepsilon - \varepsilon_b)\mathbf{E}] \quad (4.18.2)$$

The field solution \mathbf{E} of the latter equation is the exact solution of the initial problem. When considering the light scattering on an arbitrary shaped particle in a homogeneous medium we take the dyadic tensor Green function of the Helmholtz equation as the basic solution. With the aids of this tensor after representing the total scatterer volume by a number of sells we the operator equation (4.18.2) in the matrix form

$$E_k^\alpha = E_{0k}^\alpha + \sum_j \sum_\beta \frac{\Delta\varepsilon_j}{\varepsilon_s} \Gamma_{kj}^{\alpha\beta} E_j^\beta \quad (4.18.3)$$

where index β runs three Cartesian coordinates and index j represents different sells.

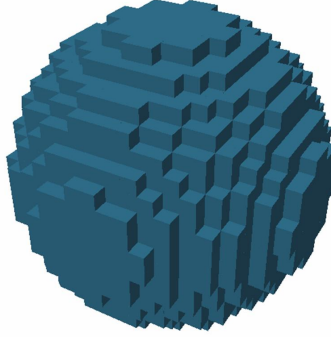


Figure 4.18.1: Sphere represented by cubic cells.

Numerical algorithm

The procedure of resolving (4.18.3) represents a nontrivial task in the source region. We propose a numerical scheme of matrix inversion that uses the Neumann series:

$$\left(I - \frac{\Delta\varepsilon}{\varepsilon_s} \Gamma\right)^{-1} = \sum_{m=0}^{\infty} \left(\frac{\Delta\varepsilon}{\varepsilon_s} \Gamma\right)^m = \sum_{m=0}^{\infty} (DC)^m I + DC + DCDC + DCDCDC + \dots \quad (4.18.4)$$

In the last equation D denotes a diagonal matrix and matrix C is a circulant. The rows of such matrix are simple cyclic permutation of the first one and its multiplication by vector is just a convolution. The convolution can be calculated by the FFT, thus, the calculation time becomes pretty linear on the matrix size. At the same time the matrix C is stored as a vector, hencefor, this approach allows to deal with very large number of sells (up to 10^6 on a personal computer) which allows for considering large variety of scatterer shapes and structure composition.

Comparison with the Mie theory

We apply our method to calculate scattering of the plane wave on a dielectric sphere to compare with the reference method - the Mie theory [6]. The sphere was embedded in a cube which was subdivided into smaller cubic sells. The dielectric permittivity of a

sell is equal to that of the sphere if it is completely in the interior and to the dielectric permittivity of the exterior medium if the sell is completely outside. When the volume of the sell contains both media the sell permittivity is found as an average value $\langle \varepsilon^\alpha \rangle$, where the best results gives power $\alpha = -0.2$. Fig. 4.18.1 shows an example of such cubic representation of a sphere by $20 \times 20 \times 20$ cells. First, we compare the far field

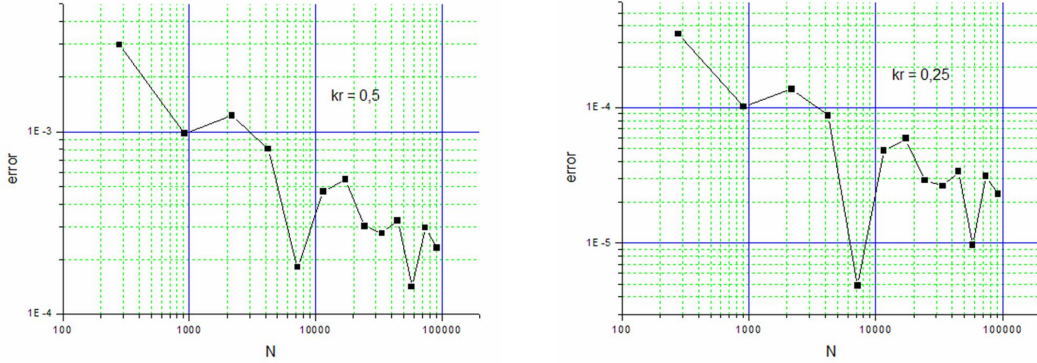


Figure 4.18.2: Absolute average error in the far field versus number of cubic cells.

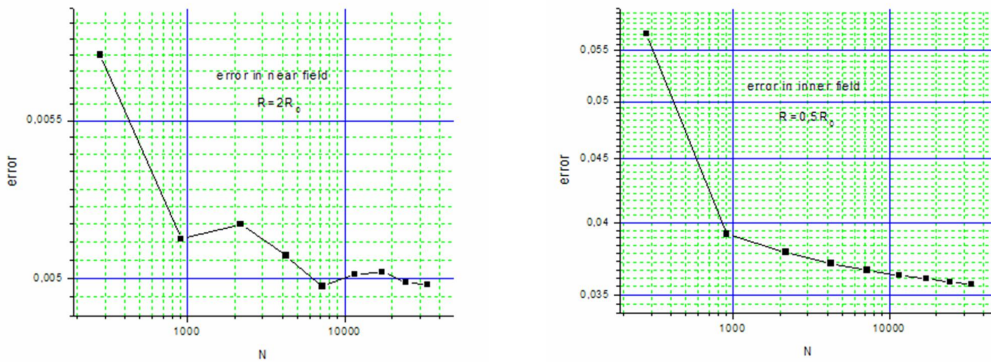


Figure 4.18.3: Absolute error in the near far field versus number of cubic cells.

calculated by two methods. Fig. 4.18.2 represents the absolute error averaged by 180 different directions and both polarisations versus the number of cells N . The normalized sphere radius k_0R is 0.25 and 0.5. This corresponds for $\lambda = 600\text{nm}$ to spheres of diameter 50 nm and 100 nm, approximately. The incident plane wave is of unit amplitude. It follows from Fig. 4.18.2 that the error decreases as $1/\sqrt{N}$.

We compare next the near field calculated by two methods. Fig. 4.18.3 represents the absolute error for point at distances $R/2$ and $2R$ from the center of the sphere versus the number of cells N . The normalized sphere radius k_0R is 0.25.

Numerical examples

We apply our method to calculate scattering of a plane wave on different dielectric structures. In the case of small contrasts $\Delta\varepsilon \propto 0.1$ and particle size of 0.1-0.5 wavelength,

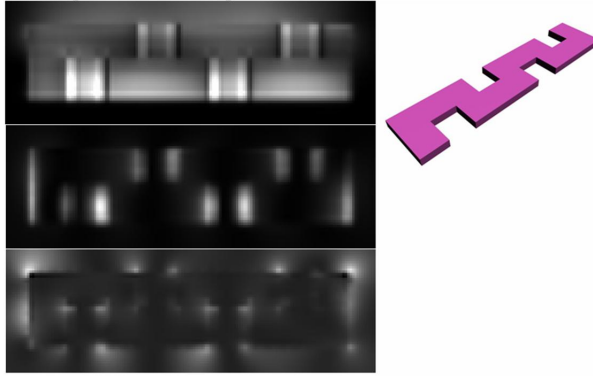


Figure 4.18.4: Near field scattering of a plane wave nm on a dielectric structure of length 450 nm and thickness 30 nm.

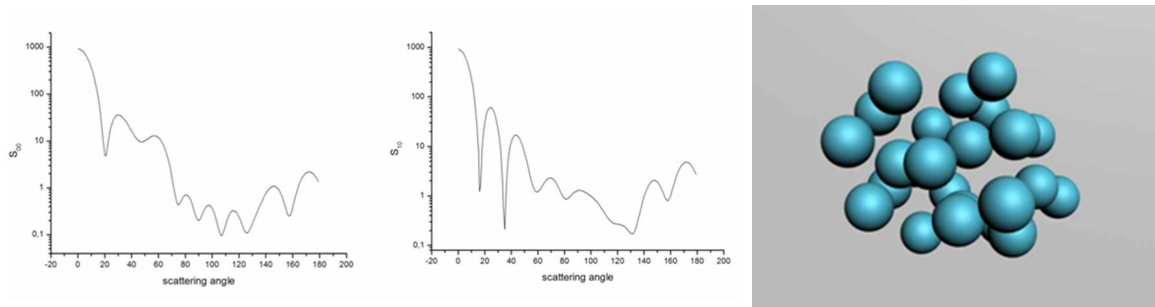


Figure 4.18.5: Far field scattering of a plane wave $\lambda = 550$ nm on an ensemble of 25 spheres of diameter 100 nm.

the length of Neuman series in calculation was about 6-20. For larger particles and contrasts this number can increase to 50-100. Fig. 4.18.4 and 4.18.5 represent two examples of the near and far field calculation.

Conclusion

Our work resulted in creating a powerful method based on GSM and FFT techniques for calculating scattering on arbitrary shaped particles. It is worth to point out however that our calculating abilities now are limited to dielectric particles which dimensions are less than several wavelengths. Such limitation arises since the Neumann series diverges under certain conditions. To avoid this one has to apply an alternative numerical algorithm to resolve the matrix equation.

References

- [1] T. Wriedt and U. Comberg, Comparison of computational scattering methods, J. Quant. Spectrosc. Radiat. Transfer, v. 60, 411 (1998)

- [2] B.T. Draine, J.J. Goodman, Application of fast-Fourier-transform techniques to the discret-dipole approximations, *Opt. Lett.*, v. 16, 1198 (1991)
- [3] B.E. Barrowes, F.L. Teixeira, J.A. Kong, Fast algorithm for matrix-vector multiply of asymmetric multilevel block-Teoplitz matrices in 3-D scattering, *Microwave and Optical Technology Letters*, v. 31, 1 (2001)
- [4] P.J. Flatau, Fast solvers for one-dimensional light scattering in the discret-dipole approximation, *Optics Express*, v.12, 3149 (2004)
- [5] A.V. Tishchenko, Generalized source method: new possibilities for waveguide and grating problems, *Opt. and Quantum Electron.*, v. 32, 971 (2000)
- [6] G. Mie, Beiträge zur Optik Trüber Medien, speziell Kolloidaler Metallösungen, *Ann. Phys.*, 25, 377-452 (1908).

4.19 Interactions of layered spheres with dipoles in direct and inverse scattering theory

Tsitsas, N. L.¹

¹School of Applied Mathematical and Physical Sciences, National Technical University of Athens, GR-15784, Athens, Greece

The scattering of a dipole generated spherical wave by a layered sphere provides interesting features, which are essentially different from those due to a plane wave. In direct scattering theory the far-field interaction of a dipole with a sphere is in general stronger than that of a plane wave. On the other hand, in inverse scattering problems the distance of the dipole from the sphere's center constitutes an additional parameter, which is encoded in the far-field pattern and is significant for the sphere's reconstruction.

Dipole excitation of a layered sphere has significant applications. The interaction between the mobile phone antenna and the human head is modelled as an exterior dipole excitation problem [1]. Besides, the interior dipole excitation has significant medical applications, such as implantations inside the human head for hyperthermia or biotelemetry purposes [2], as well as excitation of the human brain by the neurons' currents [3]. Further chemical, biological, and physical applications are discussed in [4].

In this paper we investigate the excitation of a layered sphere by a time-harmonic spherical electromagnetic wave, generated by a dipole located either in the interior or in the exterior of the sphere. The layered sphere consists of N concentric spherical layers with constant material parameters; $N-1$ layers are dielectric and the N -th layer (core) is perfect conducting, impedance or dielectric. We compute the exact Green's function by combining T-matrix [5] and Sommerfeld's methods [6]. The T-matrix method uses Mie series expansions and handles the effect of the layers, while the Sommerfeld's method handles the singularity of the dipole and unifies interior and exterior excitation. For variances of such methods see [4,7].

Moreover, we introduce the low-frequency assumption and extract from the derived exact Green's function the low-frequency far-field results for a layered sphere subject to interior and exterior dipole excitation, extending previous results on conducting spheres in [8]. The derived low-frequency results are then utilized to establish certain inverse scattering algorithms. The distance of the dipole from the sphere's center plays a significant role in the development of these algorithms. We examine three types of distinct inverse problems by utilizing the far-fields due to interior and exterior dipoles. More precisely, we determine (i) the sphere's location and the layers radii, (ii) the physical parameters of the layers, and (iii) the dipole's location.

Several numerical results will be presented, exhibiting the far-field interactions between the layered sphere and the dipole.

Acknowledgement

The author thanks sincerely Prof. C. Athanasiadis for valuable discussions.

References

- [1] M. Okoniewski, M.A. Stuchly, "A study of the handset antenna and human body interaction," *IEEE Trans. Microw. Th. Tech.* 44, 1855-1864 (1996).
- [2] J. Kim, Y. Rahmat-Samii, "Implanted Antennas Inside a Human Body: Simulations, Designs, and Characterizations," *IEEE Trans. Microw. Th. Tech.* 52, 1934-1943 (2004).
- [3] G. Dassios, A. S. Fokas, F. Kariotou, "On the non-uniqueness of the inverse magnetoencephalography problem," *Inv. Prob.* 21, L1-L5 (2005).
- [4] A. Moroz, "A recursive transfer-matrix solution for a dipole radiating inside and outside a stratified sphere," *Annals Phys.* 315, 352-418 (2005).
- [5] T. Wriedt, "A Review of Elastic Light Scattering Methods," *Part. Part. Syst. Char.* 15, 67-74 (1998).
- [6] A. Sommerfeld, *Partial Differential Equations in Physics.* (Academic Press, 1949).
- [7] N. L. Tsitsas, C. Athanasiadis, "On the scattering of spherical electromagnetic waves by a layered sphere," *Quart. J. Mech. Appl. Math.* 59, 55-74 (2006).
- [8] C. Athanasiadis, P. A. Martin, I. G. Stratis, "On the scattering of point-generated electrom. waves by a perfectly conducting sphere, and related near-field inverse problems," *Z. Ang. Math. Mech.* 83, 129-136 (2003).

4.20 The use of nano particles for patterned polarizers within the whole transparent window of soda lime glass

A. Volke¹

¹CODIXX AG, Steinfeldstr. 3 39179 Barleben/ Magdeburg, Germany

The use of nano particles in various optical applications is state of the art today. In this paper the use of non spherical nano particles in glass for a polarizer is discussed. Advantages and disadvantages of those glass filters as well as some basic applications are presented. Some methods for making polarizers with patterns in respect of polarization axis and polarization properties are introduced.

Polarizers are essential components in optical applications and, as the secrets of light are more and more disclosed, the relevance of polarizers in technical applications is growing. Consequential, the need of new and more versatile polarizers increases.

An elongated nano particle shows a strong polarization dependency. In case of many particles with parallel elongation axes, this polarization effect can be utilized. Based on a method of the Martin Luther University Halle-Wittenberg from the early 1980ies, CODIXX has brought this process of making glass polarizers with silver nano particles in soda lime glass to an industrial scale. Nowadays polarizers for the complete transparent wavelength spectrum of soda lime glass (340 nm-5 μm) based on elongated silver nano particles are commercially available.

As a specialty, CODIXX has developed a new method for making patterned polarizers. One method is based on micro lithography and lamination. Another method is based on mosaic technology and complements the lithographically made polarizers. Patterned polarizers of both technologies are successfully produced and find commercial use in various measurement applications.

4.21 Using Light Scattering for Fast Particle Sizing in Atmospheric Science: an Up-to-date White Light Optical-Particle-Counter

A. G. Wollny¹

¹ Max-Planck-Institute for Chemistry, J.-J.-Becher-Weg 27, 55128 Mainz, Germany

Particle sizing by light scattering has been used in atmospheric science for almost half a century. After large improvements in laser technology, the lower detection limit was moved far below particle diameters of 100nm. Still the problem of the non-monotonic response for particle sizes similar to the laser wavelength and above remained. In recent

years very bright broadband ('white') light emitting diodes (LEDs) have become available. These LEDs are strong enough to detect an illuminated single submicron particle by its scattered light with a photo multiplier tube (PMT). An optical particle counter using this method was deployed onboard of the NOAA WP-3D research aircraft during several field missions in the last few years. The obtained data was combined with measurements of two other particle counters using different techniques to generate a full particle size distribution on a 1Hz time base.

Introduction

Atmospheric aerosol particles have an important impact on climate and human health [1]. As pointed out in the recent IPCC report [2] our limited understanding of the aerosol effects on the radiative forcing is still the largest uncertainty in global warming predictions. Just recently the European Union has taken steps to improve air quality by introducing EU-wide limits on fine particle emissions (PM_{2.5}) for the first time ever [3]. Both topics fuel the ongoing scientific interest for the analysis of atmospheric aerosol [4] including their optical properties.

Historical background and new approaches

McMurry [5] has given an excellent review of atmospheric aerosol measurements since almost half a century; this includes a discussion of the pros and cons of using laser vs. white light for optical particle measurements based on Mie Theory. After decades of fast technique development in the field, the focus seems to be shifting to more sophisticated setups [6] to gather combined information, such as refractive index, size, shape etc., rather than 'just' measuring the optical diameter.

Instrument development

There is still the need for development of fast and compact optical particle counters especially for aircraft based measurements. Applying model simulations based on Mie Theory as previously described [7], we have build an OPC that operates with a white light LED that is temperature controlled by a thermoelectric cooler. Scattered light from a single particle traveling through the focused light is reflected by an elliptical mirror onto a PMT. The chosen design allows for a monotonic response from particles with diameter ranging from 0.5 to 8.0 μ m. The size response function was confirmed in lab experiments for particles with different refractive indices and a large number of sizes.

Application

The described instrument was operated onboard the NOAA WP-3D research aircraft during several field missions in the last years. Using a low-turbulence inlet the ambient aerosol particles are being pumped inside the aircraft and dried below 40% relative humidity before sampling. The obtained data is combined with measurements from a laser based OPC (particle diameter range from 60nm to 900nm) and a five stage

condensation particle counter (starting at a particle diameter of 5nm). A particle size concentration distribution is produced for every second for flight of up to 8 hours [8].

Acknowledgement

The author greatly appreciates the long lasting collaboration with Charles A. Brock at the Chemical Sciences Division at National Oceanic and Atmospheric Administration in Boulder, Colorado, USA; where the presented results have been obtained.

References

- [1] U. Pöschl, Atmospheric Aerosols: Composition, Transformation, Climate and Health Effects, *Angew. Chem. Int. Ed.* 44, 7520-7540, (2005).
- [2] Intergovernmental Panel on Climate Change, *Climate Change 2007 - The Physical Science Basis*, Cambridge University Press, UK and New York, US (2007).
- [3] European Union, Directive of the European Parliament and of the Council on ambient air quality and cleaner air for Europe, PE-CONS 3696/07 (2008).
- [4] K. A. Prather, C. D. Hatch, V. H. Grassian, Analysis of Atmospheric Aerosols, *Annu. Rev. Anal. Chem.* 1:16.1-16.30 (2008).
- [5] P. H. McMurry, A review of atmospheric aerosol measurements, *Atmospheric Environment*, 34, 1959-1999 (2000).
- [6] A. Nagy, W. W. Szymanski, P. Gal, A. Golczewski, A. Czitrovszky, Numerical and experimental study of the performance of the dual wavelength optical particle spectrometer (DWOPS), *Journal of Aerosol Science*, 38 (4), 467-478 (2008).
- [7] C. F. Bohren and D. R. Huffman, *Absorption and Scattering of Light by Small Particles*, New York: Wiley-Interscience Publication (1983).
- [8] C. A. Brock et al., Sources of particulate matter in the northeastern United States in summer: 2. Evolution of chemical and microphysical properties, *J. Geophys. Res.* 113, D08302, doi:10.1029/2007JD009241 (2007).

4.22 Considerations to Rayleigh's hypothesis

Wauer, J.¹, Rother, T.²

¹Institute for Meteorology, University of Leipzig, D-04103 Leipzig, ²Remote Sensing Technology Institute, German Aerospace Center, D-17235 Neustrelitz In 1907 Lord Rayleigh published a paper on the dynamic theory of gratings. In this paper he presented a rigorous approach for solving plane wave scattering on periodic surfaces. Moreover he derived explicit expressions for a perfectly conducting sinusoidal surface and for perpendicular incidence of the electromagnetic plane wave. This paper was criticised by Lippmann in 1953. He assumed that Rayleigh's approach is incomplete. Since this time there have been published several arguments, proofs, and discussions concerning the correctness and the range of validity of Rayleigh's approach not only for plane wave scattering on gratings but also for light scattering on nonspherical structures, in general. In the presentation we will discuss the different points of view on what is called "Rayleigh's hypothesis" as well as the relevance of a found theoretical limit for its validity. Furthermore we present a numerical treatment of the original scattering problem of a p-polarized plane wave perpendicularly incident on a perfectly conducting sinusoidal surface (i.e., the scalar Dirichlet problem). In doing so we emphasize the near-field solution especially within the grooves of the grating up to points on the surface, and below the surface. Two different Green's function formulations of Huygen's principle are used as starting points. One of this formulation results in the general T-matrix approach which is considered to be affected by Rayleigh's hypothesis especially for near-field calculations. The other formulation provides a conventional boundary integral equation which is in accordance with Lippmann's point of view and free of problems with Rayleigh's hypothesis. But the obtained results show that Lippmann's argumentation do not withstand a critical numerical analysis, and that the independence of least-squares approaches from Rayleigh's hypothesis, as understood and proven by Millar, seems to hold also for certain methods which do not fit into such an approach.

4.23 Optical force distribution on the surface of a spheroid

Feng Xu¹, Tropea, C.¹, Lock, J.A.², Gouesbet, G.³

¹Fachgebiet Strömungslehre und Aerodynamik, TU Darmstadt, Darmstadt, Germany, ²Dpt. of Physics, Cleveland State University, Ohio, USA, ³UMR 6614/CORIA CNRS, Université et INSA de Rouen, Saint Etienne du Rouvray, France

Radiation force induced by a laser beam has been widely utilized to trap or to manipulate the particles of micrometer and nanometer scale over the past 30 years. Various

experimental instruments, e.g. optical tweezers [1] and optical stretcher [2], have been developed to meet the requirements of non-intrusive detection and control of the micro-objects, e.g. droplets, cells, and DNA strands [3]. Regarding the theoretical aspect, the Lorenz-Mie theory has been extended to deal with the case of non-plane wave illumination and the force exerted on a sphere by a focused laser beam has been analytically predicted [4]. Such a theory, referred as generalized Lorenz-Mie theory (GLMT, [5]) has the potential to be further extended to some regularly shaped particles when the incident beam is expanded in the coordinates mirroring the geometry of these particles, as exemplified by our previous work on scattering, net force and torque prediction for a spheroid [6-8]. As a further study, here we reported our progress on force density distribution on the surface of a sphere and spheroid. Influences of non-sphericity, layer-structure, and incident beam shape on the stress profile are analyzed. The results predicted by GLMT are analyzed and verified by geometrical optics which has a more straightforward physical interpretation of the mechanical effect of light.

References

- [1] A. Ashkin, *Optical Trapping and Manipulation of Neutral Particles Using Lasers: A Reprint Volume with Commentaries*. (World Scientific, Singapore, 2006).
- [2] J. Guck, R. Ananthakrishnan, T. J. Moon, C. C. Cunningham, and J. Käs, *Phys. Rev. Lett.* **84**, 5451 (2000).
- [3] K. C. Neumann and S. M. Block, *Rev. Sci. Instr.* **75**, 2787 (2004).
- [4] G. Gouesbet, B. Maheu, and G. Gréhan, *J. Opt. Soc. Am. A* **5**, 1427 (1988).
- [5] G. Gouesbet and G. Gréhan, *Atomization Sprays* **10**, 277 (2000).
- [6] F. Xu, K. Ren, G. Gouesbet, G. Gréhan, and X. Cai, *J. Opt. Soc. Am. A* **24**, 119 (2007).
- [7] F. Xu, K. Ren, G. Gouesbet, X. Cai, and G. Gréhan, *Phys. Rev. E* **75**, 026613 (2007).
- [8] F. Xu, J. A. Lock, G. Gouesbet, and C. Tropea, *Phys. Rev. A* **77**, 149806 (2008).

5 Poster contributions

5.1 Investigation of volume scattering from size distributed MgO and TiO₂ particles using Mie theory

Ahmed, G.A.¹, Gogoi, A.¹, Choudhury, A.¹

¹Department of Physics, Tezpur University, Tezpur-784028, Assam, India

MgO and TiO₂ particles of sub-micron size were embedded in a transparent polyvinyl alcohol (PVA) matrix. The intensity of the light scattered by these particles when they were exposed to visible (632.8nm) laser radiation was monitored as a function of angle and state of polarization [1,2]. The experiments were targeted at determining a large number of the elements of the Mueller scattering matrix of these particles [3]. In these investigations size distribution of the particles were considered and verified using scanning electron microscopy (SEM). Analysis of the experimental measurements was done by comparison with theoretically generated results involving Mie theory. Monte Carlo simulation of the scattering processes was also done to validate the results. It was observed that single scattering Mie theory provided a good approximation to the experimental results within acceptable limits of error. The extent of the deviations of the experimental results from the theoretical and simulated results due to increasing non-sphericity of the particles was also investigated.

References

References

- [1] G.A.Ahmed, G.K.D.Mazumdar, A.Choudhury, Investigations by a designed and fabricated laser based air quality monitoring system, *J.Instrument Soc.India* **26**(3), 734-738 (1996).
- [2] D.Das, G.A.Ahmed, G.K.D.Mazumdar, A.Choudhury, Investigations on atmospheric humidity profile at varying oxygen levels with a laser based monitoring system, *Asian J. Phys* **10**(3), 323-335 (2001).
- [3] C.F.Bohren, D.R.Huffman, *Absorption and Scattering of Light by Small Particles* (John Wiley & Sons Inc., New York, 1983).

5.2 Optical properties of dielectric media in the presence of metallic nanoparticles

S. Benghorieb¹ , R. Saoudi¹ , A. V. Tishchenko¹, F. Hobar²

¹Universitaire Jean Monnet, Laboratoire Hubert Curien, 18 rue Benoît Lauras, 42000 Saint-Etienne, France, ²Laboratoire Microsystèmes et Instrumentation, Université de Constantine, route d'Ail El Bey, Constantine 25000 Algérie

Abstract

We have applied the Mie theory to calculate the average refractive index of a dielectric with metal spherical nanoparticles. Our approach is general and applies regardless of the particle size distribution. It allows for introducing new optical properties of dispersion, absorption and transmission as well as the changes brought on the real and imaginary parts of the refractive index. We have shown in particular the influence of the nanoparticle size on the two latter parameters.

1 Introduction

The refractive index of a material is the key parameter that affects all optical properties. The possibility of change while controlling them to scale represents an interest in a wide range of applications in photonics and optoelectronics. This is done by modifying the index, by any means, to obtain new optical properties of absorption, dispersion and transmission of the medium. This helps to build a new optical response corresponding to the created index change. We are interested in index changes produced by presence of metal particles in a dielectric because of strong effects accompanying excitation of surface plasmons. This allows manufacturing highly selective filters and mastering the colors. The existing theories dealing with the change of refractive index of a material produced by the metal particles are poorly developed and not always reliable. The theory of Mie [1] did not apply to the index calculations. The electrostatic approach of Maxwell-Garnet [2] allows such calculation but has limited to particles of small size ($\sim 10nm$). The aim of our work is to fill this void by developing the theory of Mie to make it capable of calculating the change in the average dielectric in the presence of metallic nanoparticles.

2 Numerical Results

First, we consider a single sphere of silver immersed in glass matrix of permittivity $\varepsilon_m = 2.2$, the volume concentration is 0.01%. Fig. 5.2.1 shows a real and imaginary parts of the matrix index change. Obviously, we have a similar behavior as in the Lorenz dipole model [3], in this case of an isolated silver particle the surface plasmon resonant peak is located around $\lambda = 415nm$. If the particle diameter is around $10nm$ the absorption dominates over scattering and determines the dipole extinction, which can be calculated from Δk . Fig. 5.2.2 represents the extinction, scattering, and absorption. The position of the plasmon resonance will change depending on the size particle. Fig. 5.2.3 shows a comparison of real Δn and imaginary Δk parts of modified complex refractive index for spheres of different diameters $D = 10 - 30nm$. The resonance peak tends towards blue.

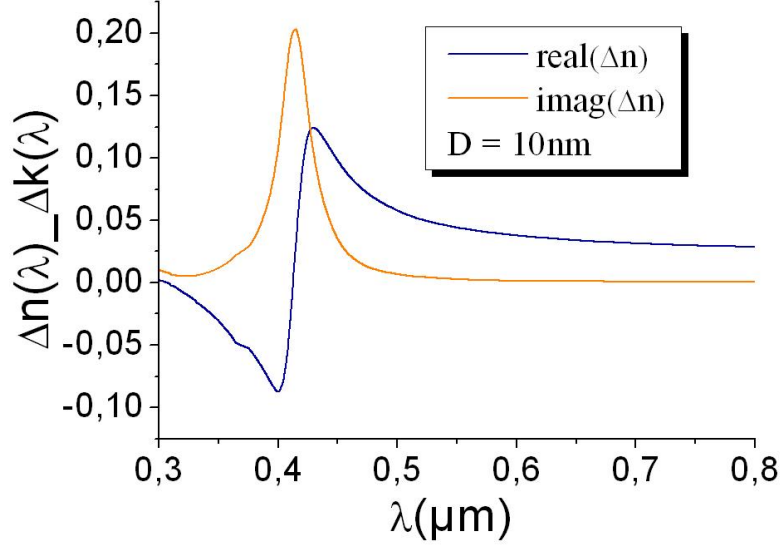


Figure 5.2.1: Real Δn and imaginary Δk of modified complex refractive index of Ag spheres of diameter $D = 10nm$ in a SiO_2 matrix.

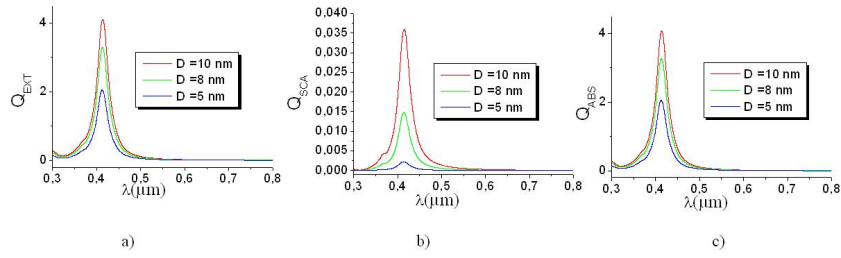


Figure 5.2.2: a) Extinction section, b) Scattering section, c) Absorption section determined from imaginary parts of modified complex refractive index Δk of a SiO_2 matrix doped by Ag spheres of diameter $D = 10nm$.

The curves show that, for a 1% volume concentration of metal we obtain a strong modification in complex refractive index, $\Delta n_{max} = 0.12$ and $\Delta k_{max} = 0.2$.

The real and imaginary parts of the index change in the dielectric as function of the radius of silver nanoparticles are shown in Fig. 5.2.4, for each wavelength there is an optimum radius at which we observe a maximum. This means that we have an average size for which the maximum absorption and dephasing is reachable. Fig. 5.2.4c represents the change in the ratio of real and imaginary parts depending on the size of the particle. Such ratio has a big value when the particle size is small. It increases with the wavelength. This allows to change the index of the dielectric medium without increasing absorption. For a given wavelength absorption curves admit a minimum value while the real part is big enough.

The preliminary results that we obtained for the real part with our method can be

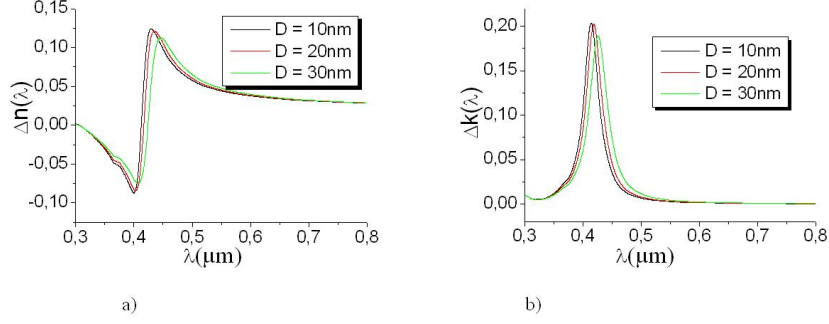


Figure 5.2.3: a) Real, b) Imaginary part of modified complex refractive index Δn , Δk of a SiO_2 matrix doped by Ag spheres of diameter $D = 10\text{nm}$.

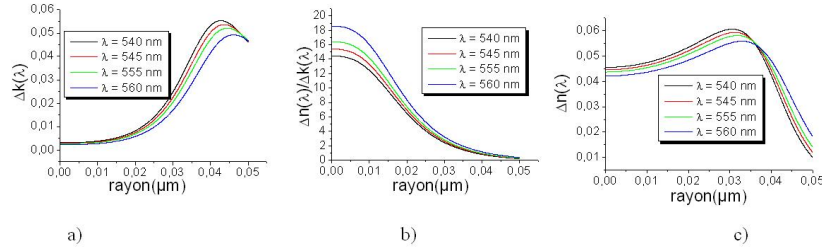


Figure 5.2.4: a) Real part Δn , b) Imaginary part Δk , c) Ratio $\Delta n/\Delta k$ of modified complex refractive index Δn , Δk of a SiO_2 matrix doped by Ag spheres of diameter $D = 10\text{nm}$.

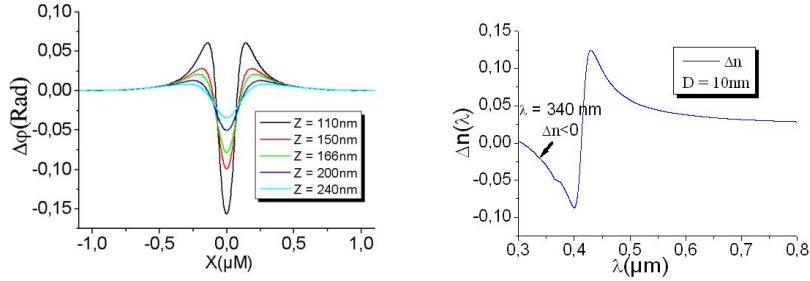


Figure 5.2.5: a) $\Delta\varphi$, b) Δn , comparison between $\Delta\varphi$ and Δn at distance $Z = 110, 150, 166, 200, 240\text{nm}$ from an Ag sphere of diameter $D = 10\text{nm}$ in SiO_2 , $\lambda = 340\text{nm}$.

verified. We present in Fig. 5.2.5a the phase curves for wavelength $\lambda = 340\text{nm}$ and at different distances from the metallic sphere. Compared to n Fig. 5.2.5b they clearly indicate that they are in a good agreement with the previous results since n has a negative value for this wavelength and $\Delta\varphi$ observed is also negative. By modeling with our technique, we are able to adjust this index by choosing the size, shape, concentration and type of particles to be included. We have in fact the approach that allows to

examine the possibility of creating new optical properties depending on the parameters and characteristics of the dielectric with metal nanoparticles.

3 Conclusion

We developed a new technique from the Mie theory. It has allowed us to study changes in the index of a dielectric in the presence of a single nanosphere shape. Our approach is also able to predict and explain the absorption, dephasing, and dispersion behavior. It applies to all types of particles and backgrounds. We develop this approach to adjust and thus to create new optical properties of materials to perform a given optical function.

References

- [1] G. Mie, "Beiträge zur Optik Trüber Medien, speziell Kolloidaler Metallösungen," Ann. Phys., 25, 377-452 (1908).
- [2] J. C. Maxwell-Garnet, "Colours in metal glasses and in metallic films," Philos. Trans. R. Soc. London, Ser. A, 203, 385 (1904).
- [3] C. F. Bohren et al, "absorption and scattering of light by small particules," Wiley, Mörlenbach, 1983

5.3 FEM simulation of light scattering by nonspherical objects

Burger, S. , Zschiedrich, L. , Kettner, B. , Schmidt, F.

Zuse Institute Berlin, Takustraße 7, 14195 Berlin, Germany
and

JCMwave GmbH, Haarer Straße 14a, 85640 Putzbrunn, Germany

Nanotechnology is rated as a key technology of the 21st century. In the field of nanooptics already at present, state-of-the-art scientific experiments and industrial applications exhibit nanometer to sub-nanometer design tolerances. This motivates the development and application of fast and accurate simulation tools for these fields.

We have developed a program package for numerical simulations of Maxwell's equations based on advanced finite-element methods (FEM). We give a short introduction to the method and report on the current status of the solvers, incorporating higher order edge elements, domain-decomposition algorithms, adaptive refinement refinement methods, adaptive transparent boundary conditions, and fast solution algorithms [1,2,3,4]. We further review recent applications of our methods to light scattering problems arising in fundamental research (metamaterials, nano-particles in a complex environment [5,6]) and industrial research (microlithography, EUV metrology, [7,8]).

References

- [1] J. Pomplun, S. Burger, L. Zschiedrich, and F. Schmidt, “Adaptive finite element method for simulation of optical nano structures,” *phys. stat. sol. (b)* **244**, p. 3419, 2007.
- [2] A. Schädle, L. Zschiedrich, S. Burger, R. Klose, and F. Schmidt, “Domain decomposition method for Maxwell’s equations: Scattering off periodic structures,” *J. Comput. Phys.* **226**, pp. 477–493, 2007.
- [3] L. Zschiedrich, S. Burger, J. Pomplun, and F. Schmidt, “Goal Oriented Adaptive Finite Element Method for the Precise Simulation of Optical Components,” **6475**, p. 64750H, Proc. SPIE, 2007.
- [4] L. Zschiedrich and F. Schmidt, “Evaluation of Rayleigh-Sommerfeld diffraction formula for PML solution,” in *Proceedings of Waves 2007 - The 8th International Conference on Mathematical and Numerical Aspects of Waves*, N. Biggs, ed., pp. 253–255, Univ. of Reading, UK, 2007.
- [5] C. Enkrich, M. Wegener, S. Linden, S. Burger, L. Zschiedrich, F. Schmidt, C. Zhou, T. Koschny, and C. M. Soukoulis, “Magnetic metamaterials at telecommunication and visible frequencies,” *Phys. Rev. Lett.* **95**, p. 203901, 2005.
- [6] T. Kalkbrenner, U. Hakanson, A. Schädle, S. Burger, C. Henkel, and V. Sandoghdar, “Optical microscopy using the spectral modifications of a nano-antenna,” *Phys. Rev. Lett.* **95**, p. 200801, 2005.
- [7] S. Burger, L. Zschiedrich, F. Schmidt, R. Köhle, T. Henkel, B. Kuchler, and C. Nölscher, “3D simulations of electromagnetic fields in nanostructures,” in *Modeling Aspects in Optical Metrology*, H. Bosse, ed., **6617**, p. 66170V, Proc. SPIE, 2007.
- [8] J. Pomplun, S. Burger, F. Schmidt, F. Scholze, C. Laubis, and U. Dersch, “Finite element analysis of EUV lithography,” in *Modeling Aspects in Optical Metrology*, H. Bosse, ed., **6617**, p. 661718, Proc. SPIE, 2007.

5.4 Experimental determination of light scattering properties of spheroidal titania particles and its comparison with Mie theory

Gogoi, A.¹, Choudhury, A.¹, Ahmed, G. A.¹

¹Optoelectronics and Photonics Laboratory, Department of Physics School of Science and Technology, Tezpur University Tezpur-784028, Assam, India

Light scattering characteristics of commercially used titania (TiO₂) particles with an average radius of 400 nm embedded in a cylindrical polyvinyl alcohol (PVA) matrix has been measured as a function of scattering angle at 543 nm, 594 nm and 632 nm laser wavelengths by using a designed and fabricated laboratory light scattering instrument. The system incorporates an array of sixteen highly sensitive static Si detectors that measured scattered light signals from 100 to 1700 in steps of 10. The experimental results were validated by tallying with theoretically generated Mie plots for titania particles of same size. The results agreed qualitatively well for both measured and theoretically calculated values within acceptable limits of deviation. A comparative analysis between the results obtained by using the three different incident wavelengths was done. It has been found that the front scattering properties of the ultrafine titania particles are very intense at 543 nm whereas the backscattering is more at 594 nm and 632 nm.

Result: A number of different experimental studies have been carried out in the past to investigate the scattering behavior of rutile titania particles [1-3]. Light scattering by titania particles are also studied theoretically by applying established theories like T-matrix [1, 3], finite element method [4] etc.

Table 5.4.1: Important parameters for Mie calculation

PARAMETERS	VALUE
Particle radius in micrometers	0.4
Environment refractive index	1.00 + i0.00000
Particle refractive index	2.73 + i0.00000
Incident light wavelength in micrometers	0.633

The experimental scattering profiles of titania particles at 543 nm, 594 nm and 632 nm laser wavelengths are shown in figure 5.4.1. To examine the validity of the experimental results, we performed theoretical analysis using Mie theory and compared the results. Some important parameters used in the theoretical calculation are tabulated in table 5.4.1. The results of these calculations are plotted in figure 5.4.1.

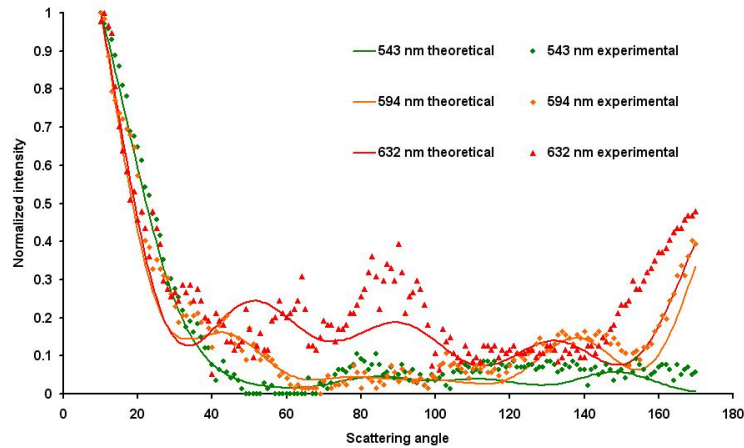


Figure 5.4.1: Experimental and theoretical graphs for particle size $0.400 \mu\text{m}$

References

- [1] H. Volten, J. -P. Jalava, K. Lumme, J. F. de Haan, W. Vassen, and J. W. Hovenier, Laboratory Measurements and T-Matrix Calculations of the Scattering Matrix of Rutile Particles in Water *Appl. Opt.*, Vol. **38**, No. 24, 5232-5240, (1999).
- [2] L. E. McNeil and R. H. French, Multiple scattering from rutile TiO_2 particles, *Acta Mater.* **48**, 4571-4576, (2006).
- [3] O. Muñoz, H Volten, J. W. Hovenier, M. Min, Y. G. Shkuratov, J. P. Jalava, W. J. Van der Zande and L. B. F. M. Waters, Experimental and computational study of light scattering by irregular particles with extreme refractive indices: hematite and rutile, *Astronomy & Astrophysics*, **446**, 525-535, (2006).
- [4] E. S. Thiele and R. H. French, Light scattering properties of representative, morphological rutile TiO_2 particles studied using a Finite-Element method, *J. Am. Ceram. Soc.*, **81**[3], 469-479, (1998).

5.5 Mie Resonances in Femtosecond Pulse Absorption by Metallic Nanoparticles

Grigorchuk, N.I.¹, Tomchuk, P.M.²

¹Bogolyubov Institute for Theoretical Physics, NAS of Ukraine,
Metrologichna Str. 14-b, 03680, Kyiv, Ukraine

²Institute for Physics, NAS of Ukraine,
Nauka Ave. 46, 03680, Kyiv, Ukraine

The metallic nanoparticles (MNP's) in transparent matrices show spectrally selective

optical absorption due to collective oscillation and interband transitions [1]. The surface plasmon frequency of MNP's unlike bulk samples and films varies critically with the geometry of nanoparticle [2], [3]. This important peculiarity is of great interest for a range of optical applications [4].

The theory is proposed which permits calculation of the energy absorbed by aspherical MNP's from the electric and magnetic fields of a femtosecond laser pulses of given duration, in the excitation region of Mie resonances. The carrying frequency of the laser beam was considered as to be changed. For particles of oblate or prolate spheroidal shape, the dependence of the absorbed energy on a number of factors, including the particle volume, the deviation of the particle shape from spherical one, the pulse duration, and the shift of the carrier frequency of a laser ray from the frequency of Mie resonance in a spherical particle, is determined [5].

Similar calculations for the energy due to only the magnetic absorption, was fulfilled by us separately in [6]. For particles of various shape it was found the dependence of absorbed energy on the orientations of the magnetic field of the laser ray upon particle and the magnitude of carrier frequency. It is established appreciable enhancement of absorption when the length of free electron path is larger comparatively with the particle size. The phenomenological and kinetic approach is compared each with other.

We develop our method for calculation of the energy absorbed by MNP's from double pulse laser-induced radiation in the region of Mie-resonances [7] as well. It was shown that depending on the time delay between two pulses the energy absorbed by a particle can be larger or smaller than the sum of the energies absorbed from two uncorrelated pulses.

References

- [1] C.F. Bohren and D.R. Huffman, Absorption and Scattering of Light by Small Particles, Wiley, Weinheim (2004).
- [2] P.M. Tomchuk, N.I. Grigorchuk. Phys. Rev. B, **73**, 155423, 2006.
- [3] N.I. Grigorchuk, P.M. Tomchuk. Fiz. Nizk. Temp. [Low Temp. Phys.], **33**, 1119, 2007.
- [4] U. Kreibig and M. Vollmer, Optical Properties of Metal Clusters, Springer, Berlin (1995).
- [5] P.M. Tomchuk, N.I. Grigorchuk. Ukr. J. of Phys., **52**, 889, 2007.
- [6] N.I. Grigorchuk, P.M. Tomchuk. J. of Phys. Studies, **12**, No. 2, 2008.
- [7] N.I. Grigorchuk, P.M. Tomchuk. Fiz. Nizk. Temp. [Low Temp. Phys.], **34**, 576, 2008.

5.6 Resonance spectra of typical particles

Yiping Han¹, Yang Zhang², Jiangyong Liu¹, Guoxia Han¹, Qiang Xu¹

¹Department of Applied Physics, School of Science, Xidian University, Xi'an, China, 710071, ²Department of Mechanical, Aerospace and Manufacturing Engineering, PO Box 88, UMIST, Manchester M60 1QD, UK

The dielectric particle possesses natural internal modes of oscillation at characteristic frequencies corresponding to specific ratios of size to wavelength, which are called morphology-dependent resonance (MDR). The strength and position of the enhanced and localized MDR spectra are highly sensitive to the environment with which the particle interacts¹⁻⁴. The properties of Morphological Dependant Resonance (MDR)'s for typical particles, such as elliptic cylinder, cylinder with rough sidewall, spheroid, etc, have been investigated. The behaviour of locations, quality factors of resonances has been discussed. The resonance spectrum is calculated and shows the strong dependence of the resonance spectrum on the size, refractive indexes of particles. The resonances associated with natural mode are shown. In order to capture the main features of processes dominated by MDR's rapidly, we used numerical results to give relatively simple empirical expressions for the positions of the resonance peaks by curve fitting. When falling droplet slightly depart from sphericity, shape distortion destroys the original spherical symmetry, and lifts the original degeneracy of $(2n+1)$ -multiplets. The properties of MDR's are investigated on impact of the deformation and surface perturbation on the intrinsic characteristics of the particles. And the resonance wavelength will be shift with respect to the distortion, the results shows that location of the resonance shifts to larger wavelengths as distortion of droplet is increased. Also the strength of resonance is sensitive to shape distortion. These results will be useful for interpreting experimental data without using the complication of the full scattering theory.

References

- [1] J A Lock, Excitation of morphology-dependent resonances and van de Hulst's localization principle *Opt. Lett.* 24 (1999) 427
- [2] H.M Lai, P. T. Leung, and K. Young, Time-independent perturbation for leaking electromagnetic modes in open systems with application to resonances in microdroplets, *Physical Review A* 41 (1990) 5187
- [3] G. Gouesbet, and G. Grehan, Generalized Lorenz-Mie theories, from past to future-Atomization and Sprays, 10 (2000) 277
- [4] G. Chern, Md. M. Mazumder, RK. Chang, Laser diagnostics for droplets characterization: application of morphology dependent resonances, *Prog. Energy Combust. Sci.* 22 (1996) 163

5.7 Categorization of light scattering programs

Hellmers, J.¹, Wriedt, T.²

¹Universität Bremen, Badgasteiner Str. 3, 28359 Bremen, Germany, ²Institut für Werkstofftechnik, Badgasteiner Str. 3, 28359 Bremen, Germany

In 1908 Gustav Mie published his paper describing a theoretical approach to calculate the light scattering by gold colloids. Today, a 100 years later, the theoretical investigation of optical properties is still a topic of high interest for different branches in scientific research - like Material Science, Biology, Meteorology, Astrophysics - and industry. The calculation of light scattering by small particles in the so called Mie range size area can only be done numerically. Therefore adequate computer programs are required. The knowledge of the optical properties of such particles helps to design new products as well to understand complex physical phenomena e.g. in atmospheric science.

As the original Mie theory is only suitable for spherical particles, advanced light scattering theories were introduced to describe the optical behavior of more complex particles as well. This was supported by the rapidly ongoing improvements in computational science (hardware as well as the understanding of implementation of mathematical problems into numerical schemes and corresponding algorithms) during the second half of the 20th century. Nowadays a broad range of sophisticated computer software is available for science and industry. The problem is, that due to the complex mathematical procedures needed to calculate light scattering by particles in the Mie range size area there is no 'ultimate' program that can handle all kind of scattering problems. Instead there exist several, different scattering theories (see e.g. Wriedt [1],[2], Mishchenko et al. [3], Kahnert [4], Veselago et al. [5] or Tsukerman et al. [6]) which are implemented - sometimes in different ways - into corresponding programs. Therefore every program has its own characteristics and is suitable just for specific scattering problems. If a user wants to solve a specific task he must choose the software that will give him the greatest advantage. A categorization scheme for light scattering programs therefore will be helpful for such a choice.

'Top-down approach': methods and algorithms

To calculate light scattering by any particle(s) the scattering problem has to be solved. It consists of a scatterer with known properties (shape, size, refractive index) which is illuminated by light with a defined wavelength. The incident light can be described by electro-magnetic waves and therefore must satisfy Maxwell's equations. This leads to an under-determined set of differential equations. Considering the particle's properties plus additional mathematical assumptions allows to overcome the under-determination and to solve the set of equations. There are different ways to do so; in principle they can be divided into four categories:

- direct solution using an initial value approach
- direct solution using a boundary value approach

- using a volume integral approach
- using a surface integral approach (Green's theorem)

In every program to calculate light scattering one of these four approaches is used. Therefore it is possible to categorize light scattering programs regarding to the theory and algorithm they are based on. The problem is though, that this is a highly theoretical approach that doesn't take into account the users need. Choosing a suitable program for a given scattering problem requires a great amount of experience and knowledge of the specific advantages and disadvantages of the underlying scattering theories. Because of this we would like to suggest an alternative procedure that should meet the users' needs in daily work.

'Bottom-up approach': particle characteristics

A user usually wants to calculate light scattering for a defined scattering problem. In most cases the particle itself will be in the center of focus. So the first question will be whether a program can calculate light scattering by the particle or not. The algorithm and theory the software then is secondary. So from a users point of view a categorization scheme for light scattering software should be orientated in regard to the particle characteristics and the scattering problem. This would imply a kind of checklist that has to be followed to get to the fitting program and that could be organized as follows:

- 1) particle shape: spherical/non-spherical, symmetrical/non-symmetrical, regular/irregular, low/high aspect ratio, convex/concave, smooth/rough, etc.
- 2) particle size: size parameter in relation to incoming wavelength
- 3) particle composition: homogeneous/inhomogeneous, etc.
- 4) refractive index: real, complex, anisotropic, bianisotropic, chiral, etc.
- 5) incident wave: plane wave, Gaussian beam, etc.
- 6) medium: absorbing/non-absorbing, etc.
- 7) results: what can be calculated - DSCS, Mueller-Matrix elements, torque, radiative force, orientation averaged results, etc.
- 8) expandability of the scattering problem: multiple scattering, particle on surface, cluster, coated particles, etc.
- 9) particle description: analytically (by formula) / model (by polygons)
- 10) method: effects on calculation time, e.g. by surface/volume discretisation

The checklist then should be continued by non-physical software properties that might have influence on the decision by the user:

- 11) availability: free to use / free to modify / proprietary software
- 12) usability: precompiled/not precompiled, running on given hardware, etc.

Finally, information without any connection to the use of program can be added to complete a categorization

- 13) metadata: author, year, published in, revision, source, similar programs, etc.

A categorization in such a way is especially helpful for scientist who are not particularly familiar with light scattering and the corresponding theories and just want to find a program as a tool for their actual work.

In a next step a categorization scheme like this should be the base for a light scattering software database with a sophisticated search tool to help scientist finding suitable light scattering programs for their work. Such a search could be made available online; corresponding developments are in progress (see Wriedt and Hellmers [7]).

We hope for contribution by our colleagues. Any comments, critic and suggestions are welcome.

Acknowledgement

We would like to acknowledge support of this work by Deutsche Forschungsgemeinschaft DFG.

References

- [1] T. Wriedt, "A Review of Elastic Light Scattering Methods," Part. Part. Syst. Char. 15, 67-74 (1998).
- [2] T. Wriedt, U. Comberg, "Comparison of computational scattering method," JQSRT 60, 411-423 (1998).
- [3] M.I. Mishchenko, J.W. Hovenier, L.D. Travis, "Light Scattering by Nonspherical Particles. Theory, Measurement and Applications," Academic Press, San Diego (2000).
- [4] M. Kahnert "Numerical methods in electromagnetic scattering theory," JQSRT 79-80, 775-824 (2003).
- [5] V. Veselago, L. Braginsky, V. Shklover, C. Hafner, "Negative Refractive Index Materials," J. Comput. Theor. Nanosci. 3(2), 1-30 (2006).
- [6] I. Tsukerman, F. Cajko, A.P. Sokolov, "Traditional and new simulation techniques for nanoscale optics and photonics," 2005 Proceedings of SPIE, Vol 5927, 128-137 (2005).
- [7] T. Wriedt, J. Hellmers, "New Scattering Information Portal for the light scattering community," JQSRT 109, 1536-1542 (2008).

5.8 Aggregate of spherical primary particle and approximations for light scattering cross section

Jacquier S.¹, Gruy F.¹

¹École Nationale Supérieure des Mines de Saint-Étienne Centre SPIN, Département GENERIC, 158 Cours Fauriel 42023 St. Étienne

To characterize the presence of spherical particle in low concentrated suspension by using a non intrusive method, the light-matter interaction is used. This interaction is measurable, for example by turbidimetry, by comparing the change of intensity of a light source which cross a medium with and without particle. The corresponding turbidity is proportional to the scattering cross section (C_{sca}) of the suspended particles. C_{sca} is a function of: the wavelength of the incident light source in the medium (λ), the refractive index of the medium surrounding the particle (n_m), the particle refractive index (n_p) and the particle size parameter ($x = 2\pi r/\lambda$ where r is the sphere radius). The sphere scattering cross section is obtained numerically from the Mie theory. This theory suitable for all sphere size parameter, is sometimes forsaken to the profit of the use of simpler approximation. These approximations have different validity range depending on: x and the ratio $m = n_p/n_m$. Among these approximations let us quote: the Rayleigh, Fraunhofer, Rayleigh-Debye-Gans and the Anomalous Diffraction approximations [1,2]. Let us recall that the Mie theory is supported by these assumptions:

- the particles are spherical,
- the wavelength between incident and diffuse radiations is the same one,
- the particles consist in a homogeneous material,
- the particles are insulated spatially i.e. there is no multiple scattering,

Therefore, in the case of multisphere aggregate the Mie theory is then not directly applicable, but requires an extension. An important literature exists on this subject [3,4]. However using C_{sca} got by generalized the Mie theory is not possible for spectral analysis during in line measurement because these calculations need long CPU time with a common computer.

Thus this paper summarizes our work about the research of approximations for the scattering cross section for a multisphere aggregate. The validity range of these approximations is carried out by comparing the values of C_{sca} obtained under the same conditions from approximation methods and an exact method (GMM). GMM (Generalized Multiparticle Mie) solution was developed by Xu in 1995 ([5] for more information see the references therein). We consider that an aggregate is composed of N identical primary spherical particles with a size parameter $x \in [0, 10]$.

This study was unrolled in 3 parts:

1. Understand the change of C_{sca} as a function of N and of a aggregate morphology parameter d_1 [6]. We conclude that the number of primary particle is the relevant parameter in the range $x \in [0, 2]$ and that N and d_1 have the same weight in the second

range $x \in [2, 10]$. This study helps us to select approximations which are testing in the next point

2. The results of these investigations are present in [7] and lead to the conclusion: methods of the Compact Sphere (CS) and Hollowing Sphere (HS) are inappropriate, methods using a fractal dimension are not very conclusive for aggregates containing a small number of primary particles, Percival-Berry-Khlebtsov (PBK) method is valid for $0 < x < 2$, with an error which increases with the refractive index of material, Anomalous Diffraction (AD) method is correct for $2 < x < 10$, and is less sensitive to the refractive index, Effective Refractive Index (ERI) method, baed on projected area of aggregate, is the method suitable on the whole size parameter.

3. Then the ERI and AD methods were improved. The ERI method was improved by the introduction of a corrected term [8]. We reformulated the Anomalous Diffraction method now completely analytically [9] by introducing the chord length distribution for various aggregates. This new expression is entitled ADr, with the r as rapid, because this one is at least a hundred times faster than the standard AD method. The initial study [9] was done for ordered clusters, then we extended the test of ADr method to a large number of random aggregates.

Acknowledgement

The authors would like to thank D. Y.-l. Xu for making his GMM code available.

References

- [1] C.F. Bohren, D.R. Huffman, Absorption and scattering of light by small particles. (Wiley-VCH, Weinheim, 1998).
- [2] H.C. van de Hulst, Light scattering by small particles. (Dover publications, Inc. New york, 1981).
- [3] F.M. Kahnert, "Numerical methods in electromagnetic scattering theory". JQSRT. 79(80), 775-824 (2003).
- [4] M.I. Mishchenko,et al., "T-matrix theory of electromagnetic scattering by particles and its applications: a comprehensive reference database". JQSRT, 88, 357-406 (2004).
- [5] Y.-l. Xu, N.G. Khlebtsov, "Orientation-averaging radiative properties of an arbitrary configuration of scatterers". JQSRT, 79-80, 1121-1137 (2003).
- [6] S. Jacquier, F. Gruy, Méthodes approchées pour les propriétés optiques d'agrégats de particules sphériques non absorbantes.(ENSM-SE, PhD thesis, 2006).
- [7] S. Jacquier, F. Gruy, "Approximation of the light scattering cross-section for aggregated spherical non-absorbent particles". JQRST, 106, 133-144 (2007).
- [8] S. Jacquier, F. Gruy, Approximation for scattering properties of aggregated spherical particles: ERI method. (PARTEC, 2007).

- [9] S. Jacquier, F. Gruy, "Anomalous diffraction approximation for light scattering cross section: Case of ordered clusters of non-absorbent spheres". JQSRT, 109, 789-810 (2008).

5.9 Probing the composition of a drying microdroplet of water suspension of nanoparticles with optical methods

Jakubczyk, D.¹, Derkachov, G.¹, Kolwas, K.¹, Kolwas, M.¹

¹Institute of Physics of the Polish Academy of Sciences
al. Lotników 32/46, 02-668 Warsaw, Poland

The evaporation of single levitated water droplets containing 200 nm's diameter polystyrene

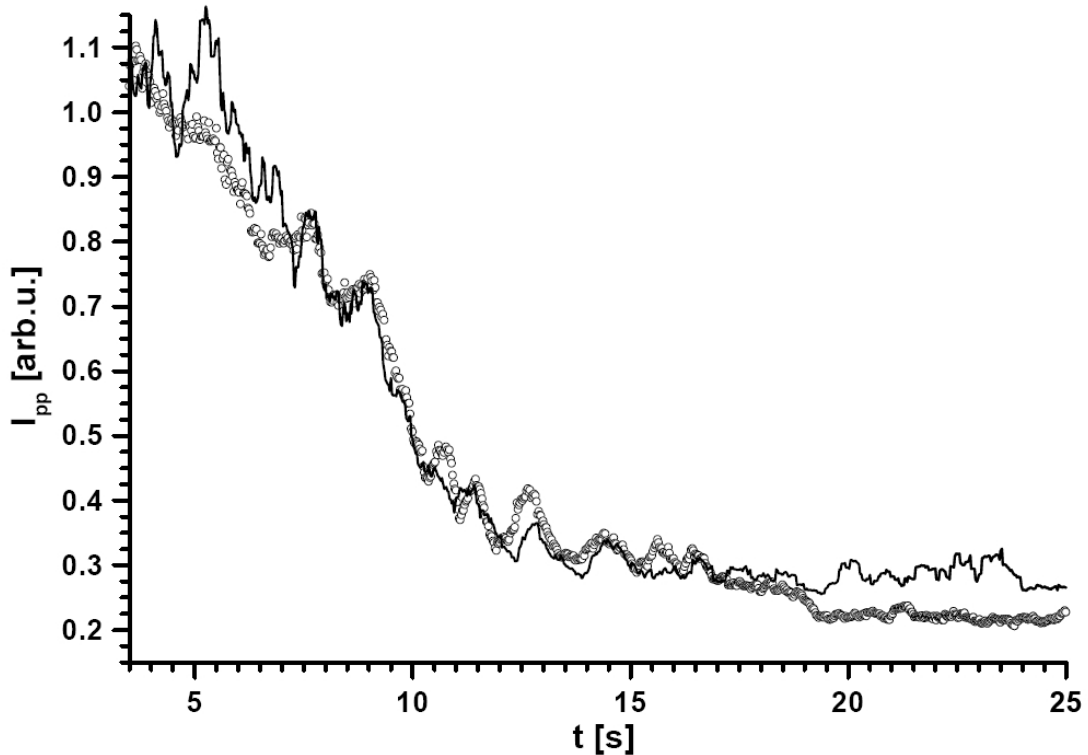


Figure 5.9.1: Temporal evolution of optical p -polarization signal: open circles experimental results, solid line - Mie theory prediction.

spheres was studied. Each such droplet was levitated in the electrodynamic quadrupole trap placed in a small climatic chamber [1] and illuminated with two coaxial laser beams:

s-polarized red and *p*-polarized green. The droplet radius was found with from the spatial frequency of the irradiance of *s*-polarized scattered light $I_{ss}(\Theta)$ (FFT method; see eg. [2]). This method is independent of the (effective) refractive index of the droplet. It was a desired quality, since in our experiments the effective refractive index of the droplets was changing. Carefully applied the method was sufficiently precise for us (± 100 nm). Another optical signal, integrated over the observation angle, $I_{pp}(t)$ (*p*-polarized scattered light, see figure 5.9.1) also provided valuable information on the droplet properties. The $I_{pp}(t)$ signal is a function of droplet size and composition (determined mostly by droplet size as well). We found, that most of its rich extrema structure was neither noise nor caused by resonances in the inclusions structures, but Mie structural resonances. For $7 < t < 19$ s they could be well reproduced (figure 5.9.1) by Mie theory with the droplet radius taken from the experiment (FFT method, not Mie theory!) and the effective refractive index taken as the simple volume mixture of the indices of water and inclusions (see eg. [3]). This seems to indicate that in some cases Mie theory may be extended to essentially inhomogeneous media and utilized to probe the composition of the droplet. This result also confirms that the radius (at least as perceived by optical phenomena) was measured quite accurately.

Since the final droplet radius could not be unambiguously found with FFT method, it served, to a certain extent, as a fitting parameter for mixing formula. Actually, all the systematical errors of the measurement as well as all approximations of the model were accounted for by this parameter. In spite of that, it was found to be reasonable (1431 nm in figure 5.9.1) .

Acknowledgement

This work was supported by Polish Ministry of Science and Higher Education grant No. 1 P03B 117 29.

References

- [1] M. Zientara, D. Jakubczyk, K. Kolwas, and M. Kolwas, "Temperature Dependence of the Evaporation Coefficient of Water in Air and Nitrogen under Atmospheric Pressure: Study in Water Droplets," J. Phys. Chem. A 112, 5152-5158 (2008), DOI: 10.1021/jp7114324.
- [2] B. Steiner, B. Berge, R. Gausmann, J. Rohmann, and E. Rühl, "Fast *in situ* sizing technique for single levitated liquid aerosols," Appl. Opt. 38, 1523-1529 (1999).
- [3] U. Kreibig, and M. Vollmer, Optical Properties of Metal Clusters. (Springer, Berlin, 1995).

5.10 Photonic/Plasmonic Structures in Nanocomposite Glass

O.Kiriyenko¹, W.Hergert¹, S.Wackerow¹, M.Beleites¹ and H.Graener¹

¹Institute of Physics, Martin Luther University Halle-Wittenberg, Friedemann-Bach-Platz 6, 06108 Halle, Germany

Glass containing metallic nanoparticles is a promising material for various photonic applications due to the unique optical properties mainly resulting from the strong surface plasmon resonance (SPR) of the metallic nanoparticles. The characteristics of the resonance can be modified by varying size, shape and concentration of the inclusions. Size and shape can be modified either by the application of mechanical stress or intensive laser pulses. [1]

Under the influence of moderate temperatures and high electric fields, silver nanoparticles embedded in a glass matrix can be dissolved. This process is used to build periodic photonic/plasmonic structures in a glass matrix. [2] The building blocks of the structure are regions formed by a two-component material consisting of glass and metallic nanoparticles. A finite element method (FEM) implemented in the software Comsol Multiphysics is used to calculate effective permittivities of this composite material.

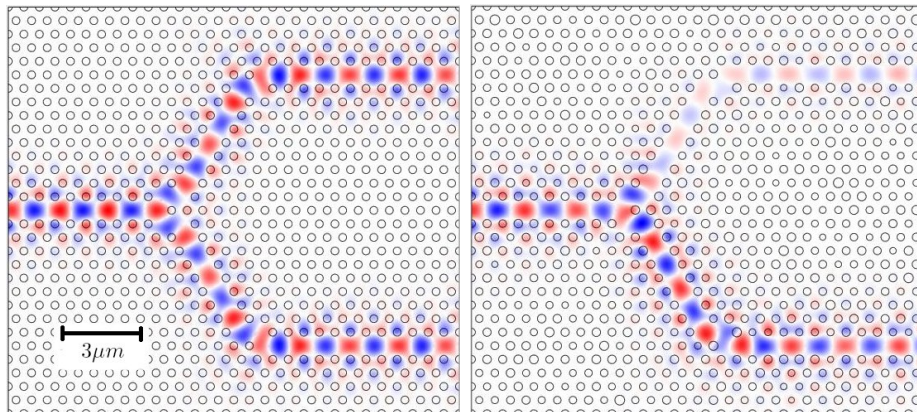


Figure 5.10.1: Electric field in a Y-waveguide in a hexagonal twodimensional photonic crystal. The background material is glass and the rods consist of metallic nanoparticles in a glass matrix. Ideal structure (left) and structure with variation of the radii of the rods (right). The lattice constant of the structure is $0.5\mu\text{m}$. The radius of the rods in the ideal structure is $0.1\mu\text{m}$. A Gaussian distribution of the radii ($\sigma = 0.01\mu\text{m}$) is used in the simulation of the non-ideal structure.

The properties of Y-waveguides in two-dimensional model structures are studied. The structure which is investigated numerically corresponds to experimental realizations of such structures based on electric-field microstructuring. Special attention is devoted

to the influence of changes of the geometrical structure and of the nanoparticle filling fraction on the waveguide properties. Fig. 5.10.1 shows, that imperfections in the structure easily destroy the symmetry in transmission properties of the Y-waveguide.

References

- [1] A.Poslipensky, A.Abdolvand, G.Seifert, H.Graener, "Femtosecond laser assisted production of dichroitic 3D structures in composite glass containing Ag nanoparticles", *Appl.Phys.A* 80, 1647-1652 (2005)
- [2] A. Abdolvand, A.Podlipensky, S.Matthias, F.Syrowatka, U.Goesele, G.Seifert, H. Graener, "Metallo-dielectric Two-Dimensional Photonic Structures Made by Electric-Field Microstructuring of Nanocomposite Glasses", *Adv.Mater.* 17, 2983-2987 (2005).
- [3] H.Graener, A.Abdolvand, S.Wackerow, O.Kiriyenko, W.Hergert, "Optical properties of photonic/plasmonic structures in nanocomposite glass", *Phys.Stat.Sol.(a)* 204, 3838-3847 (2007).

5.11 Theory of strong localization effects of classical waves in disordered loss or gain media

Lubatsch, A.^{1,2}, **Frank, R.**¹, **Kroha, J.**¹

¹ **Physikalisches Institut, Universität Bonn, 53115 Bonn, Germany,** ²**Laboratoire de Physique et Modélisation des Milieux Condensés/CNRS, 38042 Grenoble, France**

Scalar wave transport in a system of randomly distributed scatterers of finite size (Mie-scatterers) is considered in three dimensions. The presented theory is based on a self-consistent Cooperon resummation, implementing the effects of energy conservation and its absorptive or emissive corrections by means of an exact, generalized Ward identity. Substantial renormalizations are found, depending on whether the absorption/gain occurs in the scatterers or in the background medium. The possibility of oscillatory in time behavior due to memory effects caused by the interplay of interference and sufficiently strong gain are discussed, as well as the different length scales.

5.12 Optical Trapping of Carbon Nanotubes and Gold Nanorods

Maragò O.M.¹, Jones P.H.², Bonaccorso F.^{1,4}, Gucciardi P.G.¹, Iatì M. A.¹, Ferrari A.C.³, Saija R.⁴, Denti P.⁴, Borghese F.⁴

¹Istituto per i Processi Chimico-Fisici del CNR, Salita Sperone, 98158 Faro Superiore, Messina, Italy,

² Department of Physics and Astronomy, University College London, Gower St, London WC1E 6BT, UK,

³ Engineering Department, University of Cambridge, 9 JJ Thomson Ave, Cambridge CB3 0FA, UK,

⁴ Dip. Fisica della Materia e Ingegneria Elettronica, Università di Messina, Salita Sperone 31, 98166 Messina, Italy.

Optical trapping [1] of 1-d nanostructures has received much attention [2,3,4,5] due to its potential for top-down organization of complex nano-assemblies. Trapped nanoparticles can also be used to increase space and force resolution in photonic force microscopy [4]. Their small transverse size is the key to achieve nanometric resolution, while an axial dimension in the micron range ensures stable trapping and could allow force sensing in the sub-pico-Newton regime. Here we optically trap carbon nanotubes bundles in water solutions and extract the distribution of both centre-of-mass and angular fluctuations from 3-d optical tracking of the trapped nanotubes through back focal plane interferometry (see fig. 5.12.1 (a,b,c)). We measure the optical force and torque constants from auto and cross-correlation of the tracking signals. The latter allows us to isolate the angular Brownian motion. We demonstrate that nanotubes enable nanometre spatial, and femto-Newton force resolution in photonic force microscopy.

Furthermore we investigate optical trapping of gold nanorods, where the presence of plasmon resonances (defined by their aspect ratio) enables trapping [6]. We compare the mechanical effects on nanorods by different laser sources. Single nanorods and aggregates are stably trapped and oriented with laser polarization (see fig. 5.12.1 (d)). Radiation force and torque are estimated from thermal fluctuations of trapped nanoparticles. Complex field polarizations (radial, azimuthal, Laguerre-Gauss fields) are also investigated.

References

- [1] A. Ashkin, *Optical Trapping and Manipulation of Neutral Particles using Lasers*, (World Scientific Publishing, Singapore, (2007) and references therein.
- [2] S. Tan, et al., Optical trapping of single-walled carbon nanotubes, *Nano Lett.* 4, 1415-1419 (2004).

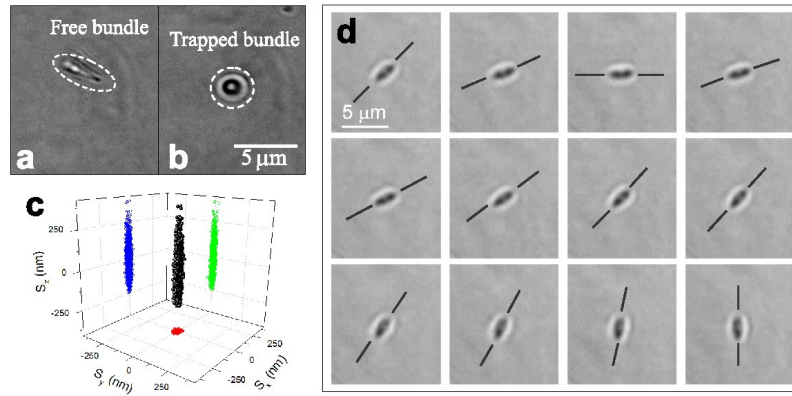


Figure 5.12.1: (a) Untrapped carbon nanotubes bundle randomly oriented, (b)trapped bundle oriented with propagation axis, (c) Brownian motion of a carbon nanotubes bundle in an optical trap reconstructed from back focal plane interferometry, (d) plasmon enhanced optical trapping of a gold nanorods aggregate aligned with polarization axis: changes in the light polarization induce rotation of the micron sized structure.

- [3] R. Agarwal, et al., Manipulation and assembly of nanowires with holographic optical traps, *Optics Express* 13, 8906-8912 (2005).
- [4] Y. Nakayama, et al. Tunable nanowire nonlinear optical probe, *Nature* 447, 1098-1102 (2007).
- [5] F. Borghese, P. Denti, R. Saia, M. A. Iatì, O. M. Maragò, Radiation torque and force on optically trapped linear nanostructures, *Phys. Rev. Lett.* 100, 163903 (2008).
- [6] Pelton, M. et al., Optical trapping and alignment of single gold nanorods by using plasmon resonances, *Optics Lett.* 31, 2075-2077 (2006).

5.13 Field enhancement through particle plasmons

Miclea, P. -T.^{1,2}, Uepping, J.², Ralf B. Wehrspohn^{2,3}

¹Fraunhofer Center of Silicon Photovoltaics, Walter-Huelse-Str.1, 06120 Halle, Germany,

² AG Microstructured Based Material Design, Martin Luther University Halle-Wittenberg, Heinrich-Damerow-Str. 4, 06120 Halle, Germany,

³Fraunhofer Institute for Mechanics of Materials, Walter-Huelse-Str. 1, 06120 Halle, Germany

We describe the optical properties of two dimensional nano arrays of gold nano particles starting from the isolated particles using Mie theory. Because of the arrangement of particles in a two dimensional assembly, we use the effective medium theory for description of the dielectric permittivity of gold nano particles and approximate the metalnanoparticles/polymer composite material with an effective medium material. In this approximation we calculate the optical transmission properties for two dimensional gold nano arrays using the finite element method (comsol). The optical properties of gold will be modeled using a analytic function [1] for the complex dielectric function. On the other hand we use the generalized Mie theory description of assembly of metal nano particles in a polymer matrix. The results are compared with the experimental data of gold nano particles embedded in polymer matrix.

References

- [1] P. G. Etchegoin, E. C. Le Ru, and M. Meyer. An analytic model for the optical properties of gold. *The Journal of Chemical Physics*, 125(16):164705, 2006.

5.14 Experimental determination of size and refractive index of colloidal particles by coherent refraction and transmittance of light

Sánchez-Pérez, C.¹, García-Valenzuela, A.¹, Sato-Berú, R.³

¹Centro de Ciencias Aplicadas y Desarrollo Tecnológico, Universidad Nacional Autónoma de México, Apartado Postal 70-186, Distrito Federal 04510, México.

Size particle determination has been a challenging area of research. Different techniques have been already proposed and commercially developed due to its importance in scientific laboratories and industrial applications. Particle sizing from optical properties has been investigated and used for many years now. We can mention two types of techniques:

scattometry and spectroturbidimetry. In the first type of techniques features from the scattering pattern of isolated particles (highly dilute limit) are measured and from it the particle size inferred [1]. In these techniques the refractive index of the particles must be known and is limited to sufficiently large particles so the scattering pattern has clearly measurable angular patterns. In spectroturbidimetry techniques, a spectrum of the extinction coefficient is measured and from it the particle size distribution is obtained. In spectroturbidimetry the refractive index of the particles must be known as well [2]. If particles are sufficiently large the inversion of the particle size distribution is a well-conditioned inverse problem. However, as the particles size gets smaller the problem becomes very sensitive to errors in refractive index of particles rendering this technique less suitable in this case.

Recently it has been shown that the effective refractive index of a colloid can be used to better infer the size of the particles without knowing a priori their refractive index, even for very small particles [3,4]. In this work we analyze the experimental measurements required to use this methodology in the case of non-absorbing colloidal particles. Specifically, the measurement of the real and imaginary parts of the effective refractive index and the volume fraction occupied by the particles is required. We discuss all the necessary precautions to be taken for these measurements and present experimental results with colloids consisting of spherical silica particles suspended in distilled water. The particle sizes we have tested are in the range of tenths of nanometers. We compare our measurements with electron transmission microscopy size measurement.

References

- [1] J. Vargas-Ubera, J. F. Aguilar, and D. M. Gale, "Reconstruction of particle-size distributions from light-scattering patterns using three inversion methods," *Appl. Opt.* 46, 124-132 (2007).
- [2] S.Y. Shchyogolev, "Inverse problems of spectroturbidimetry of biological disperse systems: an overview", *J. Biomed. Opt.*, vol.4, 490 (1999).
- [3] A. Reyes Coronado, A. García-Valenzuela, C. Sánchez-Pérez, R. G. Barrera, "Measurement of the effective refractive index of a turbid colloidal suspension using light refraction", *New Journal of Physics*, vol. 7, 89 (2005).
- [4] A. García-Valenzuela, R. G. Barrera, E. Gutiérrez-Reyes, "Firm theoretical grounds for particle sizing in turbid colloids using light refraction", to be submitted.

5.15 Equivalent refractive index for biaxially anisotropic scatterers using T-matrix approach

Schmidt, V.¹, Wriedt, Th.²

¹Universität Bremen, Badgasteiner Str. 3, 28359 Bremen, Germany, ²Institut für Werkstofftechnik, Badgasteiner Str. 3, 28359 Bremen, Germany

Simulation of optical properties of anisotropic scatterers is very important in different scientific and technology applications. Many industrial materials are anisotropic. Such particles can be found for example as white pigments in paper and colour pigments in paint.

The development of effective numerical methods for the solution of the scattering problem is very important for science and technological applications. Such methods can be used for very accurate calculations or for the determination of the area of applicability for various approximations.

A modern and effective numerical tool is the T-matrix approach based on an expansion of the total electromagnetic field by spherical vector wave functions (SVWF) [1]. The T-matrix approach has been applied mostly to isotropic scatterers (permittivity ε and/or permeability μ are scalar). There are some extensions for biaxially anisotropic spheres [2], uniaxially anisotropic spheres [3], ellipsoids [4] or non-axisymmetric scatterers [5]. We extended the method from the uniaxially anisotropic case obtained by Doicu [5] to biaxially anisotropic particles.

The differential scattering cross sections for random oriented biaxially anisotropic, uniaxially anisotropic and isotropic arbitrary scatterers that are equivalent in Rayleigh-Gans-Debye (RGD) approximation [6] are compared.

Field expansion in the anisotropic medium. The electromagnetic fields in the anisotropic medium are characterised by the stationary Maxwell equations

$$\begin{aligned} \nabla \times \mathbf{H} &= -ik\mathbf{D} & , & & \nabla \times \mathbf{E} &= ik\mathbf{B} \\ \nabla \cdot \mathbf{B} &= 0 & , & & \nabla \cdot \mathbf{D} &= 0 \end{aligned} \quad (5.15.1)$$

and the constitutive relations

$$\mathbf{E} = \bar{\varepsilon}\mathbf{D} \quad , \quad \mathbf{H} = \bar{\mu}\mathbf{B} \quad (5.15.2)$$

where ε is the tensor of electric permittivity and μ of magnetic permeability. In the biaxially anisotropic case the permittivity tensor is diagonal and has three different complex components

$$\bar{\varepsilon} = \begin{pmatrix} \varepsilon_x & 0 & 0 \\ 0 & \varepsilon_y & 0 \\ 0 & 0 & \varepsilon_z \end{pmatrix} \quad , \quad \bar{\mu} = \mu. \quad (5.15.3)$$

The basis of the quasi-spherical vector wave functions for the electromagnetic field in such medium (1)-(3) is obtained by inverse Fourier transformation. The expressions of T-matrix calculations for the new basis are similar to those for the "classical" isotropic case, except that the SVWF functions in surface integrals of the Q and RegQ matrices are replaced by the functions of the new basis.

$$\mathbf{X}_{mn}^e(k\mathbf{r}), \quad \mathbf{Y}_{mn}^e(k\mathbf{r}), \quad \mathbf{X}_{mn}^h(k\mathbf{r}), \quad \mathbf{Y}_{mn}^h(k\mathbf{r}).$$

To calculate the T-matrix for such scatterers a parallelised Fortran code using OpenMP technology was developed.

Equivalent refractive index. Bohren and Huffman [6] have shown that the scattering and absorption cross sections of random oriented biaxially anisotropic spheres in Rayleigh approximation can be exactly approximated by ensembles of three isotropic spheres

$$\langle C_{scat}^{bi}(m_x, m_y, m_z) \rangle = \frac{1}{3} (C_{scat}^{iso}(m_x) + C_{scat}^{iso}(m_y) + C_{scat}^{iso}(m_z)), \quad (5.15.4)$$

where m_x, m_y, m_z are the components of the refractive indexes of biaxially anisotropic medium, $C_{scat}^{bi}, C_{scat}^{iso}$ are scattering cross sections for biaxially anisotropic and isotropic spheres and $\langle \rangle$ denotes orientational averaging.

In the RGD approximation the scattering matrix is proportional to the factor $(m^2 - 1)$, where m_r is refractive index, then (4) is equal to

$$\langle C_{scat}^{bi}(m_x, m_y, m_z) \rangle = C_{scat}^{iso}(m_{xyz}), \quad m_{xyz} = \sqrt{(m_x^2 + m_y^2 + m_z^2)/3}. \quad (5.15.5)$$

In Fig. (5.15.1) an exemplary comparison of the differential scattering cross sec-

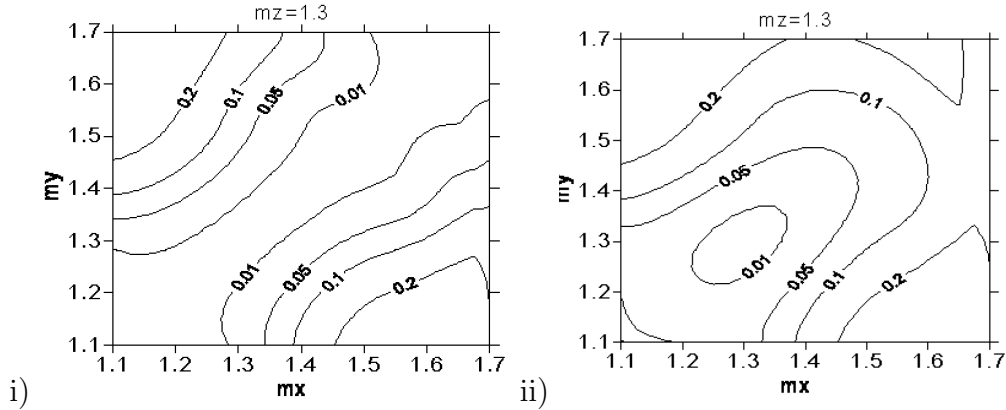


Figure 5.15.1: Exemplary comparison of DSCS: i) between random oriented biaxially and uniaxially anisotropic spheres, Δ^{uni} ; ii) between biaxially anisotropic and isotropic spheres, Δ^{iso} . Radius of spheres $r = 500\text{nm}$, wavelength $\lambda = 628.3\text{nm}$.

tions (DCSC) for different random oriented biaxially anisotropic, uniaxially anisotropic

($m_{x,y} = \sqrt{(m_x^2 + m_y^2)/2}$) and isotropic ($m_{x,y,z} = m_{xyz}$) spheres outside the RGD approximation area is presented. The relative approximation error $\Delta^* = \int_0^\pi \ln(\text{DSCS}_{bi}(\theta)) - \ln(\text{DSCS}_*(\theta))d\theta$ is plotted.

Conclusion. Further simulations for large spheres and cubes demonstrate that the optical properties (DSCS) of biaxially anisotropic random oriented scatterers (spheres with radius $kR < 5$ and refractive index $1.1 < m_{x,y,z} < 1.7$) can be accurately approximated (with relative error 1%) by ones of uniaxially anisotropic scatterers in the case of the difference between m_x and m_y is less 6-7%. For smaller particles this difference value will be higher, e.g. for spheres with $kR = 1$ it is 10%. But for each particle there are some regions (e.g. for spheres with $kR = 5$ it is $m_x \approx 1.2$, $kR = 3 - m_x \approx 1.3$, $kR = 1 - m_x \approx 1.7$) where the "equivalent" area is much broader.

The optical properties (DSCS) of biaxially anisotropic random oriented spheres (with radius $kR < 5$ and refractive index $1.1 < m_{x,y,z} < 1.7$) can be also accurately approximated (with relative error 1%) by ones of isotropic spheres if additionally the difference between $m_{x,y}$ and m_z is less 4%. This difference value increases with decreasing of kR for high values of m_z .

Acknowledgement

We would like to acknowledge the financial support of this work by Deutsche Forschungsgemeinschaft (DFG).

References

- [1] P.C. Waterman, "Symmetry, unitary and geometry in electromagnetic scattering," Phys. Rev. D, V. 3, N. 4, 825-839 (1997).
- [2] B. Stout, M. Neviere, P. Popov, "T-matrix of the homogeneous anisotropic sphere: applications to orientation-averaged resonant scattering," J. Opt. Soc. Am. A, V. 24, 1120-1130 (2007).
- [3] K.-L. Wong, H. Chen, "Electromagnetic scattering by a uniaxially anisotropic sphere," Microwaves, Antennas and Propagation, IEE Proceedings H, V. 139, 314-318 (1992).
- [4] S.N. Papadakis, N.K. Uzunoglu, C.N. Capsalis, "Scattering of a plane wave by a general anisotropic dielectric ellipsoid," J. Opt. Soc. Am. A, V. 7, 991-997 (1990).
- [5] A. Doicu, "Null-field method to electromagnetic scattering from uniaxial anisotropic particles," Optics Communications, V. 218, Iss. 1-3, 11-17 (2003).
- [6] C.F. Bohren, D.R. Huffman, "Absorption and scattering of light by small particles," Wiley (1998).

5.16 Interstellar Extinction by Spheroidal Grains

D. B. Vaidya¹

¹Gujarat College, Ahmedabad 380006 India

The exact solution to Maxwell's equations to calculate absorption, scattering and extinction of electromagnetic waves by homogeneous spheres is provided by Mie theory [1] and spherical grain models are commonly used to evaluate the interstellar extinction curve [2]. However, spherical grains can not explain the observed interstellar polarization that accompanies interstellar extinction. Since there is no exact theory to study the scattering properties of non-spherical (e.g. spheroids, cylinders) and inhomogeneous (porous, fluffy, composite) grains there is a need for formulating models of electromagnetic scattering by the irregularly shaped and inhomogeneous grains.

In the present study, we use discrete dipole approximation (DDA) [3] to calculate the extinction efficiencies of spheroidal silicate and graphite grains. We use the extinction efficiencies of the spheroidal grains to evaluate the interstellar extinction curve in the wavelength region; $3.4\mu m - 0.1\mu m$ [4][5]. The model extinction curves of spheroidal grains with not very large axial ratio fit the observed extinction reasonably well. We have also computed the volume extinction factor V_c , which is an important parameter from the point of view of the cosmic abundance, for the spheroidal grain models that reproduce the observed interstellar extinction curve. Our results show that the shape of the grains do not affect the volume extinction factor [6].

We have also studied the extinction and linear polarization efficiencies for aligned spheroids. These results show considerable variation in the linear polarization with the shape of the grains as well as with the orientation angles of the spheroids.

References

- [1] Mie G. (1908), *Ann. Phys.*, 25, 377
- [2] Mathis J.S., Rumpl W., Nordsieck K.H., (1977), *ApJ*, 217, 425
- [3] Draine B.T. (1988), *ApJ*, 333, 848
- [4] Vaidya D. B., Gupta R., Dobbie J.S., Chylek P. (2001), *A & A*, 375, 584
- [5] Vaidya D.B., Gupta R., Snow T.P., (2007), *MNRAS*, 379, 791
- [6] Gupta R , Mukai T., Vaidya D.B., Sen A., Okada Y., (2005), *A & A*, 441, 555

5.17 New life of Mie's approach with other bases, potentials, methods, etc.

Farafonov, V.G.¹, Il'in, V.B.², Vinokurov, A.A.¹

¹University of Aerocosmic Instrumentations, Bol.Morskaya 67, 190000 St.Petersburg, Russia, ²St.Petersburg University, Universitetskij pr. 28, 198504 St.Petersburg, Russia

In foundation of Gustav Mie's solution to the light scattering problem for a homogeneous sphere presented in [1] and called Mie theory one can find *harmonic fields' expansion in terms of the spherical wave functions* connected with the Debye scalar potentials, which for the scattered field is

$$\vec{E}^{\text{sca}}(\vec{r}) = \sum_{\nu} E_{\nu} \left(b_{\nu} \vec{M}_{\nu}^r(\vec{r}) + c_{\nu} \vec{N}_{\nu}^r(\vec{r}) \right), \quad (5.17.1)$$

where

$$\vec{N}_{\nu}^a = \frac{1}{k} \vec{\nabla} \times \vec{M}_{\nu}^a, \quad \vec{M}_{\nu}^a = \vec{\nabla} \times (\vec{a} \psi_{\nu}) \quad (5.17.2)$$

are solutions to the vector Helmholtz equation with the wavenumber k , $\nu = (\frac{e}{o}, 1, n)$ and, e.g., $\psi_{e1n}(r, \theta, \varphi) = h_n^{(1)}(r) P_n^1(\cos \theta) \cos \varphi$. Mie's coefficients a_{ν}, p_{ν} used in his expansions of the r, θ, φ -components of \vec{E}^{sca} (see Eqs. (52) in [1]) are naturally related with b_{ν}, c_{ν} : $a_n = (2n + 1)i^{2n+1}b_n$, $p_n = -(2n + 1)i^{2n+1}c_n$ (see for more details [2]).

The approach based on such field expansions in terms of wave functions was used by Rayleigh to consider scattering of sound waves [3] and by Mie to study that of electromagnetic ones [1] and is still widely required. Naturally, there are many works on its generalization. Here we present a review and new results of our *developments of the approach* with all details and codes' description being given in [4].

First, we have considered not only homogeneous spheres, but *multilayered axisymmetric scatterers* and homogeneous *ellipsoids*.

Second, in our works not only spherical, but *spheroidal and ellipsoidal bases* are applied. The expansions (5.17.1) in terms of spherical and spheroidal functions are used to consider light scattering by homogeneous and multilayered axisymmetric scatterers. We extensively utilized field expansions in spheroidal wave functions to study homogeneous and confocal layer spheroids and for the first time involved ellipsoidal ones to treat ellipsoids.

Third, we introduced *other scalar potentials* that were found to be in particular efficient for highly elongated/flattened particles. The fields were divided into two parts with specific properties and the Debye ($\vec{a} = \vec{r}$ in Eq. (5.17.2)) and "cylindric" ($\vec{a} = \vec{i}_z$) potentials were used for one field part and modified Abraham potentials for another.

Forth, besides Mie's way of finding the field expansion coefficients that is traditionally called the separation of variables method (SVM), we involved others, namely the *extended boundary condition* (EBCM) and *generalized point matching methods* (GPMM).

We report results of extensive numerical comparison of solutions obtained by these methods for particles of various shapes, sizes, and compositions. Because of different problem formulations used by the methods, properties of the solutions essentially differ.

At last, our progress in analytical and numerical study of *Rayleigh's hypothesis* about field expansion convergence at any point up to the scatterer surface is outlined. We determined regions of scatterer parameter values where the expansion (5.17.1) with the coefficients derived by the EBCM converges in near- and far-field zones (necessary conditions are quite different). This expansion with the coefficients obtained by the SVM is found to converge always in the far-field zone like in the case when the GPMM is applied.

Acknowledgement

We thank the grants RFFI 07-02-00831, RNP 2.1.1.2852, NSh 1318.2008.2.

References

- [1] G. Mie, "Beiträge zur Optik trüber Medien, speziell kolloidaler Metallösungen," *Annal. Physik* 25, 377-445 (1908).
- [2] C.F. Bohren, D.R. Huffman, *Absorption and Scattering of Light by Small Particles*. (J. Wiley & Sons, New York, 1983).
- [3] J.W. Strutt (Baron Rayleigh), *The Theory of Sound*. (Macmillan, London, 1877).
- [4] V.G. Farafonov, V.B. Il'in, *Light Scattering by Simple Model Nonspherical Heterogeneous Particles*. (Springer-Praxis, Berlin, 2009), in prep.

5.18 Scattering data base scatdb

Wauer, J.¹, Rother, T.², Schmidt, K.²

¹Institute for Meteorology, University of Leipzig, D-04103 Leipzig, ²Remote Sensing Technology Institute, German Aerospace Center, D-17235 Neustrelitz

Scattering of electromagnetic waves on nonspherical dielectric particles becomes of growing importance in remote sensing of the earth's atmosphere as well as in technical diagnostics. Studying the influence of dust like particles on our climate system and analyzing powder probes are only two examples in this context. There can be stated an increasing amount of modern measurement techniques which makes it necessary to take electromagnetic wave scattering on nonspherical particles into account. But there are especially two aspects which make this necessity a complex task. First, the numerical effort is much higher than that one known for spherical particles within Mie theory. It strongly depends on the morphology of the particle and can be performed on-line only in very specific situations. Second, the convergence procedures of the existing approaches

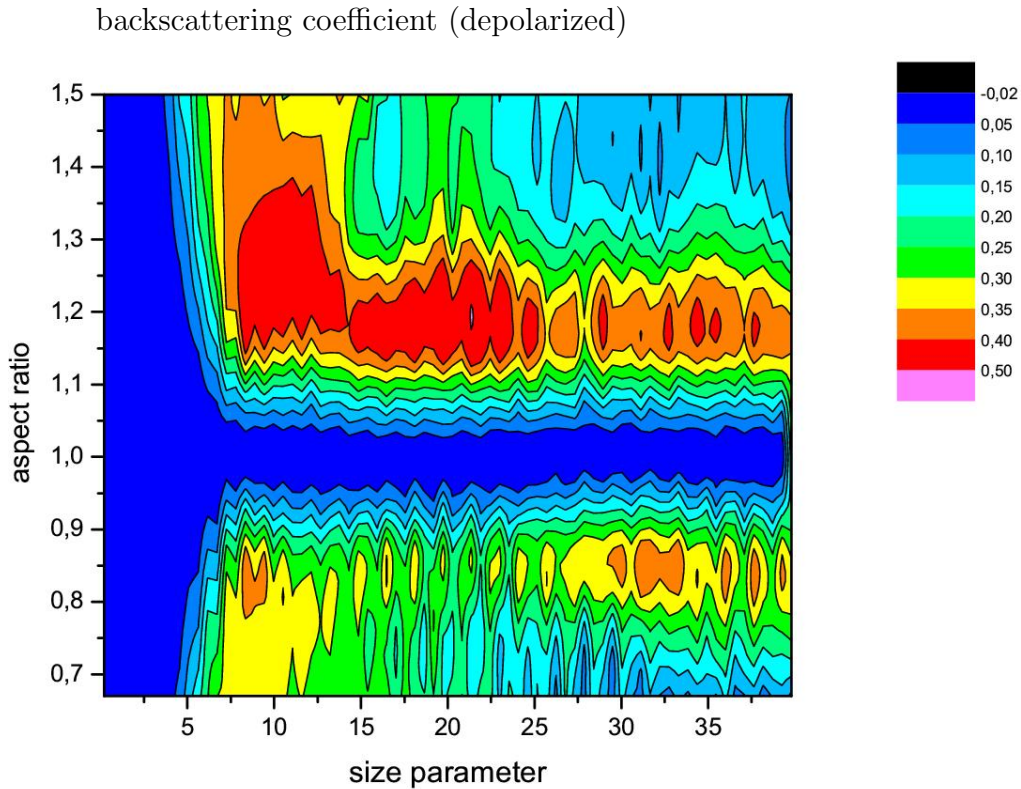


Figure 5.18.1: Backscattering coefficient $\sigma_{vh}^{back} / (\sigma_{vv}^{back} + \sigma_{vh}^{back})$ of spheroids as a function of aspect ratio (av) and size parameter for $n = 1.33$ (prolate spheroids: $av > 1$, oblate spheroids: $av < 1$).

are much more complex as compared to spheres. To obtain reliable results requires a detailed knowledge of the methodology behind a certain approach. Otherwise, one can run into a lot of pitfalls.

With the data base described in this presentation we will release interested users from dealing with those aspects and provide an easy access to scattering data of nonspherical particles. Therefore we present well tested scattering properties as benchmark results with a given accuracy and an estimated error bar. In this first version of the data base we consider only spheroidal particles. But the general structure of this data base will be used later on for other geometries, too. The calculations have been performed by use of the program `mieschka`[1] which is based on the T-matrix approach.

We have developed an user interface which allows external users an easy access to the scattering data. For the access we have realized the following functionality:

- scattering data for a fixed parameter set (i.e. a given wave length, refractive index and geometry)
- a specific scattering quantity as a function of the radius and optionally a second parameter (i.e. aspect ratio or real part of the refractive index)

- averaged (i.e. size and aspect ratio averaged) scattering data.

In this presentation we will also provide first results which can be obtained by using the scattering data base.

References

- [1] Wauer, J., et. al. "Two software tools for plane-wave scattering on nonspherical particles in the German Aerospace Center's virtual laboratory," *Applied Optics*, vol. **43** pp. 6371-6379 (2004).

Contributors

- Ahmed, G.A., 78, 84
Alegret, J., 41
Andersen, A. C., 22
Apeksimov, D.V., 52
- Böckmann, C., 22
Barrera, R.G., 50
Bech, H., 42
Beleites, M., 94
Benghorieb, S., 44, 78
Bonaccorso, F., 96
Borghese, F., 38, 56, 96
Burger, S., 82
- Cacciola, A., 56
Cecchi-Pestellini, C., 56
Choudhury, A., 78, 84
Cojoc, D., 49
- Damaschke, N., 24
Datsuyk, V.V., 48
Denti, P., 38, 56, 96
Derkachov, G., 93
Doicu, A., 26
Doll, U., 62
- Farafonov, V.G., 104
Ferrari, A.C., 96
Ferrari, E., 49
Frank, R., 49, 96
Frisvad, J. R., 26
- Garbin, V., 49
García-Valenzuela, A., 50, 99
Geints, Yu.E., 52
Germer, T.A., 28
Gogoi, A., 78, 84
Gouesbet, G., 29, 76
- Graener, H., 94
Grigorchuk, N.I., 85
Gruy F., 90
Gucciardi, P.G., 96
Guoxia Han, 86
Gupta, R., 53
Gutiérrez-Reyes, E., 50
- Heckenberg, N. R., 37
Hellmers, J., 87
Hergert, W., 54, 94
Hesse, E., 31
Hobar, F., 44, 78
Hu, Y., 37
- Iatì, M.A., 38, 56, 96
Il'in, V.B., 104
- Jacquier S., 90
Jakubczyk, D., 93
Jones, P.H., 96
- Köhler, U. , 64
Kawaguchi, T., 58
Kaye, P.H., 31
Kettner, B., 82
Kiriyyenko, O., 94
Knöner, G., 37
Kokhanovsky, A.A., 60
Kolwas, K., 93
Kolwas, M., 93
Kroha, J., 49, 96
- Laven, P., 34
Leder, A., 42
Lock, J.A., 76
Lubatsch, A., 49, 96
- Maragò, O.M., 38, 96

Martín-Moreno, L., 41
 Martin, P. A., 36
 Mc Call, D.S., 31
 Miclea, P.-T., 99
 Mölter, L., 63

 Nieminen, T. A., 37

 Okada, Y., 60
 Osterloh, L., 22

 Petrov, D., 49
 Pornsawad, P., 22

 Qiang Xu, 86

 Randeu, W.L., 65
 Rausch, A., 62
 Roehle, I., 62
 Rother, T., 76, 106
 Rubinsztein-Dunlop, H., 37

 Sánchez-Pérez, C., 50, 99
 Saija, R., 38, 56, 96
 Saito, Takushi, 58
 Saoudi, R., 44, 78
 Sato-Berú, R., 99
 Satoh, I., 58
 Schmidt, F., 82
 Schmidt, K., 106
 Schmidt, M., 63
 Schmidt, V., 100
 Schweiger, G., 40
 Shcherbakov, A., 67
 Stübinger, Th. , 64
 Stilgoe, A. B., 37
 Stopford, C., 31

 Teschl, F., 65
 Tishchenko, A.V., 44, 67, 78
 Tomchuk, P.M., 85
 Tropea, C., 76
 Tsitsas, N. L., 71

 Ulanovsky, Z., 31

 Vaidya, D.B., 53, 103

 Versluis, M, 49
 Vinokurov, A.A., 104
 Volke, A., 72
 Volpe, G., 49

 Wackerow, S., 94
 Wauer, J., 76, 106
 Wehrspohn, R.B., 99
 Witt, W. , 64
 Wollny, A. G., 73
 Wriedt, T., 87, 100

 Xu, F., 76

 Yang Zhang, 86
 Yiping Han, 86

 Zemlyanov, A.A., 52
 Zschiedrich, L., 82

 Üpping, J., 99

Index

- analytical orientation averaging, 60
- Bateman, 36
- biaxially anisotropic scatterers, 101
- colloids
 - effective refractive index, 51
- coronas, 34
- cross sections, 61
- discrete-dipole approximation (DDA), 41, 53, 67
- drying microdroplet, 93
- Dunhem-Quine theorem, 29
- extended boundary condition method (EBCM), 105
- extreme precision calculations, 64
- femtosecond pulse absorption, 85
- field distribution of plasmons, 45
- field enhancement, 99
- finite element method (FEM), 82
- frequency-pulsed excitation, 53
- gas density measurements, 62
- generalized Lorenz-Mie theory, 76
- generalized source method, 67
- glories, 34
- Green's tensor (GT) formalism, 41
- Harry, 36
- ill-posed problem, 23
- interferometric laser imaging, 58
- interstellar
 - extinction, 53, 104
 - grain aggregates, 56
 - photochemistry, 56
- inverse scattering theory, 71
- layered spheres, 71
- light scattering
 - cross section, 91
 - features on surfaces, 28
 - programs, categorization, 88
 - small particles, 31
- localization effects
 - of classical waves, 96
- Lorenz-Mie theory, 29, 40
 - extension, 48
 - generalized (GLMT), 76
 - graphics, 26
 - milk, 27
 - optical tweezers, 37
- Lorenz-Mie-Debye theory, 40
- Maxwell's equations
 - numerical simulation, 82
- metallic nanoparticles, 79, 85, 95
- microbubble sizing, 58
- microphysical properties, 23
- Mie particles, 23
- Mie scattering, 71
 - pulse induced, 42
- Mie, Gustav
 - life and work, 55
- morphology dependent resonances (MDR), 40, 87
- multilayered axisymmetric scatterers, 105
- multiple scattering, 61
- nanooptics, 82
 - mesh based calculations, 41
- nanoplasmonics, 48
- nanorods
 - gold, 97

- nanotubes
 - carbon, 97
- nonspherical objects, 82
- numerical orientation averaging, 60
- optical aerosol spectrometers, 63
- optical force distribution, 76
- optical trapping, 38, 97
- particle plasmons, 99
- particles
 - aggregate of, 91
 - arbitrarily shaped, 66
 - atmospheric sciences, 73
 - characterization, 24
 - colloidal, 99
 - MgO, 78
 - size analysis, 64
 - sizing, 73
 - small, densely packed, 60
 - spheroidal titania, 84
 - TiO₂, 78
- patterned polarizers, 73
- point matching method (GPMM), 106
- prebiotic molecules
 - formation of, 56
- quasi-Monte-Carlo method, 60
- rainbow techniques, 24
- rainbows, 34
- Raman lidar, 22
- random media
 - light transport, 49
- Ray Tracing with Diffraction on Facets
 - model (RTDF), 31
- Rayleigh scattering, 62
- Rayleigh's hypothesis, 76, 106
- refractive index, 61
- regularization, 23
- rendered images, 27
- scatdb, 106
- scattering database, 106
- scattering properties, 26
- separation of variables method, 105
- small particles
 - densely packed, 60
- soda lime glass, 73
- supernovae, 22
- systems of particles
 - near plane surface, 26
 - scattering properties, 26
- T-matrix, 53, 101
 - method for clusters of spheres, 60
- tightly-focussed beam, 37
- time resolved analysis, 42
- topological charge, 49
- transparent spherical microparticle, 53
- whispering gallery modes, 40
- white dwarfs, 22